Diss. ETH Nr. 14959

# Isolation of binding molecules to the EDB domain of fibronectin, a marker of angiogenesis

A dissertation submitted to the

SWISS FEDERAL INSTITUTE OF TECHNOLOGY ZURICH

for the degree of

DOCTOR OF NATURAL SCIENCES

Presented by

Jörg Scheuermann
Dipl. Chem. ETH – ETH Zürich
born April 16, 1970
from Mannheim, Germany

accepted on the recommandation of

Prof. Dr. Dario Neri, examiner

Prof. Dr. Leonardo Scapozza, co-examiner,

Dr. Oliver Zerbe, co-examiner

Zürich, December 2002

# TABLE OF CONTENTS


**1 SUMMARY 5**

**1 ZUSAMMENFASSUNG 7**

**2 INTRODUCTION 9**

**2.1 Fibronectin, a protein of the extracellular matrix 9**

2.1.1 Structure of fibronectin 9

2.1.2 Alternatively spliced fibronectin isoformes 11

**2.2 The EDB domain of fibronectin: an oncofetal marker 12**

2.2.1 Structure of the EDB domain 12

2.2.2 Occurrence of EDB 14

2.2.3 Therapeutic relevance of EDB as a marker of angiogenesis 16

**2.3 Human antibody technology for the generation of specific EDB binders 17**

2.3.1 Antibodies and antibody phage technology 17

2.3.2 Monoclonal anti-EDB antibodies, from BC-1 to L19 24

2.3.3 L19 derivatives and L19 fusion proteins for the treatment of angiogenesis-associated cancer 28

**2.4 Tumor therapy: From antibodies to low-molecular weight synthetic binders 30**

2.4.1 Antibodies – advantages and drawbacks 30

2.4.2 High-affinity low-molecular weight synthetic binders 35

2.4.2.1 Drug discovery at present 35

2.4.2.2 Combinatorial Chemistry and High-throughput screening 38

2.4.2.2.1 Combinatorial Chemistry 38

2.4.2.2.2 High-Throughput Screening (HTS) 40

2.4.2.3 Screening by NMR 43

2.4.2.3.1 General techniques 43

2.4.2.3.2 SAR by NMR 45

2.4.2.4 Virtual Screening 46

**3 RESULTS, METHODS AND DISCUSSION 49**

**PART I: Low-molecular weight binders to EDB**

**3.1 Discovery and investigation of lead-compounds as binders to the EDB domain 49**

3.1.1 Abstract 49

3.1.2 Introduction 51

3.1.3 Materials and Methods 54

3.1.3.1 Production of $^{15}$N-labeled EDB 54

3.1.3.2 NMR and spectra analysis 54

3.1.3.3 Chemical synthesis 55

3.1.4 Results 61

3.1.4.1 Library design 61

3.1.4.2 NMR analysis of EDB binding 61

3.1.4.3 Derivatives of 2,2-diphenylethylamine 67

3.1.5 Discussion 72

**PART II: High-molecular weight binders to EDB**

**3.2 Unexpected observation of concentration-dependent dissociation rates for antibody-antigen complexes in competition experiments 75**

3.2.1 Abstract 75

3.2.2 Introduction 76

3.2.3 Experiments and Methods 79

3.2.3.1 Antibodies, antigens and calmodulin 79

3.2.3.2 Competition experiments 79

3.2.4 Results and Discussion 82

**3.3 Robotic Isolation of EDB-specific derivatives of the L19 antibody 86**

3.3.1 Abstract 86

3.3.2 Introduction 87

3.3.3 Materials and Methods 93

3.3.3.1 Library construction 93

3.3.3.2 Biopanning 97

3.3.3.3 ELISA 98

3.3.3.4 Robotization 100

3.3.4 Results and Discussion 102

3.3.4.1 Robotization of antibody screening 102

3.3.4.2 ELISA screening of antibody fragments with improved dissociation rate for the antigen 104

3.3.4.3 Construction of a library of L19 mutants 107

3.3.4.4 Biopanning experiment 110

3.3.4.5 Characterization of L19 mutants 112

**4 CONCLUSIONS 116**

**5 REFERENCES 118**

**6 ABBREVIATIONS 140**

**7 CURRICULUM VITAE 141**

**8 ACKNOWLEDGEMENTS 143**

# 1 SUMMARY

Aggressive solid tumors induce the formation of new blood vessels from preexisting ones, a process termed angiogenesis. As a growing tumor heavily relies on the supply of nutrients via the blood stream, blocking this blood supply should constitute an appropriate avenue towards cancer therapy. Alternatively, molecules capable of a selective localization on new blood vessels could be used for the selective destruction of endothelial cells lining the tumor blood vessels, without affecting mature endothelial cells.

The extra-domain B (EDB) of fibronectin, a domain which — by alternative splicing of the primary RNA transcript — is either present or omitted in fibronectin molecules of the extracellular matrix, represents a good-qualitiy marker of angiogenesis, as it is abundantly expressed around new blood vessels, but undetectable in virtually all normal adult tissues (exeption made for uterus and ovaries).

The selective targeting of neovasculature of solid tumors with anti-EDB antibodies (conjugated to an appropriate effector function such as a cytotoxic or an immunostimulating agent) has proven to be successful in animal experiments.

Two factors play an important role in the specific targeting of new formed blood vessels: I) Abundance and accessibility of the targeted antigen. (the latter is strongly influenced by the size of the targeting molecule; which may limit tissue penetration and body clearance) and II) the affinity of the targeting molecule towards the marker of angiogenesis of choice.

Molecules with a smaller size than antibodies and a comparable affinity towards the target antigen are expected to be superior to antibodies in terms of pharmacokinetic properties and immunogenicity.

In this thesis, we first aimed at discovering a low-molecular weight organic molecule which binds specifically to the EDB domain of fibronectin.

The structure of the EDB domain evidences the presence of a major and of a minor hydrophobic patch on the surface of this protein domain. Since the EDB domain is highly negatively charged (it contains no lysine residue and only two arginine residues but 5 glutamate residues and 7 aspartate residues), we have screened a library of 113 primary amines containing an aromatic moiety for their interaction with

$^{15}$N-labeled recombinant EDB, using SAR by NMR technology. One compound, 2,2-diphenylethylamine, exhibited a specific binding to EDB, with an affinity in the millimolar range.

Further investigation on the molecular scaffold of this binder led to the identification of structural determinants which are required for the binding. While the affinity of the initial binder could not be improved by the chemical modifications performed onto the basic 2,2-diphenylethylamine structure, these analogues showed which chemical derivatives of 2,2-diphenylethylamine retain the binding affinity for the EDB. We are currently using this information for the construction of high-affinity bidentate EDB ligands.

In parallel to the small molecule approach a macromolecule-based approach has been used. As affinity of the targeting agent towards its cognate antigen is of great importance for molecular targeting approaches, we aimed at increasing the affinity of a single-chain antibody fragments towards EDB ("L19", available in the laboratory).

For that purpose, we created a library of antibody fragments based on the "L19" antibody. Binders were first enriched by means of biopanning and afterwards subjected to high-throughput robotic screening.

For the screening, we established a novel ELISA-screening based approach which is able to rank the binding antibodies based on their kinetic dissociation constants, regardless of their oligomeric state.

During the setup of this competition-ELISA assay, we discovered and further investigated an unexpected effect of concentration dependent kinetic dissociation rates of antibody-antigen complexes which might be of general validity for bidentate binders.

Using this novel screening approach we were able to identify several binders from the library with high affinity to EDB.

# 1 ZUSAMMENFASSUNG

In einem als Angiogenese bezeichneten Prozess induzieren solide Tumoren, ausgehend von bereits existierenden Blutgefässen, die Bildung neuer Blutgefässe.
Da ein wachsender Tumor in starkem Masse auf die Nährstoffversorgung durch die Blutzirkulation angewiesen ist, sollte die Unterbrechung der Blutzufuhr des Tumors einen möglichen Weg der Tumortherapie darstellen. Wahlweise könnten Moleküle, welche in der Lage sind, sich selektiv an neue Blutgefässe anzulagern, für die selektive Zerstörung der die tumoralen Blutgefässe umgebenden neu gebildeten Endothelzellen herangezogen werden, ohne dadurch die bereits existenten Endothelzellen ebenfalls zu betreffen.
Die Extra-Domäne B (EDB) von Fibronektin, welche in Fibronektinmoleküle der extrazellulären Matrix aufgrund alternativen Spleissens des primären RNA Transkripts eingebaut werden kann, ist ein geeigneter Angiogenesemarker von hoher Qualität, da sie gehäuft in der Umgebung neovaskularisierender Blutgefässe exprimiert wird, jedoch in normalen erwachsenen Geweben nicht detektiert werden kann (mit Ausnahme des Uterus und der Ovarien).
Versuche mit EDB-spezifischen Antikörpern, welche an die neu gebildeten Blutgefässe banden und mit einer geeigneten zytotoxischen oder immunstimulierenden Effektorfunktion verknüpft waren, erwiesen sich bei der Tumortherapie im Tierexperiment als erfolgreich. Beim spezifischen Abzielen (targeting) auf die neu geformten Blutgefässe spielen zwei Faktoren eine bedeutsame Rolle:
I) Die Menge sowie die Zugänglichkeit des Antigens, auf das man abzielt (letzteres ist stark beeinflusst von der Grösse des bindenden Moleküls, welche wiederum die Gewebepenetration und die Ausscheidung aus dem Körper beeinträchtigt) und II) die Affinität des bindenden Moleküls zu dem gewünschten Angiogenesemarker.
Moleküle kleineren Molekulargewichts im Vergleich zu Antikörpern, welche vergleichbare Affinität zum entsprechenden Antigen aufweisen, sollten diesen bezüglich ihrer pharmakokinetischen Eigenschaften und ihrer Immunogenität überlegen sein.

Das Ziel dieser Dissertation war zunächst die Entdeckung kleiner organischer Moleküle, welche in der Lage sind, spezifisch an EDB zu binden.
Die EDB-Domäne besitzt eine grössere sowie eine kleinere hydrophobe Region. Aufgrund der stark negativen Ladung der EDB-Domäne (sie enthält keinen Lysin- und lediglich zwei Argininreste, hingegen 5 Glutamat- und 7 Aspartatreste) untersuchten wir mittels „SAR by NMR“-Technologie eine Bibliothek, bestehend aus 113 primären Aminen, welche jeweils einen aromatischen Rest besassen, auf Interaktion mit $^{15}$N-markiertem EDB.
Eine Verbindung aus dieser Bibliothek, 2,2-Diphenylethylamin, zeigte eine spezifische Bindung an EDB mit millimolarer Affinität. Eine weitergehende Untersuchung des molekularen Gerüsts dieses Binders offenbarte die für die Bindung notwendigen strukturellen Determinanten. Während es nicht möglich war, durch chemische Modifikationen an 2,2-Diphenylethylamin die Affinität zu erhöhen, zeigten die erhaltenen Analoga, welche 2,2-Diphenylethylamin-Derivate weiterhin Affinität zu EDB aufwiesen. Wir sind im Begriff, die daraus erhaltenen Informationen für die Herstellung hochaffiner bidentaler EDB-Binder zu nutzen.
Da die Affinität des bindenden Agens zu dem entsprechenden Antigen von grösster Wichtigkeit für Targeting-Anwendungen ist, setzten wir uns wir im zweiten Teil dieser Dissertation das Ziel, die Affinität eines EDB-spezifischen scFv Antikörper-Fragments zu erhöhen („L19“, aus unserem Laboratorium).
Zu diesem Zweck erzeugten wir eine Bibliothek von Antikörper-Fragmenten, basierend auf dem Antikörper „L19“. EDB-Binder wurden zunächst durch Biopanning-Experimente angereichert und anschliessend mit Hilfe Robotik-gestützten High-Throughput-Screenings untersucht. Wir entwickelten eine neuartige Methode, welche auf ELISA-Screening basiert und welche die Einteilung der Antikörper anhand ihrer kinetischen Dissoziationskonstanten und ohne Rücksicht auf ihren oligomeren Zustand ermöglicht. Während des Etablierens der neuen Kompetitions-ELISA-Methode beobachteten wir einen unerwartet auftretenden Effekt einer Konzentrationsabhängigkeit der Dissoziationsgeschwindigkeit eines Antikörper-Antigen-Komplexes, welcher für bidentale Binder von allgemeiner Gültigkeit sein könnte. Mithilfe der neu entwickelten Methode war es möglich, aus der Bibliothek mehrere hochaffine EDB-Binder zu isolieren.

# 2 INTRODUCTION

## 2.1 Fibronectin, a protein of the extracellular matrix

### 2.1.1 Structure of fibronectin

Fibronectin (FN) is one of the largest multi-domain proteins for which domain organization and molecular interactions have been resolved in detail [Hynes, 1990; Pankov and Yamada, 2002]. Fibronectin is found in a soluble form in the plasma (300µg/ml) and in an insoluble form in the extracellular matrix (ECM), to which most of the FN activities in the body have been ascribed: binding to cell surfaces and various compounds, including collagen, fibrin, heparin, DNA, and actin. Fibronectins are involved in a number of important functions like wound healing, cell adhesion, blood coagulation, cell differentiation and migration, maintenance of the cellular cytoskeleton, hemostasis and thrombosis, wound healing, oncogenic transformation as well as in tumor metastasis migration [Hynes, 1990; Magnusson and Mosher, 1998]. These essential functions are underlined by the fact that mouse embryos which are homozygous for the loss of the FN gene have been observed to die at about 8.5 days of gestation. Embryonal death is associated with widespread defects in mesoderm-derived structures, including absence of somites and notochord, as well as developmental defects in the heart and vascular system. [George et al., 1993]. In a soluble form fibronectin (pFN) is abundant in plasma and other body fluids, while insoluble fibronectin (cFN) is a major component of the extracellular matrix (ECM). FN usually exists as a dimer of two nearly identical ~250 kDa (≈ 2500 amino acids) subunits, covalently linked by a pair of disulfide bonds near the C-terminal end of the

subunits [Alitalo and Vaheri, 1982; Yamada, 1983 ; Hynes, 1985; Ruoslahti, 1988]. Each monomer comprises 3 types of repeating units, termed type-I (ca. 40 amino acid residues), type-II (ca. 60 amino acid residues) and type-III (ca. 90 amino residues), arranged like beads on a string: 12 type-I repeats, 2 type-II repeats and 15-17 type-III repeats [Leahy et al., 1996; Pankov and Yamada, 2002 ], see Figure 2.1.1. These modular repeating units are resistant to proteolysis and contain binding sites for extracellular matrix proteins such as collagen and thrombospondin, cell-surface receptors such as integrins, circulating blood proteins such as fibrin and glycosaminoglycans such as heparin and chondroitin sulphate.

FNs are glycoproteins containing up to 9% carbohydrate, depending on the cell source. Glycosylation sites are found predominantely within the type-III repeats and the collagen-binding domain.

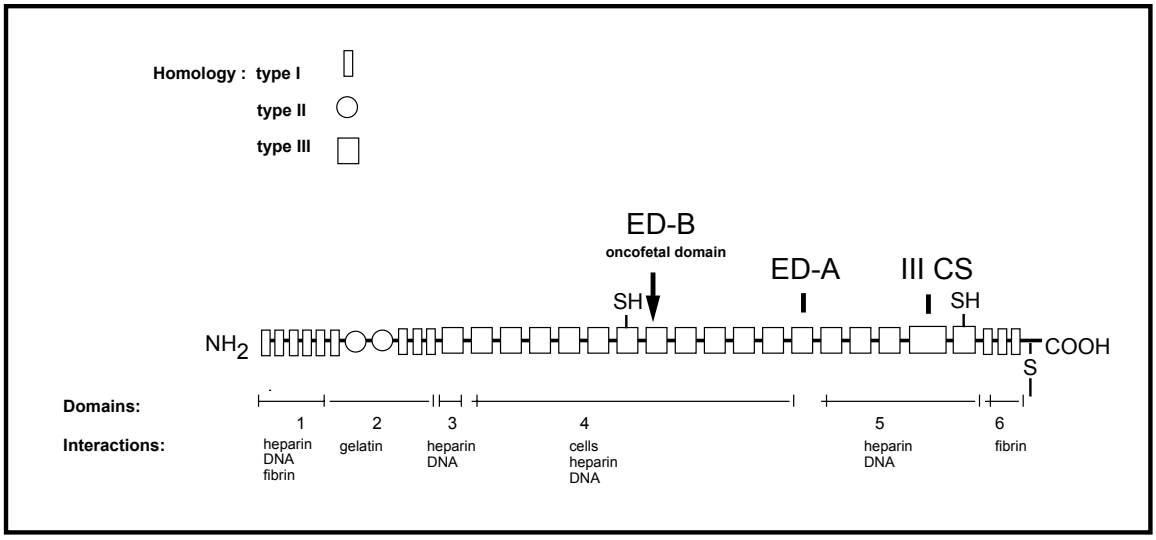


**Figure 2.1.1**

Representation of the domain structure of a subunit of human Fibronectin. Fibronectin subunit is made up of a series of repeating units of three different types (type-I, type-II, type-III). Two subunits are joined by two disulfide bonds at their carboxyl termini. Three repeats can be either inserted or omitted in the molecule by a mechanism of RNA alternative splicing: EDB, EDA, IIICS. Separate functional regions (in the figure named domains) have been identified that contain binding activities for other components of the ECM: domain 1 (can bind to heparin, DNA, fibrin), domain 2 (can bind to gelatin), domain 3 (can bind to heparin and DNA), domain 4 (can bind to cells, heparin, DNA), domain 5 (can bind to heparin and DNA), domain 6 (binds to fibrin).

### 2.1.2 Alternatively spliced fibronectin isoformes

Although FNs are the product of the single *FN* gene, the resulting protein can exist in multiple forms which — apart from posttranslational modifications — arise from alternative splicing of its primary RNA transcript (for reviews see: [Ffrench-Constant, 1995 ; Kosmehl et al., 1996]. This polymorphism which leads to as many as 20 different isoforms in human FN, thereby generating FNs with different solubility, cell-adhesive and ligand-binding properties, provides cells with the possibility to modify the composition of the ECM in a tissue-specific manner. Alternative splicing takes place in three regions of the primary RNA transcript: Exon usage or skipping leads to either inclusion or omission of two type-III repeats, extra-domain B (EDB, also termed EIIIB or EDII), which is inserted between FN type-III repeats $III_7$ and $III_8$, or/and extra-domain A (EDA, also termed EIIIA or EDI), inserted between FN type-III repeats $III_{11}$ and $III_{12}$. This type of splicing occurs in many vertebrates, including *Xenopus*, chicken, rat, dog and human. These extra-domains are almost always absent from plasma-fibronectin but can be found in ECM-fibronectin. A third region of splicing occurs at a non-homologous stretch termed V (variable) region or IIICS (type-III connecting segment), respectively. The structural variations at this locus are by far more complex and species dependent. Not only can this extra-domain be completely in- or excluded but also partially in- or excluded: In human, five different V-region variants have been found. Other types of splicing have been detected in cartilage, where the whole V-region along with $III_{15}$ and $I_{10}$ is missing. This form exists not only as a homodimer but also in an unusual monomeric configuration. These alternatively spliced variants are of huge importance since in transformed cells and in malignancies, the splicing pattern of FN pre-mRNA is altered leading to an increased expression of FN isoforms containing the IIICS, EDA and EDB sequences [Castellani et al., 1986 ; Borsi et al., 1987 ; Vartio et al., 1987 ; Zardi et al., 1987 ; Carnemolla et al., 1989 ; Oyama et al., 1989 ; Oyama et al., 1990 ; Borsi et al., 1992 ; Castellani et al., 1994; Kaczmarek et al., 1994 ].

## 2.2 The EDB domain of fibronectin: an oncofetal marker

### 2.2.1 Structure of the EDB domain

The 3D-structure of the alternatively spliced-in typeIII-like EDB domain, a 91 amino acid sequence, has been solved by NMR spectroscopy in solution in the group of Kurt Wüthrich at the ETH Zurich (PDB entry 2FNB)[Fattorusso et al., 1999], and is characterized by two antiparallel β sheets that form a β sandwich (Figure 2.2.1). One β sheet is formed by three β strands (A, B and E), and the other by four β strands (C, C', F and G). The two β sheets enclose a hydrophobic core of 25 amino acid sidechains. EDB is highly acidic (net charge: -10 at pH 7.4) and contains only two positively charged residues. The negatively charged residues are uniformly distributed over the protein surface, except for a solvent-exposed hydrophobic patch formed by residues Ile35, Phe54, Ile78 and Leu80 [Fattorusso et al., 1999].

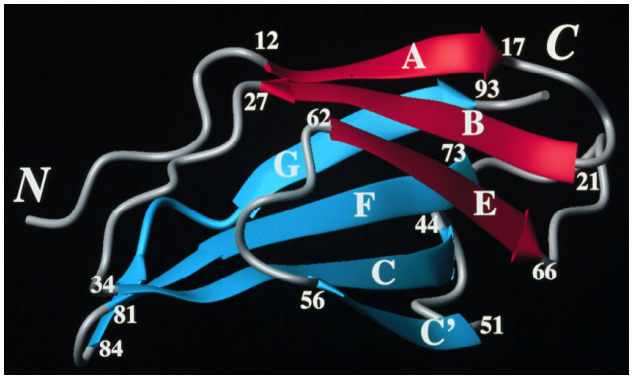


**Figure 2.2.1**

**Structure of the EDB domain of fibronectin.**

Ribbon drawing of one of the 20 energy-minimized conformers of human EDB (PDB entry 2FNB). The 2 β-sheets formed by 3 and 4 β-strands, respectively, are colored in red and cyan. The β-strands are labeled A to G following the nomenclature used for other FN typeIII domains. For the individual β-strands, the first and last sequence positions are indicated, N- and C-termini are also indicated.

Crystal and solution structures of type-III domains of fibronectin have been solved (PDBentries 1TTF;1TTG;1FNA;1CFB;1FNF;2FN2;1MFN;2MFN;2FNB;1FNH;1J8K).
The crystal structure of a FN fragment containing the type-III domains 7-10 [Leahy et al., 1996] (PDB entry 1FNF) shows a rod-like molecule with highly variable relationships between the individual pairs of adjacent domains. The relative orientations of adjacent pairs of domains are fine-tuned by interactions at the interdomain interfaces. These are largely composed of the loops located at the N and C termini of each domain. Detailed structure comparisons of EDB with FN type-III repeats 7 and 8 (FN7 and FN8) show that marked differences in corresponding loop structures cause significant differences in the relative orientation of the adjoining domains in EDB-containing fibronectin and fibronectin without EDB [Leahy et al., 1996]. This finding is supported by the observation that a specific monoclonal antibody, BC-1, recognizes an epitope in FN7 that is inaccessible in FN but becomes unmasked in EDB-containing fibronectin [Carnemolla et al., 1992].

### 2.2.2 Occurrence of EDB

The 91 amino acid alternatively spliced-in EDB domain is identical in mouse, rat, rabbit, dog, monkey and human (Figure 2.2.2). It has a restricted pattern of expression: undetectable in normal adult tissues and in mature blood vessels, but accumulating in regenerating tissues and around new blood vessels [Nicolo et al., 1990 ; Halin et al., 2001].

EDB protein sequence in different species

```
                   10         20         30         40         50
Human     ...EVPQLT DLSFVDITDS SIGLRWTPLN SSTIIGYRIT VVAAGEGIPI
Dog       ...EVPQLT DLSFVDITDS SIGLRWTPLN SSTIIGYRIT VVAAGEGIPI
Rat       ...EVPQLT DLSFVDITDS SIGLRWTPLN SSTIIGYRIT VVAAGEGIPI
Mouse     ...EVPQLT DLSFVDITDS SIGLRWTPLN SSTIIGYRIT VVAAGEGIPI
Chicken   ...EVPQLT DLSFVDITDS SIGLRWTPLN ASTIIGYRIT VVAAGESVPI
Xenopus   ...EIPQLT DIKYDDVTDT SIDLRWTPLN SSNIIGYRIT VVAAGESVPI

                       60         70         80         90
Human       FEDFVDSSVG YYTVTGLEPG IDYDISVITL INGGESAPTT LTQQT
Dog         FEDFVDSSVG YYTVTGLEPG IDYDISVITL INGGESAPTT LTQQT
Rat         FEDFVDSSVG YYTVTGLEPG IDYDISVITL INGGESAPTT LTQQT
Mouse       FEDFVDSSVG YYTVTGLEPG IDYDISVITL INGGESAPTT LTQQT
Chicken     FEDFVDSSVG YYTVTGLEPG IDYDISVITL INGGESAPTT LTQQT
Xenopus     YEEFVGPTDG YYKVSGLEPG IDYEISLITL INGGESAPTT IIQHT
```

**Figure 2.2.2**

Comparison of the aminoacid sequence of EDB in different species. Human EDB sequence is identical to that of dog, rabbit (not shown), rat, mouse. It has a homology of 96% with the chicken and of 80% with the Xenopus EDB sequence. (Numbering according to[Fattorusso et al., 1999])

EDB has been discovered through proteolytic cleavage of FN molecules obtained from different sources: In 1985, a site within the cell-binding domain 4 (see Figure 2.1.1) was found in tumor-derived or SV-40-transformed human cells which was

cleaved by the proteolytic enzyme cathepsin-D and which was undetectable in plasma-FN and FN from normal human cells [Borsi et al., 1985]. This suggested a new splicing site and a transformed cell-specific splicing pattern leading to the expression of a new sequence in FN from transformed cells. In 1987, a large percentage of FN molecules from transformed human cells was shown to contain the EDB domain, in the middle of the cell-binding domain 4 [Zardi et al., 1987]. Since then, immunohistochemical studies were performed, first with a murine monoclonal antibody binding to FN only in the presence of EDB [Carnemolla et al., 1989] and later with recombinant antibody fragments specific for the EDB domain [Carnemolla et al., 1996], which have allowed the identification of EDB as an angiogenesis-associated marker (see next section).

The EDB containg fibronectin isoform ($B^+$-fibronectin), apart from the female reproductive cycle and some very rare exceptions, is undetectable in normal human adult tissues, but exhibits expression in foetal and tumor tissues as well as during wound healing [Zardi et al., 1987 ; Carnemolla et al., 1989 ; Ffrench-Constant and Hynes, 1989 ; Ffrench-Constant et al., 1989 ; Laitinen et al., 1991]. It is expressed mainly by cells in neovascularizing conditions and accumulates around neovascular structures and is therefore considered to be a marker of angiogenesis. This selective expression pattern has been extensively demonstrated in studies on many different tumor types, in particular on invasive ductal carcinoma [Kaczmarek et al., 1994] and brain tumors [Castellani et al., 1994], but also in an ocular angiogenesis model [Birchler et al., 1999a].

### 2.2.3 Therapeutic relevance of EDB as a marker of angiogenesis

The formation of new blood vessels (angiogenesis) is an important process in the progression of cancer and many other fast progressing diseases. Angiogenesis, therefore, offers an ideal point of intervention in order to attack these disorders at the level of their sustaining processes.

Angiogenesis has been shown to be associated with EDB expression around the newly forming blood vessels virtually in all the cases studied, leading to the conclusion that EDB is a marker of angiogenesis [Castellani et al., 1994; Pujuguet et al., 1996; D'Ovidio et al., 1998; Karelina and Eisen, 1998; Midulla et al., 2000; Castellani et al., 2002]. So far, the EDB domain of fibronectin is one of the few markers of angiogenesis, which have extensively been characterized and validated by biodistribution analysis *in vivo* [Tarli et al., 1999; Viti et al., 1999]. Since angiogenesis is a feature common to almost all kinds of solid tumors, an angiogenesis-based therapeutic approach would be a unique strategy to fight all kinds of genetically different tumors relying on neovascularization: the inhibition of tumor-associated angiogenesis will “starve” the tumor and thus block its growth and metastatic spreading. In principle, two kinds of anti-angiogenesis therapeutic strategies are thinkable: the first (and more exploited) one is based on the inhibition of angiogenesis while the second one consists of targeting and delivering toxic molecules to new blood vessels, so called vascular targeting. Angiogenesis-based therapies target endothelial cells which, unlike cancer cells, are genetically stable and less prone to mutation [Kerbel, 1997]. Thus, the risk of developing resistance to the therapeutical agent is low. Another advantage is given by the fact that a targeted antiangiogenic therapy would generally be less toxic than conventional therapies, since neovasculature is almost undetectable in normal adult tissue.

The EDB domain specific for neovascularizing tumors therefore offers all advantages of a good molecular target.

## 2.3 Human antibody technology for the generation of specific EDB binders

### 2.3.1 Antibodies and antibody phage technology

Antibodies, also called immunoglobulins, are important functional units of the immune system. They are B cell-produced glycoproteins which can trigger an immune response by directly interacting with the big variety of antigens that an organism encounters. It has been estimated that a human being makes at least $10^{15}$ different antibody molecules, each of them specific for a different antigen. Antibodies can be highly specific for their antigen, with affinities typically $10^5$-$10^7$ $M^{-1}$ for a primary and $10^8$ $M^{-1}$ or more for a secondary immune response [Winter et al., 1994]. Their affinities are improved by avidity, i.e. one antibody molecule has two binding domains which, when bound to the same target at the same time, increases the functional affinity of the antibody.

The basic structure of an antibody consists of two identical light chains and two identical heavy chains which are linked by disulfide bonds. Each heavy and light chain contains a variable sequence (VH and VL respectively) in the amino-terminal 110 residues, and constant sequences (CH and CL respectively) in the remaining portion of the chain. Variability of the antibodies, which accounts for their different binding specificity, is located in the VL and VH, clustered in several hypervariable regions: the complementarity determining regions (CDRs). These regions form the antigen binding site of the antibody molecule and determine its specificity.

Immunoglobulin light chains (which are of two types: κ and λ) and heavy chains are encoded by three separate multigene families located on different chromosomes. In germline DNA, each multigene family contains numerous gene segments. In vivo, diversity in antibody combining sites is produced by multiple variable (V), diversity (D), and joining (J) gene segments and somatic mutation.

CDRs 1 and 2 of H and L chains are encoded by V regions. Light chain CDR3 (LCDR3) is produced by the combination of V and D regions, whereas heavy-chain CDR3 (HCDR3) is formed by the combination of V, D and J regions.

The diversity is created by random rearrangement of the variable gene segments in germ-line DNA: conserved DNA sequences flank each V, D, and J segment and direct their joining. During this process, many different combinations of V, D, J fragments are obtained. Major sources of antibody diversity are the random joining of multiple V, J and D germline gene segments, random association of a given heavy-chain and light-chain, junctional flexibility and N-region nucleotide addition, somatic mutation following antigenic stimulation.

Since 1986, when the first three-dimensional structure of an antigen-antibody complex was solved [Amit et al., 1986], it is known that most of the contacts with the antigen are made by the heavy chain and in particular by HCDR3. Moreover, HCDR3 are the only CDRs which are not structurally constrained to canonical structures [Barre et al., 1994].

In 1975 the invention of hybridoma technology by Milstein and Köhler [Kohler and Milstein, 1975] revolutionised the use of antibodies in cell biology, immunology and medicine. The technique allows the production of rodent monoclonal antibodies against a given antigen in virtually unlimited amounts. However, rodent antibodies are immunogenic in humans. Furthermore, it is difficult to make rodent monoclonal antibodies against highly conserved antigens, or human monoclonal antibodies, especially against human self-antigens. For therapy of human tumors, the efficacy of murine antibodies appears to be hindered by additional obstacles, including the induction of a human anti-mouse antibody (HAMA) response [Frodin et al., 1992 ; Maher et al., 1992 ; Berkower, 1996]. An avenue towards the solution of the HAMA problem is to use human antibodies. In principle, however, anti-idiotypic response could still develop upon repeated administration of human antibodies and has indeed been documented in patients [Isaacs et al., 1992 ; Schneider et al., 1993]. Human antibodies can be generated by humanisation of murine antibodies, for example by CDR grafting [Jones et al., 1986 ; Riechmann et al., 1988], by immunisation of transgenic mice expressing human antibodies [Taylor et al., 1992 ; Tuaillon et al.,

1993 ; Lonberg et al., 1994 ; Taylor et al., 1994 ; Jakobovits, 1998], or by using antibody phage technology [Winter et al., 1994].

Phage antibody technology appears to offer a solution, as human antibody fragments can be isolated from repertoires of fragments displayed on filamentous bacteriophage [Winter et al., 1994]. The process does not require immunisation of humans, and antibody fragments can be made against both foreign and human self-antigens. Phage display is a powerful technology which allows to select a particular phenotype (for example a protein which specifically bind to an antigen) from repertoires of proteins displayed on phages. The technology was originally described in 1985 by Smith [Smith, 1985; Smith, 1991] who presented the use of the non-lytic filamentous bacteriophage fd for the display of specific binding peptides on the phage coat. The power of the methodology was further enhanced by the groups of Winter [McCafferty et al., 1990] and Wells [Lowman et al., 1991], who demonstrated the display of functional folded proteins on the phage surface.

The technology is based on the principle that a polypeptide (capable of performing a function, typically the specific binding to a target of interest) can be displayed on the phage surface by inserting the gene coding for the polypeptide in the phage genome. Doing so, genotype and phenotype are coupled in a single unity.

It is possible to create repertoires of phages, called phage display libraries, in which the proteins displayed on each phage are slightly different from each other. If one is able to purify from this large phage repertoire a phage particle by virtue of the phenotype (for instance the binding specificity) displayed on its surface, one also isolates the genetic information coding for the binding protein, and can amplify the corresponding phage by bacterial infection. As an example, let us consider the selection of a binding specificity from a repertoire of binders (Figure 2.3.1).

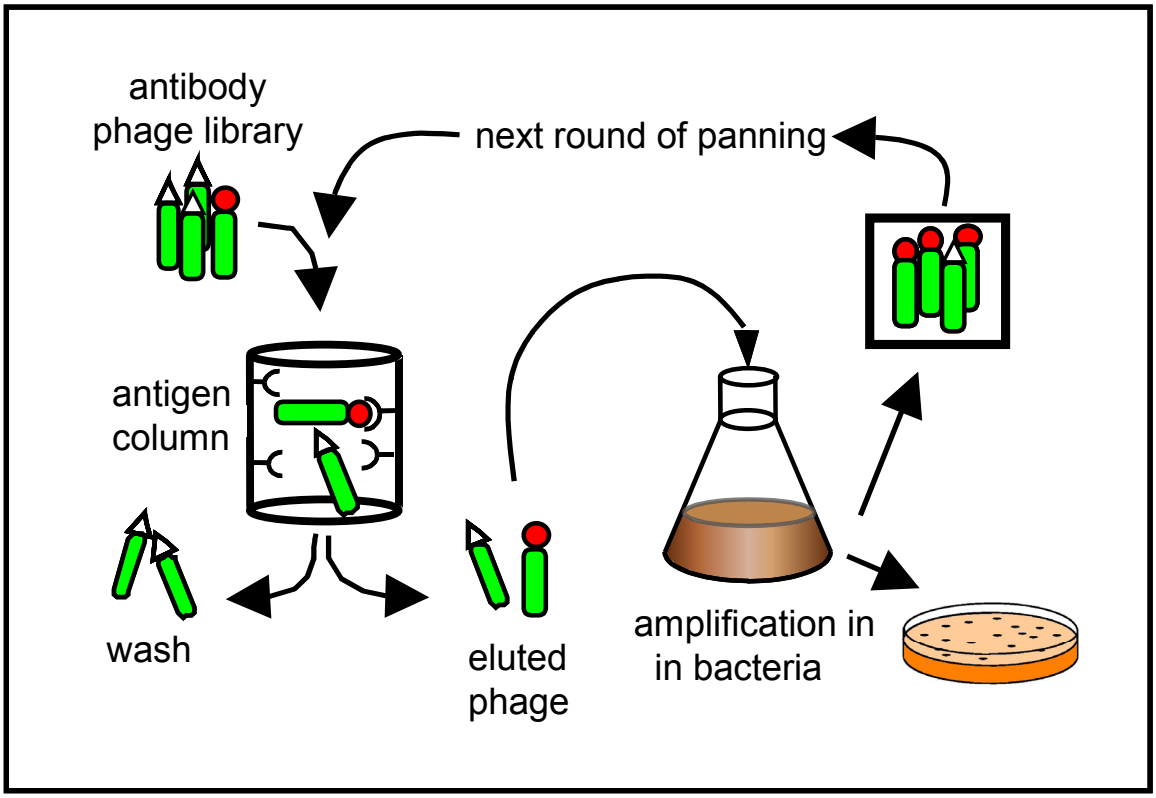


**Figure 2.3.1**

Schematic representation of a round of panning. A phage display library is applied onto a solid support, coated with the antigen of interest. Only some binding specificities (circles) are retained on the affinity support and can selectively be eluted after washing. The eluted phage can be amplified by bacterial infection and used for a further round of panning. Alternatively, its genetic material can be used for the expression of the corresponding recombinant polypeptide in a suitable over-expression system.

The library on phages is biopanned against the antigen of interest; unbound phages are discarded, specifically binding phages collected and amplified in bacteria. Several rounds of selections can be performed (typically 2-4 rounds of panning using antibody phage libraries). As a consequence, even very rare phenotypes present in large repertoires can be selected and amplified from a background of phages carrying undesired phenotypes. Phage remains infective when treated with acids, bases, denaturants and even proteases. These properties allow a variety of selective elution protocols and have also been used for applications other than selection for binding,

such as the selection of proteins with altered thermal stability [Bothmann and Plückthun, 1998; Kristensen and Winter, 1998 ] or the selection of catalytically active enzymes [Pedersen et al., 1998; Demartis et al., 1999]. The possibility to amplify in bacteria the phages selected during panning allows to enrich the pool of phages with the desired phenotype.

Filamentous phage infect strains of *E. coli* that harbour the F conjugative episome. Phage particles infect bacteria by attaching to the tip of the F pilus, and by translocating the phage genome (a circular single-stranded DNA molecule) into the bacterial cytoplasm. The genome is replicated involving both phage- and host-derived proteins, and packaged into elongated ("filamentous") viral particles of approximately 6 nm diameter and 900 nm length. For a review on phage biology, see [Webster, 1996].

Filamentous phage particles are covered by approximately 3000 copies of a small major coat protein (pVIII). Few copies of the minor coat proteins pIII and pVI are displayed at one extremity of the phage particle, while pVII and pIX are present at the other extremity. The minor coat protein pIII, the product of gene III, is displayed in 3-5 copies and mediates the adsorption of the phage to the bacterial pilus. Peptides and/or proteins have been displayed on phage as fusions with the coat proteins pIII [Smith, 1985 ; Parmley and Smith, 1988] or pVIII [Greenwood et al., 1991]. Display of proteins encoded by a cDNA library as carboxy-terminal fusion with the minor coat protein pVI has also been reported [Jespers et al., 1995].

The first peptides and proteins were displayed on phage using phage vectors (essentially the phage genome with suitable cloning sites for pVIII or pIII fusions and an antibiotic resistance gene) , see Figure 2.3.2

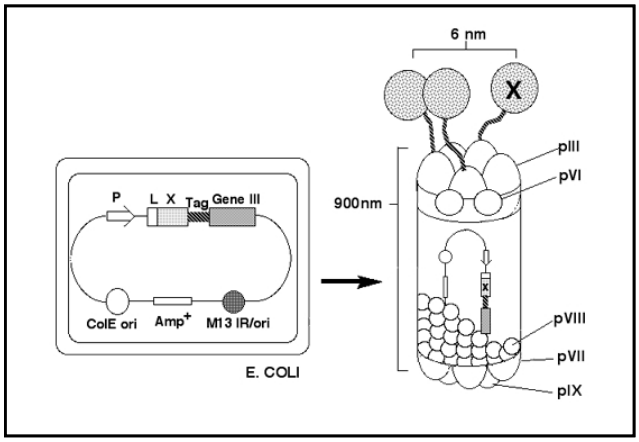


**Figure 2.3.2**

Schematic representation of a phage or phagemid vector, carrying a promoter P, a leader peptide L, a gene X, a tag sequence, fused to filamentous phage geneIII. This gives rise to a phage particle, displaying the protein "X" fused to the N-terminal extremity of the geneIII product pIII, at the tip of the phage. The peptidic tag is important for the efficient recognition of the product with an anti-tag antibody. (pIII, pVI, pVII, pVIII, pIX: phage coat proteins)

Phage vectors carry all the genetic information necessary for phage life. With pIII fusions in phage vectors, each pIII coat protein displayed on phage would be fused to the heterologous polypeptide. Using phage vectors, most peptides and folded proteins can be displayed as pIII fusions, while only short peptides containing no cysteine and 6-7 residues give rise to functional phage when displayed as pVIII fusions [Iannolo et al., 1995]. Phagemids, a more popular vector for display, are plasmid vectors that carry gene III with appropriate cloning sites and a phage packaging signal [Bass et al., 1990 ; Garrard et al., 1991; Hoogenboom et al., 1991 ]. Phagemids encoding the polypeptide-pIII fusion are preferentially packaged into phage particles using a helper phage that contains a slightly defective origin of replication, such as M13K07 or VCS-M13, which supplies all the structural proteins. The resulting phage particles may incorporate either pIII derived from the helper phage or the polypeptide-pIII fusion, encoded by the phagemid. Depending on the type of phagemid, growth conditions used and the nature of the polypeptide fused to pIII, ratios of (polypeptide-pIII):pIII ranging between 1:9 and 1:1000 have been reported [Bass et al., 1990 ; Bothmann and Plückthun, 1998 ; Kristensen and Winter, 1998 ; Sieber et

al., 1998; Demartis et al., 1999 ]. Furthermore, the proteolytic cleavage of protein-pIII fusions have been reported, contributing to further elevated levels of full-length wild type pIII ([McCafferty et al., 1990 ; McCafferty, 1996]). Besides N-terminal fusions full-length pIII, fusions to sites downstream of gene III have been reported [Barbas et al., 1991; Lowman et al., 1991 ; Krebber et al., 1997 ].

The binding antibody fragments derived from phage display technology can be secreted into the bacterial periplasm and culture medium [Better et al., 1988; Skerra and Plückthun, 1988 ] and can be produced in a large scale [Carter et al., 1992 ; Pack et al., 1993].

### 2.3.2 Monoclonal anti-EDB antibodies, from BC-1 to L19

After the discovery of the EDB domain in the laboratory of Luciano Zardi in 1987 [Zardi et al., 1987] attempts were made to raise monoclonal antibodies specific for EDB-containing fibronectin ($B^+$-FN) and antibodies specific only for the EDB-negative splice form. The resulting monoclonal antibody BC-1 which recognizes human $B^+$-FN was used in the immunohistochemical analysis of angiogenesis [Castellani et al., 1994]. However, this antibody showed species-specificity as it could not bind to mouse and chicken $B^+$-FN, thus precluding its usage in animal angiogenesis models. Furthermore, it does not recognize EDB directly but an epitope spanning over FN typeIII repeat $III_7$ and EDB. Nevertheless, the tumor targeting potential of BC-1 was assessed in nude mice bearing human tumor implants and showed to be promising [Mariani et al., 1997a; Mariani et al., 1997b]. The monoclonal antibody IST-6, specific only for EDB-negative fibronectin, together with BC-1 demonstrate the conformational change which occurs in the structure of FN when EDB is inserted.

In 1996, two affinity-matured monoclonal antibodies against EDB were derived from phage display selection [Carnemolla et al., 1996] using a synthetic human scFv phage library (this library encodes for antibodies with human VH chains, randomized in the loop region of CDR3 and linked to a human light chain) (see Figure 2.3.3) [Nissim et al., 1994] and were further characterized for their binding and tumor-targeting properties [Neri et al., 1996a]: scFv(CGS-1) was derived from a clone which resulted from 3 rounds of panning against a FN fragment containing the complete typeIII repeats 7B89 and further selection of an affinity-maturation library based on this clone (randomization of positions in the CDR3 of the light chain variable domain). scFv(CGS-2), likewise, resulted from panning against the recombinant EDB domain alone.

scFv(CGS-1) and scFv(CGS-2) were shown to recognize two distinct epitopes on EDB and to recognize EDB comprising fibronectin in tumoral tissue, as demonstrated in immunohistochemical studies [Carnemolla et al., 1996]. The scFv(CGS-1) and scFv(CGS-2) were reported to target tumors of F9 teratocarcinoma-grafted mice,

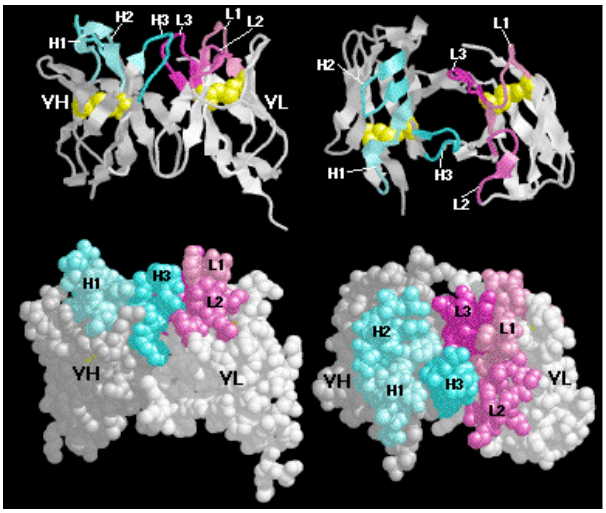


**Figure 2.3.3**

Structure of a scFv antibody fragment from two different views (left and right): The structures are depiced as backbone- (upper half) and space-fill representation (lower half), respectively. VH CDR determining regions 1, 2 and 3 are marked as H1, H2 and H3, respectively. VL CDR determining regions 1, 2 and 3 are marked as L1, L2 and L3, respectively.

especially dimeric scFv $(CGS\text{-}1)_2$, which was modified with a homodimerization tag [Pack et al., 1993], has been shown to have considerably better tumor targeting properties than its monomeric counterpart [Neri et al., 1997].

In 1998, Francesca Viti and Alessandro Pini, aiming at a highly diverse library of functional antibodies with good expression and performance, constructed a new antibody phagemid library (termed ETH-1 library) [Pini et al., 1998]. Combinatorial diversity was introduced into the CDR3 regions of the heavy chain (VH DP47 germline gene) and light chain (Vκ DPK22 germline gene) by means of degenerate primers (Figure 2.3.4)

At the C-terminal end of the scFv a phosphorylation sequencence and two versatile tags (FLAG tag and $His_6$ tag) were appended [Neri et al., 1996b] allowing easy detection and purification. In this library 8 amino acid positions (in the CDR3 domains) were randomized giving rise to a theoretical library size of ca. $2.5 \times 10^{10}$. Due to the limitation of electroporation efficiency, a real library size of ca. $3 \times 10^{8}$ was obtained. This library expressed functional scFv fragments (88% of the clones tested) and performed well upon panning against numerous different antigens [Pini et al., 1998].

Panning of this library against EDB resulted in several binders of moderate affinity ($K_D$ = $10^{-7}$ - $10^{-8}$ M) which performed well in immunostaining EDB containing fibronectin in glioblastoma multiforme, an aggressive neoangiogenic brain tumor.

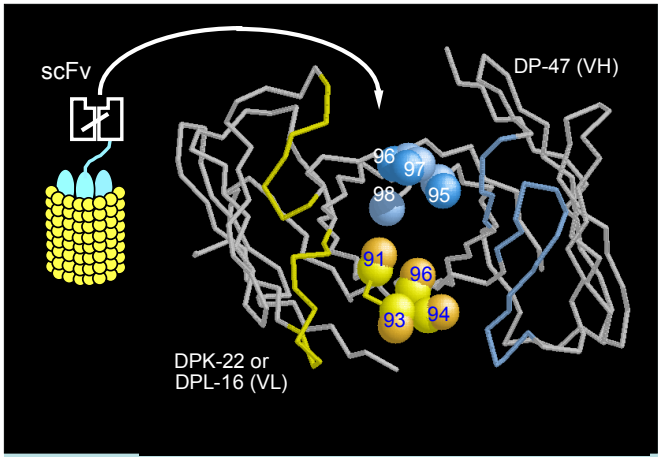


**Figure 2.3.4**

VH CDR3 and Vκ CDR3 amino acid residues subjected to random mutations are numbered and depicted in blue and yellow, respectively. Cβ atoms of their side chains are depicted in darker color. In gray, CDR1 and CDR2 sites are shown which can further be mutated to improve affinity.

Using one of these clones (termed "E1") as a scaffold, an affinity maturation library was created by randomizing 3 amino acid residues in the CDR1 and the CDR2 of VH, respectively. This library with the size of 4 x $10^8$ was selected for binding to EDB (2 rounds of panning) and a binder with 27 fold higher affinity compared to E1 could be obtained (termed H10) [Pini et al., 1998]. Further affinity maturation by randomizing two further amino acid residues of the VL chain and selection of the resulting phage display library for EDB binding finally yielded a high-affinity clone of $K_D$ = 54pM, termed L19. [Pini et al., 1998 ; Viti et al., 1999].

The enhanced binding affinity of L19 is mainly due to a lower kinetic dissociation constant ($k_{off}$ <$10^{-6}$ $s^{-1}$, compared to $k_{off}$ = 3.5 x $10^{-3}$ $s^{-1}$ of E1). The enhanced binding affinity of L19 as well as valence (monomeric scFv vs. dimeric scFv) lead also to improved targeting of tumoral angiogenesis, as was shown in biodistribution studies in F9 murine teratocarcinoma bearing nude mice by Viti et al. [Viti et al., 1999].

Furthermore, L19 was radioiodinated with $^{125}I$ and biodistribution using radioiodinated L19 demonstrated its rapid specific localization around tumor blood vessels [Demartis et al., 2001]. Recently, first immunoscintigraphy trials for the imaging of primary tumors and metastatic lesions in cancer patients have started, using L19 labeled with the γ-emitter $^{123}I$ [Santimaria et al., 2003], showing selective targeting of tumor lesions in aggressive types of lung cancer and colorectal cancer. Thus, the selective localization of radiolabeled L19 promises its future use in diagnostic oncological applications.

### 2.3.3 L19 derivatives and L19 fusion proteins for the treatment of angiogenesis-associated cancer

Molecules that selectively target and occlude new blood vessels would be useful for the diagnosis and treatment of pathologies associated with angiogenesis. One therapy approach is represented by the targeted delivery of photosensitizers, i.e. molecules that upon irradiation and in the presence of oxygen release diffusible agents, such as toxic singlet oxygen or reactive radicals. Birchler et al. chemically coupled L19 to a photosensitizer [Birchler et al., 1999a]. In a rabbit model of ocular angiogenesis irradiation with infrared light demonstrated the selective occlusion of ocular neovasculature and promotion of apoptosis of the corresponding endothelial cells. For tumor therapy, this strategy is limited by the accessibility of the targeted locus for the light of the required wave length.

Radioimmunotherapy is another possible therapeutic targeting strategy. In order to be successful, a high dose of a toxic radionuclide, preferably an α-emitter with sufficiently long half-life, must specifically be targeted to the tumor neovasculature [McDevitt et al., 2000]. Attempts in this respect have been made in our lab by labeling L19 with $^{211}$At, an α-emitter of short half-life [Demartis et al., 2001].

An alternative to direct damaging of neovascularizing tissue by radionuclides would be the site-specific delivery to the angiogenic site of effector molecules (e.g. peptides or proteins) fused to L19. Several L19 fusion proteins have been and are being produced in our laboratory:

An L19 - tissue factor (TF) fusion protein was produced, based on the concept that thrombosis of tumor vessels may stop the supply of nutrients and oxygen to tumor cells, thereby causing their death. It was shown that L19-TF selectively targets tumor blood vessels *in vivo* and that it mediates the complete and selective infarction of three different types of solid tumors in mice. At the highest doses administered, complete tumor eradication was observed in 30% of the mice treated, without apparent side effects [Nilsson et al., 2001].

Another approach is based on the observation that systemic treatment of patients with cytokines, such as IL-2, TNFα, GM-CSF or IL-12 can render some non-immunogenic tumors immunogenic, thereby activating a protective immunity [Ruef and Coleman,

1990; Tsung et al., 1997; Rosenberg et al., 1998]. However, systemic administration of cytokines is often associated with severe toxic side effects that make it impossible to administer an effective dose and to reach high concentrations at the site of the tumor. Fusion of cytokines to tumor-targeting antibodies like L19 may overcome these drawbacks. In fact, in the past decade, several groups have reported on different antibody-cytokine fusion proteins for different tumor associated antigens. These novel proteins were shown to retain both antibody and cytokine functions and to show superior anti-cancer activity as compared to equivalent amount of free cytokines.

In our laboratory, a fusion protein in which the murine p40 and p35 domains of IL-12 were sequentially fused to L19 was produced. This fusion protein exhibited potent antitumor activity, markedly superior to that of untargeted IL-12, in a mouse lung-metastasis model and in two different subcutaneous tumor models established in immunocompetent mice [Halin et al., 2002a]. Moreover, in mice treated with IL12–L19, the tumor environment became infiltrated with macrophages, lymphocyte-activated killer (LAK) cells, NK cells, and T lymphocytes.

Furthermore, Carnemolla et al. have recently shown that a fusion protein of L19 and interleukin 2 (L19-IL2) mediates the selective delivery and concentration of IL-2 to tumor vasculature, thereby leading to a dramatic enhancement of the therapeutic properties of the cytokine [Carnemolla et al., 2002]. Immunohistochemical analysis of tumor infiltrates demonstrated a significantly higher number of T lymphocytes, NK cells and macrophages, as well as increased interferon γ (IFNγ) accumulation, in tumors from animals treated with L19-IL2 compared to tumors from control groups.

## 2.4 Tumor therapy: From antibodies to low-molecular weight synthetic binders

### 2.4.1 Antibodies – advantages and drawbacks

As already mentioned in the preceding chapter, nowadays specific antibodies against almost any type of antigen with excellent binding properties can easily be produced by either hybridoma or phage display technology. High affinity towards the target antigen located at the site of the tumor is a prerequisite for good tumor targeting. Therefore, antibodies seem to be extraordinarily suited for therapeutic targeting approaches. Adams et al. examined tumor targeting properties of 3 different scFv ($K_D$ = 3.2 x $10^{-7}$ M, $K_D$ = 1.6 x $10^{-8}$ M and $K_D$ = 1.0 x $10^{-9}$ M) directed against the same epitope of the HER2/neu tumor marker [Adams et al., 1998] in mice xenografted with a human tumor. This study revealed an apparent affinity threshold that must be overcome in order to achive specific tumor accumulation. This observation could also be confirmed by studies in our research group when comparing the targeting properties of the anti-EDB scFv fragments E1 ($K_D$ = 4.1 x $10^{-8}$ M) and L19 ($K_D$ = 5.4 x $10^{-11}$ M), binding to the same EDB epitope [Tarli et al., 1999; Viti et al., 1999]. They showed that the high-affinity scFv L19 was able to target the tumoral neovasculature significantly better than E1. The antibody format used (Figure 2.4.1) constitutes another important function for targeting:

Multivalent antibodies (like IgG, SIP (small immunoprotein) or mini-antibodies [Li et al., 1997], $F(ab)_2$, $(scFv)_2$) usually have apparently higher affinity constants than their monovalent counterparts due to an effect termed avidity [Crothers and Metzger, 1972] which means that bivalent antibodies can simultaneously bind to 2 antigen molecules. Furthermore, rebinding can take place since upon dissociation of the antibody from the antigen at one or both binding sites, the antibody is likely to rebind again to the antigen before complete dissociation occurs (Figure 2.4.2)

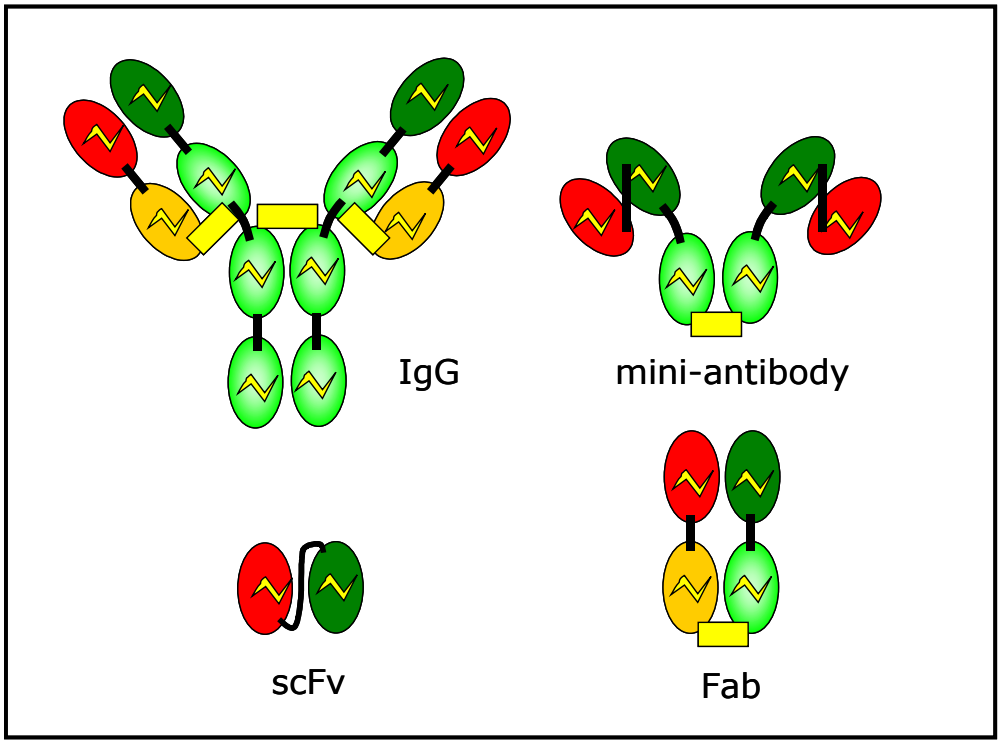


**Figure 2.4.1**

**Schematic representation of different formats of antibodies and antibody fragments**.

Heavy chains are depicted in dark/light green, light chains are depicted in red/orange. Variable regions are depicted in red and dark green, respectively; constant regions are depicted in light green and orange, respectively.

= intradomain disulfide bond = interdomain disulfide bond(s)

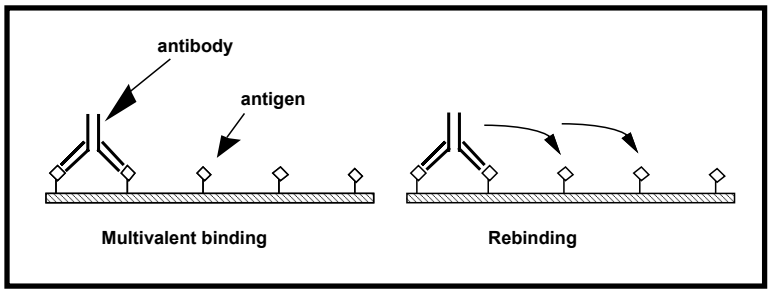


**Figure 2.4.2**

The effect of avidity on antibody binding to an antigen can be due to multivalent binding and/or rebinding

In 1993, Adams et al. showed experimental evidence of this effect when comparing the biodistribution of a $(scFv)_2$ diabody with the corresponding monovalent Fab fragment, both having almost the same molecular weight [Adams et al., 1993]. As expected, the diabody showed better tumor uptake than the Fab fragment.

Moreover, the size of the antibody plays a crucial role for its targeting properties as it influences drastically its pharmacokinetic properties [Hakimi et al., 1991; Stephens et al., 1995].

Here, two effects come into play:

First, body clearance of immunoprotein constructs of different molecular weight is performed mainly by the kidney which means that the heavier complete IgG immunoglobulins are removed much more slowly from the plasma by renal clearance than scFv fragments [Yokota et al., 1992]. The influence of rapid clearance rate has been underlined by a study of Adams et al. in which they performed biodistributions in normal and in anephric mice [Adams et al., 1998]. This effect gives rise to much better tumor/blood ratios upon targeting and cannot be overcompensated by the somewhat higher *in vivo* stability of IgGs compared to other antibody fragments: When comparing biodistributions experiments in F9 tumor bearing mice using radioiodinated L19 $(scFv)_2$, L19 SIP and L19 IgG1, Borsi et al. demonstrated that L19-SIP offers the best compromise between molecular stability, clearance rate and tumor accumulation [Borsi et al., 2002]. Using the SIP, radioactive uptake in tumors was 2-5 times higher than with $(scFv)_2$, reaching a maximum 4-6 hr after injection. In contrast, the accumulation of IgG1 in tumors constantly rose during the experiments. However, due to its slow clearance, the IgG1 tumor-blood ratio after 144 hr was only about 3 compared to a ratio of 10 for the $(scFv)_2$ and 70 for the SIP. Thus, for whole IgGs, the tumor/blood ratio is typically poor because of slow blood clearance. In contrast, scFvs typically give rise to particularly high tumor/blood ratios, even though the total amount of antibody localizing on the tumor is rather low, since scFvs clear rapidly from the blood. Several other comparative studies on tumor localization of radiolabelled intact IgGs and smaller fragments in mice, have described the advantages and disadvantages of differently sized constructs in terms of tumor targeting [Yokota et al., 1992; King et al., 1994; Behr et al., 1995].

The second effect of the relatively high molecular size (ranging between ca. 25 kDa for a scFv fragment and 150 kDa for a whole IgG) of antibodies also consitutes one of their major drawback for therapeutic targeting applications: Poor extravasation and poor tissue penetration efficacy, for penetration efficacy and size are inversely correlated [Yokota et al., 1992]. Since the antigen is most likely localized in the abluminal site of the vessels, a multi-compartment situation occurs, where extravasation into the perivascular space has to precede antibody binding to its antigen.

Though scFv fragments of the size of ca. 25 kDa only have 1/5 of the mass of a complete IgG molecule and are therefore able to extravasate more easily and diffuse deeper into the tumor than IgGs [Jain and Baxter, 1988; Yokota et al., 1992] their molecular weight still is by orders of magnitude higher than that of low-molecular weight compounds. The high interstitial pressure will also favor the diffusion and tumor penetration of smaller molecules.

For this reason, in order to achieve a better tumor/non-tumor ratio, so-called pretargeting strategies have been developed in which first a tumor-antigen specific antibody fused to another binding effector is administered. The antibody is then allowed to accumulate at the tumor site and to be cleared from the rest of the body. At a timepoint, when tumor/non-tumor ratio is optimal, a small molecule which binds to the other binding effector and which is rendered cytotoxic (e.g. by an attached radiolabel) is given to the patient. This compound then binds to its binding partner at the tumor site with high affinity but is also cleared fast from the blood by renal clearance, thereby reducing background cytotoxicity to a minimum.

Examples for this pretargeting strategies are e.g. antibody – avidin resp. antibody – streptavidin fusions combined with radiolabeled biotin [Paganelli et al., 1991a; Paganelli et al., 1991b] , (Avicidin™, NeoRX Corporation, Seattle, U.S.A.) which is presently in clinical evaluation for radioimmunotherapy (RIT). Other pretargeting strategies based on the (strept)avidin – biotin system have been studied, e.g. a three-step avidin-biotin pretargeting approach aiming at improving the tumor/non-tumor ratio of radioactivity in RIT of malignant glioma patients [Paganelli et al., 1999; Grana et al., 2002].

Immunogenicity of proteins (in this case of (strept)avidin) may develop when administered to the patient, finally impairing the therapeutic use. This, of course, also applies for antibodies:

Typically, monoclonal antibodies derived from hybridoma technology are of murine origin. For therapy of human tumors, the efficacy of murine antibodies is severely hindered by their immunogenicity, leading to the induction of a human anti-mouse antibody (HAMA) response [Frodin et al., 1992; Berkower, 1996]. Even the use of human antibodies – which could e.g. also be made by humanization of murine antibodies [Jones et al., 1986; Carter et al., 1992] - cannot exclude an anti-idiotypic response upon repeated administration to humans.

Furthermore, as polypeptides, antibodies cannot be rendered an orally available drug which would be the formulation best accepted by the patient, but have to be injected intravenously.

Finally, antibody production is very expensive compared to the production of a low-molecular weight compound, also as it has to meet strict quality control (GMP production) in order not to harm the patient. Whilst antibodies can so far only be produced in small amounts, rendering them expensive therapeutics, the production of organic molecules can easily be scaled up. Moreover, small molecules as drugs do usually not give rise to immunogenicity.

### 2.4.2 High-affinity low-molecular weight synthetic binders

#### 2.4.2.1 Drug discovery at present

A low-molecular weight drug has to meet a set of different requirements in oder to be a useful drug: It has to be able to be formulated in a stable, orally active manner. It eventually has to overcome barriers in the body like lymphatic barriers, endothelial barriers, blood-brain barriers, and blood-retina barriers which are all blocking the movement of the molecule to the appropriate site of action. Furthermore, the body will metabolize, conjugate and finally eliminate it to a different extent. Sufficient selectivity for the site of action is required to yield an acceptable benefit. These requirements are the reason why it still takes more than a decade of research time for bringing a drug to the market, while, in parallel, many more drugs fail [Drews, 2000].
In principle, 4 different strategies lead to the discovery of new low-molecular weight drugs:

1) Modification of the structure of known drugs
2) Exploiting the pool of natural (low-molecular weight) products
3) Modification of the structure of an enzyme substrate or a receptor ligand (ligand-based design)
4) Structure-based design

The first two points represent the history of drug discovery until the 1970s whereas the latter 2 points emerged in the past 15 years and are nowadays gaining importance.
Examples for modified known drugs are e.g. angiotensin converting enzyme (ACE) inhibitors [Dina and Jafari, 2000] and quinolone antibiotics [Bronson and Barrett, 2001].
Making use of the natural pool of drugs is quite an archaic but also a quite effective way to find new drugs. Many of the early drugs came from plant sources or microorganisms. Traditional medicines contributed largely to the non-random discovery of these drugs. Examples in that respect are e.g.: Macrolides, β-lactames, aminoglycosides and tetracyclins as antibiotics [Wise, 1999]; digoxin for the treatment of angina pectoris [Ravi Kumar and Kurup, 2000]; mevinolin (lovastatin) as

a medicament for atherosclerosis [Klungel et al., 2002]; vinca alcaloids, anthracyclins, etoposide, mitomycin and taxol as anti-cancer drugs [Hanauske, 1996]; cyclosporin as an immunosuppressive [Jacobsohn, 2002]. The category of drugs derived from natural products and derivatives is extensive.

This sourcing of drugs from natural products has changed over the past 5-10 years, with increasing numbers of drugs coming from chemical libraries rather than from natural products [Drews, 2000]. The reason for this is that over the last decades, pharmaceutical companies and chemical companies have established significant inventories of small molecules. These inventories were nevertheless not exploited as potential sources of drugs because of the absence of broad-based, automated screening methods and biologically relevant assays. This has changed dramatically in the last decade and today one can come up with an extensive list of potential drug candidates coming from the screening of chemical libraries, thereby creating the basis for significant new technologies in the area of high-throughput screening and combinatorial chemistry. The third approach to drug discovery, the modification of natural substrates, so far had less success in yielding new drugs. These include adenosine deaminase inhibitors, renin inhibitors, angiotensin receptor antagonists and cholecystokinin B (CCK-B) receptor antagonists [Chen and McLennan, 1993; Roques and Noble, 1996; Dina and Jafari, 2000]. While this is another valid approach for drug discovery, one subset of this approach - peptidomimetics as drugs -continues to be characterized by poor pharmacokinetic properties and administration problems. One the other hand, chemical libraries have successfully been created and screened leading to receptor agonists and enzyme inhibitors (for a review, see: [Dolle, 1998; Floyd et al., 1999]):

G-Protein coupled receptors: substance P (NK), oxytocin and vasopressin, bombesin/GRP, bradykinin, cholecystokinin, NPY, adrenergic/serotinergic/ dopaminergic; Chemokine/lymphokine receptors: MCP-1, CCR-5, IL-8; Glutamatergic receptors: AMPA, NMDA, m-Glu; Nuclear receptors: ER, PR, PPAR/RXR-RAR; Integrins: gP IIb/IIIa. Enymes: Asp proteases: renin, HIV-1; Ser proteases: thrombin, factor Xia; Matrix metalloproteases: MMP 1-13; Kinases: cyclin dependent, tyrosine, ser/thr; Phosphodiesterases; Polymerases/reverse transcriptases; Topoisomerases; Ion channels: calcium (L, N), sodium, K/ATP.

Rational drug design is most often thought of as structure-based and computer-aided drug design [Gane and Dean, 2000]. This approach to drug discovery started in the early 1980s and is driven by the need of drug discovery to find agents that are more specific for a particular molecular target, since this leads to increased efficacy, reduces side effects, and thus yields a drug against a particular pathology. Specificity can be achieved through the use of hydrogen bonds, ionic interactions, hydrophobic interactions, or best by exploiting the overall three-dimensional structure. Whereas achieving specificity is less problematic if repeating units can be used (large molecules like proteins (e.g. antibodies) or DNA (e.g. antisense specificity), it is quite difficult to achieve specificity with small molecules. So far, most success has been achieved with enzymes in this respect [Klebe, 2000].

On the other hand, it is known that several naturally occuring low-molecular weight molecules bind to their macromolecular targets in an extremely specific manner: steroids, leukotrienes, nucleosides, mononucleotides, catecholamines, excitatory amino acids, or even acetylcholine. This provides the hope that small molecules can yield the desired degree of selectivity necessary to be useful as a drug. Here, focused high-throughput organic synthesis and screening come into play, as they have drastically advanced in speed, quality, and in diversity of sources and targets.

#### 2.4.2.2 Combinatorial Chemistry and High-throughput screening

##### 2.4.2.2.1 Combinatorial Chemistry

Combinatorial chemistry, i.e. the creation of compounds resulting from the combinatorial synthesis of smaller building blocks, thereby generating huge compound libraries, has been pioniered by Merrifield with his solid-phase peptide syntheses in the 1960s [Merrifield, 1963].

From this time on, great efforts have been made in solid-phase chemistry, from peptide synthesis to oligonucleotide synthesis and chemical synthesis of small building blocks [Patchornik and Kraus, 1970; Camps et al., 1971; Leznoff and Wong, 1972; Frechet, 1981](Camps et al. even applied solid-phase synthesis to the pharmaceutically relevant benzodiazepine system [Camps et al., 1974]).

In the 1980s Frank and coworkers synthesized collections of oligonucleotides and peptides on circles of cellulose paper [Frank et al., 1983]. Geysen et al. prepared a library of peptides [Geysen et al., 1984] on functionalized polypropylene pins by immersing them sequentially into various solutions of activated amino acids held in the wells of a microtiter plate, whereas Houghten synthesized a library of 260 peptides [Houghten, 1985] in polypropylene mesh containers encapsulating polystyrene resin, a strategy now known as the "tea-bag" strategy. Both the pin and the “tea-bag” techniques gained wide popularity and led to new generations of improved technologies for combinatorial chemistry: Researchers at Affymax reported very large spatially addressable libraries on glass chips using photolithographic techniques in conjunction with photolabile protecting group chemistry [Fodor et al., 1991; Cho et al., 1993].In 1992, Bunin and Ellman [Bunin and Ellman, 1992] reported another synthesis of a benzodiazepine library using the "multi-pin" technology pioneered by Geysen. At about the same time, a group of scientists at Parke-Davis reported the construction of hydantoins and benzodiazepines using a semiautomated robotic synthesizer [DeWitt et al., 1993]. In addition, a Chiron group reported the synthesis of a library of peptoids [oligo(N- substituted glycine)] and a robotic synthesizer of such compounds [Zuckermann et al., 1992]. In the meantime, an elegant and ingenious strategy for combinatorial synthesis was proposed and

demonstrated. This strategy called "split synthesis" or "split and pool" was introduced by Furka and coworkers in 1988 [Furka et al., 1991] and independently by the groups of Lam [Lam et al., 1991] and Houghten [Houghten et al., 1991]. These strategies led to the concept of "one bead-one compound" and opened a way to the simultaneous synthesis of millions of on beads with unprecedented rapidity. As elegant as it is, this method left much to be desired in terms of structure deconvolution and quantity of material produced. To solve the first problem, a number of encoding strategies were developed based on technologies ranging from DNA sequences to polychlorinated aromatics as well as nonchemical encoding methods such as radiofrequency tagging and two-dimensional bar-coding. From the early 1990s onwards, the chemical literature exploded with reports addressing all aspects of combinatorial synthesis, including solid-phase chemistry, encoding strategies and molecular diversity. In the late 1990s alternative strategies were investigated, and an interesting compromise between solid-phase and solution-phase chemistry was found with polymers which are soluble in certain solvents but can be precipitated efficiently in others [Gravert and Janda, 1997]. Thus the reactions on such polymers are carried out in homogeneous solution while the convenience of purification via a simple filtration is maintained. In a highly efficient extension of this principle, Curran and coworkers [Studer et al., 1997] developed a number of fluorocarbon tags which allow extraction of tagged compounds into a three-phase separation system (aqueous, organic, and fluorocarbon extraction phase). Today, many well-known solution-phase reactions have been demonstrated to perform equally well on solid phase [Hermkens et al., 1997]. This leads to high-speed purification procedures and higher yields of the desired products, giving rise to an increase in efficiency and productivity. Chemists were concerned with conferring small organic molecules more "lead-like" and"drug-like" structures. Of particular interest were new solid-phase synthetic strategies, new linkers for solid-phase chemistry [James, 1999], and new polymer-bound reagents [Bhattacharyya, 2000].

Synthesizing millions of compounds randomly was a new challenge to the chemists of biotechnology and pharmaceutical companies. Soon thereafter, however, one had to realize that a multitude of randomly created molecules not necessarily leads to a higher amount of hits coming from a high-throughput screen, not to mention the

immense costs involved. The prevailing approach today is based on both solution-phase and solid-phase chemistry applied in parallel or split-and-pool formats and directed at discrete and high-purity compounds [Weller et al., 1997; Zeng et al., 1998]. Initial-phase combinatorial chemistry is applied to discover lead compounds rapidly which are then subjected to lead optimization to produce drug candidates. The last part of the process is the domain of the medicinal chemists,who may also practice combinatorial strategies to achieve their goals. Thus, smaller focused libraries are carefully designed and synthesized, either in parallel or by the split-and-pool strategy using solution- or solid-phase chemistry. Thus, combinatorial chemistry has strongly influenced medicinal chemists who recognized its power in delivering the targeted compounds in a much faster way, and in acceptable quantities and purities.

2.4.2.2.2 High-Throughput Screening (HTS)

Over the past decade the most dramatic changes in drug discovery since the launch of antibiotic research in the 1940s took place: Dramatic progress in genetic engineering and molecular biology was made, along with the emergence of economical access to a multitude of biological reagents. The ability to explore specific macromolecular interaction in rapid biochemical and cellular screens became an economic reality [Petsko, 1996]. Targets and protein ligands were soon identified (e.g., the interleukins [Curfs et al., 1997]) that promised new forms of therapy by useful intervention with small molecules. Whole-animal or tissue models, which had been the main-stay of primary screening for decades were replaced by target-based (biochemical) and function-based (cellular) assays that reflected mechanistic responses rather than whole-organism behavior [Hertzberg and Pope, 2000]. Screening became specific and economical. With new biomolecular assays available and the ability to screen larger numbers of test compounds than the conventional pharmacological models, the management of pharmaceutical companies turned to the chemists with the need for the millions of compounds required as screening candidates. Here the first problem appeared: Designing a synthesis program that would ultimately yield a drug-like hit that interferes at a biological target is an difficult task when there is no chemical structural precedence [Lahana, 1999]. At the beginning, this "random screening"

approach was not very well received by scientists who better liked more targeted research activities. Available instrumentation was based on a variety of liquid handlers redesigned from diagnostic applications. In 1990, assay throughput was at best 100 compounds per week, but that level was sufficient to handle the limited compound collections available at that time (the compound archives of most companies were large but highly focused and low in diversity). Robotic systems were developed to accommodate the microplate and integrated test systems established [Merritt, 1998]. Targets and assays were primarily developed in-house, however, novel and more sensitive detection systems evolved externally that provided useful tools in optimal protocol development. New microplate designs were similarly created in the support industries that saved time and reagents in assay development and operation. Packaged data management systems evolved from companies such as Molecular Design (now MDL Information Systems) and Tripos. In 1993, MicroSource Discovery Systems pioneered the provision of test compounds in microplate format. This approach provided efficiency, economy, and diversity in a single product with full data support. It was based on the realization that even with a modest level of assay miniaturization, a few milligrams of a test compound were sufficient to support years of screening. By 1994, HTS had become an integral part of the drug discovery process [Broach and Thorner, 1996]. Large companies reorganized their internal structure to accommodate the multi-disciplinary character of this new technology. Assay miniaturization, integrated automation, compound acquisition, and data management became key activities in discovery operations.

HTS, as applied in the pharmaceutical industry today, refers to the integrated technologies that permit the rapid evaluation of millions of compounds annually in scores of bioassays in search for new therapeutic agents [Hertzberg and Pope, 2000]. There are three objectives: *de novo* discovery, hit development, and the preliminary assessment of the metabolism and toxicity of lead candidates. *De novo* discovery addresses the search for compounds that interact with a new biochemical or cellular target for which there is no precedence in chemical structure. The identification of both ligands and antagonists for most orphan receptors is an excellent example of such applications. The discovery of drugs against diseases that cannot be satisfactorily treated with existing therapies or for which no treatment is available is another. *De*

*novo* discovery requires the use of large compound collections with a structural diversity as broad as possible and bioassays that are specific for each target. The goal is to find one or more "hits" that can provide a chemical focus for further screening [Lam, 1997]. Such hits need not be at the activity level anticipated for a development candidate; structural information about a weak inhibitor is good enough [Carr and Jhoti, 2002]. *De novo* HTS generally addresses a broad spectrum of targets. Unlike *de novo* HTS, hit development begins with some level of chemical intuition. Such information may be derived from *de novo* programs, from historical data on the character of ligands or antagonists, or from computational analysis of the structure of the target receptor. This is the area where the use of high-throughput organic synthesis has provided the greatest benefit so far and has resulted in important advances in optimization of a lead and dramatic reduction in the time required for lead-development [Viswanadhan et al., 2002]. The demand for large and complex chemical libraries as test resources in HTS programs continues to grow to meet the dramatic increase in throughput potential. Compound collections that are truly diverse in skeletal and functional array are especially important. The classical approach in *de novo* discovery has been to use a well-designed and stocked compound collection. The structural richness of the numerous natural products and their derivatives that are commercially available must also be included, since these frameworks cannot be completely mimicked by current combinatorial chemistry. So far, it remains to be proven that high-throughput solid-phase and solution-phase chemical synthesis is a reliable source for the generation of the necessary diversity as a small but carefully selected collection of thousands of compounds might be a much better resource for drug discovery than a mass produced library with millions of components [Goodnow, 2001]. This obstacle might be overcome when large multitemplate based libraries are used for the screening. Thus, the main advantage of HTS, namely its applicability even for structurally undefined targets has to meet its most important drawbacks: occurrence of false positives, costs and usage of a sufficiently big and diverse chemical library.

### 2.4.2.3 Screening by NMR

#### 2.4.2.3.1 General techniques

In the recent years, nuclear magnetic resonance (NMR) based screening has gained importance in the field of drug discovery and is likely to play a major role in future drug discovery research [Diercks et al., 2001; Pellecchia et al., 2002]. NMR screening offers a multitude of advantages for drug research: (for a detailed review, see: [Zerbe, 2002])

NMR is able to detect even the slightest drug-target interaction ($K_D$ > 1mM) and is so far unprecendenced in its ability to reveal hits with low affinity which often escape conventional HTS. Moreover, NMR screening needs no bioassay development which is required for each biological target in conventional HTS, as it directly monitors drug-target interactions. Furthermore, NMR can be used to directly determine the binding constant of a drug-target complex (e.g. by titration) [Fielding, 2000]. Depending on the NMR technique used, drug-target interactions can be monitored on the drug or on the target. If the 3-dimensional structure of the target is known, direct predictions of the binding mode (so-called structure-activity reletionships (SAR)) can be made which are of great importance for the rational design of affinity-matured drugs. As it is predictable that 3D structures of target proteins are revealed more and more rapidly, SAR determined by NMR will become even more important.

On the other hand, NMR screening still has some considerable drawbacks:

Both the drug and its target (mostly a protein) must be soluble (in buffered aqueous solution) which cannot always be achieved. Furthermore, even if the sample throughput could dramatically be improved in the recent years thanks to reduced dead-times in sample-handling (e.g. by Flow-probes [Ross et al., 2000] and improved hardware, NMR still is considered to be a slow screening methodology. Furthermore, it is not a very sensitive method, therefore needing substantially high amounts of both drug and target, though recently developed Cryotube technology has greatly improved sensitivity (allowing to use less concentrated sample) [Ross et al., 2000].

Typically, for more elaborate screens quantities of proteins in the 100mg range are required [Marchioro et al., 2002].

Unfortunately, target proteins need to be produced recombinantly, preferably in bacterial expression systems, thus excluding heterologous and high-molecular weight proteins from being screened. Moreover, special problems occur for membrane-bound receptors like the pharmacologically relevant G-protein coupled receptors: These usually glycosylated proteins not only need to be produced but also be reconstituted in functional form in a membrane-mimicking environment.

While to date NMR is applied to protein targets with molecular weight < 30 kDa, NMR screening is likely to be extended in the future to a broader range of larger targets (e.g. receptors).

To date, different NMR screening approaches are used for drug discovery. Ligand-based approaches, in which observable effects on the ligand are measured so far play a major role compared to target-based screening.

In principle, three types of NMR experiments can be defined: The target-based observation chemical shift changes induced by the binding event (e.g. HSQC screening with $^{15}N$ / $^{13}C$ labeled targets [P. J. Hajduk et al., 1999a; P. J. Hajduk et al., 1999b; Hajduk et al., 2000c], and ligand-based experiments which either detect the large mass- and thus mobility differences of the ligand upon binding to the target or exploit differences in the relaxation efficiency of ligand and ligand-target complex [Peng et al., 2001]. For screening purposes, of course only fast NMR experiments can be considered. While experiments based on the ligand (like e.g. 1D-$^{1}H$-NMR line-broadening assays) or experiments used to determine differential diffusion or relaxation rates only can reveal neat binding, target-based experiments directly can provide direct information about the site of binding, which in turn can help reducing the number of false positive binding events (However, a new ligand-based method has been introduced by Jahn et al. [Jahnke, 2002] which yields some spatial resolution by site-specific introduction of spin-labels into the target protein). Especially suited in this respect is the [$^{15}N$, $^{1}H$]-HSQC experiment, on which an important new drug discovery methodology is based: SAR by NMR (see below).

#### 2.4.2.3.2 SAR by NMR

In 1996, Fesik and coworkers introduced a novel NMR-based concept for achieving high-affinity low-molecular weight binders to protein targets: SAR (structure-activity relatioship) by NMR [Shuker et al., 1996]. This methodology is based on chemical shift changes of the target protein (for which $^{15}N$-$^{1}H$ backbone resonance assignment has been made) in an [$^{15}N$, $^{1}H$]-HSQC experiment which result upon binding. A library of low-molecular weight compounds is screened as mixtures of (usually 10) compounds. Mixtures displaying strong chemical shift changes are then deconvoluted and the compound responsible for the binding is determined and can eventually be optimized, while the shifting backbone amide resonance signals reveal the binding site. This procedure can then be repeated in order to find a further library member which binds to a binding site in close proximity to the one of the initial binder. Aim of this approach is to drastically improve binding affinity when two molecules binding to different proximal binding sites are fused to each other, thereby exploiting the chelate effect.

This approach proved to be successful in the discovery of binders to the FK506 binding protein (FKBP) [Shuker et al., 1996], inhibitors of the matrix metalloprotease Stromelysin [Hajduk et al., 1997c], binders to the DNA-binding domain of the human papilloma virus E2 protein [Hajduk et al., 1997b], inhibitors of the Erm methyl transferase [P. J. Hajduk et al., 1999c], phosphotyrosine mimetics binding to Src homology 2 (SH2) domains [P. J. Hajduk et al., 1999b] and inhibitors of Urokinase [Hajduk et al., 2000b].

Yet, the SAR by NMR methodology has several drawbacks. First, the 3D-structure of the target protein has to be revealed and NMR peak assignment has to be done before the screening process can be started, which cannot easily be performed for large proteins (larger than 30 kDa) by standard NMR-equipped laboratories. Second, large amounts of $^{15}N$-labeled protein are necessary for the screening process (in the milligram scale). Selective labeling $^{13}C$ methyl groups of the target protein and monitoring of the binding by means of [$^{13}C$,$^{1}H$]-HSQC might be suitable for the screening of proteins with molecular masses greater than 40 kDa. [Hajduk et al., 2000c].

#### 2.4.2.4 Virtual Screening

Virtual screening, also called *in silico*–screening, means the use of computational strategies for screening large databases of chemical compounds in order to prioritize compounds which are expected to bind for synthesis and later on real screening [Walters et al., 1998; Good, 2001; Schneider and Bohm, 2002]. Clearly, this implies that information about the target binding site or the type of ligand that is expected to bind is available. It can be used to produce either a very focused subset of compounds (e.g. only structural analogs of a lead compound are of interest) or an open subset when few constraints are applied (e.g. just restriction in molecular weight). It may for example prove useful when a decision is requested about which subset of a real compound is to be screened first by HTS. Three different virtual screening categories can be distinguished:

In the first approach, libraries of compounds are screened for "drug-like" compounds, regardless of whether useful information about the target is known. "Drug-likeliness" is used to evaluate a broad range of properties or structural features which are important in the various stages of drug development, such as stability, solubility, lipophilicity and hydrophilicity (Pharmaceutical companies try to evaluate compounds in respect to their toxicological and pharmacokinetic profiles as early as possible in the drug development process). Generally accepted in this respect is Lipinski's "rule of five " [Lipinski et al., 1997] which classifies compounds based on their molecular weight, partition coefficient in octanol and abundance of hydrogen bond donors and acceptors. An example of this filtering is the REOS (rapid elimination of swill) procedure which tries to eliminate undesired compounds, thereby reducing the number of compounds for more extensive computational evaluation. [Walters et al., 1998].

The second (ligand-based) approach tries to select compounds by means of a target-specific pharmacophore, which means the three-dimensional key features of a set of known binders or targets. These features are usually described in terms e.g. of hydrogen bond donor or acceptor functions and lipophilic moieties, separated in specific distance ranges. Such a pharmacophore is then used to search a database of 3 dimensional chemical structures, preferentially with conformational flexibility. A

limitation of this strategy is often represented by “over-definition”, i.e., a well-defined pharmacophore will usually be too restrictive, thus yielding only few interesting hits, whereas a less well-defined pharmacophore will lead too may hits to be useful. Furthermore, hits cannot be classified in terms of a ranking but only for similarity to initial binders. Usually, structures similar to the already known binders are found rather than novel structures.

The third virtual screening (structure-based) approach is the most sophisticated approach and tries to select compounds by means of ligand-target docking. Often, compounds are selected from the ACD database in order to be able to experimentally verify the results obtained from *in-silico*-screening. This methodology which needs large computational resources tries to dock compounds of a virtual library to the target of interest. Hence, it requires a three-dimesional database of the ligands and a 3D structure of the target (either a “real” physico-chemically characterized structure if available or just a homology model) and a docking algorithm consisting of a search algorithm and a “scoring” function which tries to optimally calculate ligand-target interaction. [Charifson et al., 1999]. Typically, a grid box of is superimposed to the binding site of the target, individual grid points are then used for the docking calculations. The scoring methods typically are empirically derived functions for the estimation of the free binding energy, evaluating ligand-target interaction in terms of geometry of hydrogen bond contacts, lipophilic contacts, eventually metal binding contacts and the entropic penalty payed by freezing the ligand’s conformation upon binding. These functions are calibrated against a data set of heterogenous ligand-target complexes. As the accurate prediction of the influence of water molecules on the binding still is impossible, the quality of the docking results poses the problem that predicted binding-affinities have an accuracy of only ca. 9 kJ/mol, equal to around 2 orders of magnitude in $K_D$.

So far, several virtual screening approaches based on ligand-target binding have been published [Burkhard et al., 1999; Tondi et al., 1999; Aronov et al., 2000; Baxter et al., 2000; Boehm et al., 2000; Filikov et al., 2000; Hopkins et al., 2000; Perola et al., 2000; Schapira et al., 2000]. Enrichment of already known binders which were included in the screened library was clearly demonstrated, yet correct ranking according to binding affinity remains problematic.

Recently, a virtual screening approach for novel inhibitors of human carbonic anhydrase has been published which allowed the identification and experimental confirmation of novel subnanomolar inhibitors of the enzyme. However, all the newly identified compounds were structurally similar to known sulfonamide inhibitors [Gruneberg et al., 2002].

# 3 RESULTS, METHODS AND DISCUSSION

## PART I: Low-molecular weight binders to EDB

## 3.1 Discovery and investigation of lead-compounds as binders to the EDB domain

### 3.1.1 Abstract

Angiogenesis, i.e. the growth of new blood vessels from pre-existing vessels, is a rare event in the adult (exception made for the female reproductive cycle), but is a characteristic feature of relevant diseases such as cancer, blinding ocular disorders and rheumatoid arthritis. The EDB domain of fibronectin, a domain of 91 aminoacids, inserted by a mechanism of alternative splicing of the primary transcript into the fibronectin molecule, is a good-quality marker of angiogenesis and a target for molecular intervention, characterized by a high number of acidic residues on its surface, as well as some solvent-exposed hydrophobic residues.

A library of 113 low-molecular weight organic compounds, containing both an aromatic moiety and at least one positive charge, was screened for binding to the EDB domain, using two-dimensional heteronuclear NMR-spectroscopy. One lead-compound, 2,2-diphenylethylamine, was found that binds specifically to the EDB domain, yet with a dissociation constant in the millimolar range. Chemical modification of this scaffold revealed structural determinants required for binding, as well as amino acid residues in the EDB domain responsible for the interaction. The results presented in this thesis represent the basis for the development of high-affinity, low-molecular weight binders by either using a linked-fragment approach or elongation of the scaffold by means of combinatorial chemistry.

A test library comprising 113 commercially available compounds was selected from the ACD-database using the program ISIS Base 2.2 (MDL Information Systems, San

Leandro, CA). The selected low-molecular weight compounds were chosen according to the following criteria: 1) presence of an aromatic core for binding to hydrophobic patches of the EDB, e.g. phenyl-, naphthyl-, biphenyl- or heteroaromatic derivatives; 2) availability of a primary amino group (in this case a 1,1-unsubstituted ethylamino group) for achieving solubility in 50mM phosphate buffer, pH=7.4 and improved affinity for the highly negatively charged EDB; 3) presence of functional groups that allow suitable routes for derivatization without requiring the excessive use of protection groups; 4) absence of acidic groups, since a negative charge was expected to reduce binding affinity to the negatively charged EDB; 5) Molecular weight < 350 Da.

The selected amino-compounds were ordered on a 2mg scale in 96-well plates from Aldrich Chemie / FLUKA Chemie AG, Buchs, Switzerland, preferentially as hydrochlorides if available, and if chiral, as racemates rather than as enantiomerically pure compounds. Before HSQC-measurement of mixtures of 5 compounds, the compounds were individually prepared as 25mM solutions in 100mM phosphate buffer, pH=7.0, occasionally by adding small amounts of diluted hydrochloric acid.

### 3.1.2 Introduction

The formation of new blood vessels from pre-existing blood vessels (angiogenesis) is an essential pre-requisite for the growth of most aggressive solid tumors, but a rare event in adult physiology, except for the female reproductive cycle [Folkman, 1995 ; Carmeliet and Jain, 2000]. Furthermore, over-exuberant angiogenesis is a characteristic feature of blinding ocular disorders (such as diabetic retinopathy and age-related macular degeneration) and rheumatoid arthritis. Markers of angiogenesis, therefore, represent an ideal target for biomolecular intervention in cancer and other relevant diseases.

Fibronectin is a multi-domain adhesive glycoprotein, abundant in plasma and in tissues, which is present in different isoforms, due to a mechanism of alternative splicing at the level of its primary transcript [Zardi et al., 1987; Carnemolla et al., 1989; Castellani et al., 1994; Kaczmarek et al., 1994; Birchler et al., 1999a]. One of its extra-domains, the EDB domain, has a 91 aminoacid sequence which is identical in mouse, rat, rabbit, dog, monkey and man. EDB-containing fibronectin (B-FN) has a restricted pattern of expression, being undetectable in normal adult tissues and in mature blood vessels, but accumulates in regenerating tissues and around new blood vessels [Nicolo et al., 1990; Halin et al., 2001]. The 3D-structure of EDB has been solved by NMR spectroscopy in solution, and is characterized by a β–sandwich with a negatively charged protein surface (at neutral pH), displaying a hydrophobic patch of 4 apolar aminoacid residues [Fattorusso et al., 1999] (Figure 3.1.1).

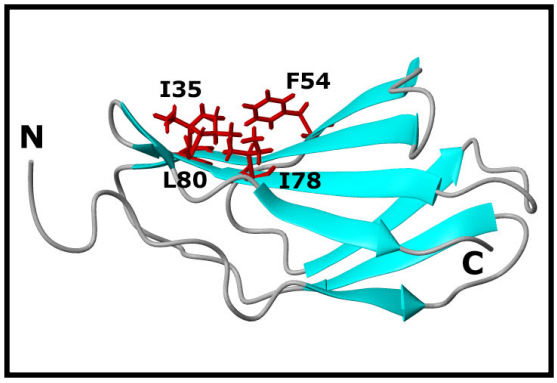


**Figure 3.1.1**

Ribbon drawing of one of the 20 energy-minimized solution structures of the EDB domain of fibronectin. β-strands are depicted in cyan.
Residues I35,F54,I78,L80, forming a solvent-exposed hydrophobic patch, are depicted in red.

Due to the high level of conservation of the EDB sequence, the generation of monoclonal antibodies by immunization has not been successful, until now. However, in collaboration with Prof. L. Zardi (Genova, Italy), our laboratory has generated a number of high-affinity human antibody fragments specific for the EDB domain, one of which (termed "L19") has a dissociation constant for the target in the picomolar range [Pini et al., 1998]. It has been extensively characterized in animal models of angiogenesis [Birchler et al., 1999b; Birchler et al., 1999a; Tarli et al., 1999 ; Viti et al., 1999 ; Demartis et al., 2001 ; Nilsson et al., 2001; Carnemolla et al., 2002; Halin et al., 2002a] and is currently in clinical trials for the immunoscintigraphic detection of tumor lesions in cancer patients. For a number of applications, nonetheless, it would be desirable to have a low-molecular weight binder specific for EDB. Such a compound would ideally be easier to produce in large amounts, could be coupled to bioactive drugs (e.g., photosensitizers or cytotoxics), should not be immunogenic and could readily cross the endothelial cell layer which separates the blood stream from $B^+$-fibronectin, which is typically located in the abluminal aspects of new blood vessels (C. Halin, H. Wunderli-Allenspach, D. Neri, unpublished results).

At present, target-based drug discovery and optimization is mainly carried out by the pharmaceutical industry, using high-throughput screening (HTS) of libraries containing several thousands of organic molecules. While bioassay development and automation play important roles in the discovery process, the nature of the chemical diversity contained in the library may be equally important. In particular, while the pharmaceutical industry has a good success rate for targets containing clefts or crevices (e.g. enzymes), more difficulties are encountered with hydrophilic protein targets, characterized by flat, hydrophilic surfaces, such as EDB [Stockman, 1998; P.J. Hajduk et al., 1999; Moore, 1999; Drews, 2000.

In order to facilitate the drug discovery process, some companies have begun to use screening methodologies based on two-dimensional heteronuclear NMR spectroscopy for protein targets of MW < 30'000 Da ; Roberts, 2000; Peng et al., 2001]. Such methodologies have allowed the discovery of high-affinity ligands for a number of relevant target proteins, such as the FK506 binding protein FKBP [Shuker et al.,

1996] and the matrix-metalloprotease stromelysin [Hajduk et al., 1997b]. A distinctive advantage of target-based NMR screening methodologies over conventional HTS is represented by the information gained about the nature of the binding site for the drug under investigation. In a typical NMR experiment a binding event between a $^{15}$N-labeled protein and an organic compound is detected by changes in positions of cross-peaks in a [$^{15}$N,$^{1}$H]-heteronuclear single quantum coherence (HSQC) experiment [Bodenhausen and Ruben, 1980]. This experiment yields a two-dimensional spectrum, in which each amide moiety of all non-prolyl residues gives rise to a cross-peak due to scalar coupling between the amide proton and its attached nitrogen nucleus in the uniformly $^{15}$N-labeled protein. The peaks which shift upon binding of a compound to the protein correspond to protein residues which are in close contact with its binder.

NMR screening methods are low-throughput and require substantial amounts of both protein and ligand, but the structural information gained in the process may be invaluable for the conjugation of two binding molecules of intermediate affinity, yielding a high-affinity bidentate ligand [Shuker et al., 1996; Hajduk et al., 1997a], or for the design of focused affinity-matured secondary libraries of lead-compounds. While the library to be used in NMR screening methodologies has to be reasonably small in size, it should contain molecules which match some properties of the target proteins (e.g., positively charged compounds if one targets a highly acidic protein) and which fit drug-like criteria, i.e. less than 5 H-bond donors, less than 10 H-bond acceptors, molecular weight < 500 Da, calculated Log P (ClogP) < 5 (or MlogP < 4.15) [Lipinski et al., 1997; Fejzo et al., 1999; Hajduk et al., 2000a; Lipinski, 2000; Lepre, 2001]. Solubility of the compounds in aqueous solution at the relevant pH at concentrations required for NMR experiments (approx. millimolar) is another important pre-requisite in library design.

In this study, we aimed at identifying lead-compounds specific for the EDB domain of fibronectin, using [$^{15}$N,$^{1}$H]-HSQC NMR screening and a small, rationally designed library of low-molecular weight organic compounds. Furthermore, having isolated a promising candidate compound from the library, we investigated which positions in this molecule could be chemically modified without losing EDB binding properties.

### 3.1.3 Materials and Methods

#### 3.1.3.1 Production of $^{15}$N-labeled EDB

The expression vector pFVEDB containing the gene encoding the EDB-domain was overexpressed in bacterial *E.coli* strain TG1 as previously described [Fattorusso et al., 1999] in minimal medium using $^{15}NH_4Cl$ as the sole nitrogen source.
Sonication of the bacterial pellet yielded crude labeled protein which was first subjected to a weak anion exchange column (DEAE-Sepharose) and dialyzed against 25mM phosphate buffer, pH = 7.4. Further purification was performed by ion exchange chromatography, using a strong anion exchange column (ResourceQ, 6ml, Amersham Pharmacia) and a salt gradient [25mM phosphate buffer (pH = 7.4) and 500mM NaCl/50mM phosphate buffer (pH=7.4)]. The yield was >10mg $^{15}$N-labeled EDB per 1g of $^{15}NH_4Cl$ (in 1l of bacterial culture). The purified EDB proved to be >95% pure as determined by SDS gel analysis and comparison of the [$^{15}$N,$^{1}$H]-HSQC with published data [Fattorusso et al., 1999].

#### 3.1.3.2 NMR and spectra analysis

All NMR spectra were recorded on a BRUKER DRX500 spectrometer at 298K. 2D-[$^{15}$N,$^{1}$H]-HSQC spectra were performed with pulsed-field gradients [Keeler et al., 1994] for coherence selection and water suppression and incorporated water flip-back methodology [Grzesiek and Bax, 1993]. Typically, data matrices comprised 2048*200 complex data points, each increment averaged over 16 scans. HSQC experiments of mixtures of 5 compounds, 2.5mM each, were carried out at 0.65mM EDB / 100mM phosphate buffer / pH=7.0 (uncorrected meter reading) and were measured in 280 µl of 90%$H_2O$/10%$D_2O$ in a shigemi tube. HSQC experiments of individual compounds, unless otherwise denoted, were carried out on 2.5mM compound, 0.65mM EDB / 50mM phosphate buffer, pH=7.0. Light-scattering experiments showed that EDB is monomeric at concentrations as high as 1.3mM in 40mM NaCl and 20mM phosphate buffer at pH=7.0 [Fattorusso et al., 1999]. 2D-NMR spectra were processed with 70°

shifted sine-bell window functions in both dimensions within the spectrometer software xwinnmr 2.1 and then transferred into the program XEASY [Bartels et al., 1995] for spectral analysis. Chemical shift values for amide protons and nitrogens were downloaded from the protein data bank (entry code 2FNB) and converted into the XEASY peaklist format using in-house written scripts.

It has been realized by many investigators that changes in the positions of cross peaks in the [$^{15}$N,$^{1}$H]-HSQC spectrum may also be due to other (non ligand-binding) effects (solvent effects etc.). Hence, we have verified ligand binding by comparing values of the proton transverse relaxation times T2 of the ligand in the presence and in the absence of EDB. The T2 data were recorded using a slightly modified CPMG sequence [Meiboom and Gill, 1958] with added DPFGSE water suppression [Hwang and Shaka, 1995]. In the analysis, a non-linear least squares fit of peak intensities of the corresponding 1D spectra recorded for T2 delays of 0.005 sec up to 7 sec against the peak intensities was performed with xwinnmr. Moreover, binding of the ligands to EDB was also verified from a reduction of the translational diffusion constant in the complex mixture, measured by a modified BPP-LED sequence [Wu et al., 1995; Johnson, 1999]. In those measurements the diffusion delay was set to 100 ms and the gradients were applied as block-shapes with strengths between 0.05 and 40 G/cm.

#### 3.1.3.3 Chemical synthesis

<u>2-(9-fluorenyl)ethylamine hydrochloride (**5**)</u>

1) 9-Fluorene carboxylic acid chloride

630mg (3mmol) 9-fluorene carboxylic acid (Aldrich Chemicals) was refluxed in 20ml thionyl chloride for 3 hours under argon. Residual thionyl chloride was removed under high vacuum over-night and the resulting oily crude product was used without further purification.

2) 9-fluorene carboxamide

To 25ml condensed $NH_3$, crude 9-fluorene carboxylic acid chloride was added dropwise as a suspension in 3ml acetone, thereby changing its color into orange. After evaporation of the $NH_3$, water and ethyl acetate were added to the dry solid. The

aqueous phase was extracted twice with ethyl acetate and the combined organic phases were washed neutral with 0.1M HCl, aqueous solutions of saturated $NaHCO_3$ and NaCl, successively. After drying over $MgSO_4$,, solvent was removed under high vacuum to yield 508mg (2.45mmol) of crude product, used without further purification.

3) 2-(9-fluorenyl)ethylamine hydrochloride

To 530mg (14mmol) $NaBH_4$ a solution of 290mg (ca. 1.4mmol) of crude 9-fluorene carboxamide in 10ml dry dioxane was added. The suspension was chilled to 10°C and a solution of 1072µl (14mmol) TFA in 5ml dry dioxane was added slowly.

After stirring at 10°C for an additional 10min, the yellowish suspension was heated slowly. At 50°C, strong $H_2$ –formation occurred. The mixture was then allowed to reflux for 5 hours. The solvent was removed *in vacuo* and 10ml methylene chloride were added followed by careful addition of 15ml water, until no more $H_2$ – formation was detectable. The organic phase was extracted 5 times with 5 ml of 2N hydrochloric acid, the combined aqueous phases filtered and all solvent removed under high vacuum. The crude product was recrystallised twice from water/methanol and dried under high vacuum.

$^1$H-NMR (DMSO-$d_6$, 295K): 3.36 (d,2H); 4.31 (t,1H); 7.39 (t,2$H_{ar}$); 7.46 (t,2$H_{ar}$); 7.74 (d,2$H_{ar}$); 7.93 (d,2$H_{ar}$); 8.03 (br.,$H_N$)

[*N*-(2,2-diphenyl)ethyl]acetamide (**6**)

95µl (1mmol) acetic anhydride was dissolved in 3ml dry dioxane and added dropwise to 400mg (2mmol) 2,2-diphenylethylamine (Aldrich Chemicals), dissolved in 5ml dry dioxane. Precipitation of a colorless solid occurred and the reaction mixture was stirred for 4 hours. After removal of solvent *in vacuo*, diluted hydrochloric acid was added and the crude product extracted three times with ether. The organic phase was dried over $MgSO_4$ and the solvent removed *in vacuo*. The resulting crude product was purified by HPLC on a reversed phase $C_{18}$-column (VYDAC®) using a linear gradient from 0.1%TFA in water to 100% methanol.

$^1$H-NMR (DMSO-$d_6$, 298K): 1.64 (s,3H); 3.60 (t,2H); 4.10 (t,1H); 7.11 (t,2$H_{ar}$); 7.19-7.23 (m,8$H_{ar}$); 7.81 (t,$H_N$)

(*S*)-2,6-diaminohexanoyl-(2,2-diphenyl)ethylamide bistrifluoroacetate

[ L-lysyl-(2,2-diphenyl)ethylamide bistrifluoroacetate ] (**7**)

110mg (0.25mmol) Boc-Lys(Boc)-OSu (BACHEM AG, Bubendorf, Switzerland) were dissolved in 3ml dry acetone. After addition of 70mg (0.35mmol) 2,2-diphenylethylamine (Aldrich Chemicals) the mixture was stirred for 2h at RT and all solvent removed *in vacuo*. For deprotection, 1ml of TFA was added. After stirring for 15min and removal of TFA *in vacuo* the resulting crude product was dissolved in water/0.1%TFA, aliquots of which were purified by HPLC on a reversed phase $C_{18}$-column (VYDAC®) using a linear gradient from 0.1%TFA in water to 100% methanol.

$^1$H-NMR ($H_2O$ / 10% $D_2O$, 298K): 0.72 (m,2H); 1.24 (m,2H); 1.37 (m,2H); 2.56 (br,2H); 3.51 (m,1H); 3.57 (t,1H); 4.01 (m,1H); 4.14 (t,1H); 7.07-7.12 (m,2$H_{ar}$); 7.17-7.21 (m,8$H_{ar}$); 7.31 (very br.,$H_N$); 8.34 (br,1$H_{amide}$)

[*N*-(2,2-diphenyl)ethyl]ethylamine trifluoroacetate (**8**)

35.5mg (0.23mmol) iodoethane and 112mg (0.57mmol) 2,2-diphenylethylamine were dissolved in 1ml dry DMF. The reaction mixture was stirred over-night at RT under Ar. To 1 volume of reaction mixture, 1 volume of 10% TFA was added. Aliquots of the mixture were then purified by HPLC on a reversed phase $C_{18}$-column (VYDAC®) using a linear gradient from 0.1%TFA in water to 100% acetonitrile.

$^1$H-NMR (DMSO-$d_6$, 298K): 1.16 (t,3H); 2.99 (m,2H); 3.70 (m,2H); 4.32 (t,1H); 7.25 (t,2$H_{ar}$); 7.35 (t,4$H_{ar}$); 7.40 (t,4$H_{ar}$); 8.28 (br.,$H_N$)

[2-(2',2'-diphenyl)ethylamino]ethanesulfonate sodium trifluoroacetate (**9**)

55.7mg (0.26mmol) Na-2-bromoethylsulfonate and 130mg (0.66mmol) 2,2-diphenylethylamine were dissolved in 2ml dry DMF. The reaction mixture was stirred over-night at RT under Ar. To 1 volume of reaction mixture, 1 volume of 10% TFA was added. Aliquots of the mixture were then purified by HPLC on a reversed phase $C_{18}$-column (VYDAC®) using a linear gradient from 0.1%TFA in water to 100% acetonitrile.

$^1$H-NMR (DMSO-$d_6$, 298K): 1.23 (t,2H); 3.56 (m,4H); 4.23 (t,1H); 7.25 (t,2$H_{ar}$); 7.33-7.37 (m,8$H_{ar}$); 7.78 (br.,$H_N$)

[*N*-(2,2-diphenyl)ethyl]-1,2-diaminoethane bistrifluoroacetate (**10**)

51.9mg (0.25mmol) 2-bromoethylamine hydrobromide and 125mg (0.63mmol) 2,2-diphenylethylamine were dissolved in 2ml dry DMF. The reaction mixture was stirred over-night at RT under Ar. To 1 volume of reaction mixture, 1 volume of 10% TFA was added. Aliquots of the mixture were then purified by HPLC on a reversed phase $C_{18}$-column (VYDAC®) using a linear gradient from 0.1%TFA in water to 100% acetonitrile.

$^1$H-NMR (50mM phosphate buffer, pH=7, 10% $D_2O$, 298K): 3.00 (d, 2H); 3.04 (d,2H); 3.43 (d,2H); 4.25 (t,1H); 7.33-7.38 (m,8$H_{ar}$); 7.26 (t,2$H_{ar}$)

[*N*-(2,2-diphenyl)ethyl,*N'*-trimethyl]-1,2-diaminoethane bistrifluoroacetate (**11**)

62.7mg (0.25mmol) (2-bromoethyl)trimethylammoniumbromide and 125mg (0.63mmol) 2,2-diphenylethylamine were dissolved in 2ml dry DMF. The reaction mixture was stirred over-night at RT under Ar. To 1 volume of reaction mixture, 1 volume of 10% TFA was added. Aliquots of the mixture were then purified by HPLC on a reversed phase $C_{18}$-column (VYDAC®) using a linear gradient from 0.1%TFA in water to 100% acetonitrile.

$^1$H-NMR (DMSO-$d_6$, 298K): 1.23 (s,9$H_{Me}$); 3.10 (br.,2H); 3.51 (br.,2H); 3.77 (br.,2H); 4.37 (br.,1H); 7.28 (br,2$H_{ar}$), 7.38 (br.,8$H_{ar}$), 8.78 (br,$H_N$)

**Synthesis of the analogous compounds 12-18 was performed on the basis of a literature recipe** [Tucker et al., 1997]**:**

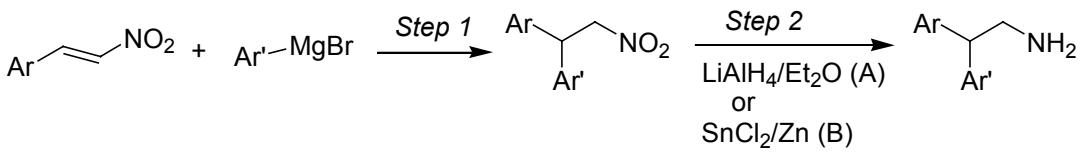


Step 1. Michael additions of Grignard reagents to 2-nitro-styrenes. *General procedure.* A catalytic amount of $I_2$ was added to a suspension of metallic Mg (1 equiv.) in dry $Et_2O$, followed by a dropwise addition of an aryl bromide (1 equiv.)

solution in dry $Et_2O$, such that a gentle reflux is maintained. The mixture was refluxed until metallic Mg disappeared. The resulting solution was warmed up to room temp. and added dropwise to a cooled solution of β-nitro styrene derivatives (1 equiv.) in dry $Et_2O$ at –20 °C under $N_2$ atmosphere. After disappearance of the starting material (monitored by TLC) the reaction was quenched with saturated aqueous $NH_4Cl$ solution, warmed up to RT and extracted with ethyl acetate. The collected organic layers were dried with anhydrous $Na_2SO_4$, filtered, and the solvent was removed *in vacuo*. Purification of the crude product by flash chromatography (FC) on silica gel afforded the corresponding 2,2-diaryl-nitroethane.

Step 2, method A. Reduction with $LiAlH_4$. *General procedure*. A solution of 2,2-diaryl-nitroethane (1 equiv.) in dry $Et_2O$ at 0°C, under $N_2$ atmosphere, was added to a stirred suspension of $LiAlH_4$ (4 equiv.) in dry $Et_2O$. The mixture was allowed to reach RT and stirred over-night. After disappearance of the starting material (monitored by TLC) the reaction was quenched with water and extracted with ethyl acetate. The collected organic layers were dried with anhydrous $Na_2SO_4$, filtered, and the solvent was removed *in vacuo*. Purification of the crude product by FC afforded the corresponding pure 2,2-diaryl-ethylamine.

Step 2, method B. Reduction with $SnCl_2$/Zn. *General procedure*. A 37% aqueous solution of HCl (4 equiv.) was added to a suspension of 2,2-diaryl-nitroethane (1 equiv.), $SnCl_2 \times 2H_2O$ (3 equiv.) and Zn dust (3 equiv.) at RT in AcOH. The mixture was stirred over-night. The solution was cooled to 0 °C and diluted with a 30% aqueous solution of NaOH until basic pH was reached. Then, the mixture was diluted with $CH_2Cl_2$, filtered on a Celite pad, and extracted with $CH_2Cl_2$. The collected organic layers were dried with anhydrous $Na_2SO_4$, filtered, and the solvent was removed *in vacuo*. Purification of the crude product by FC afforded clean 2,2-diaryl-ethylamine.

Deprotection of the benzyl moiety. A catalytic amount of $Pd(OH)_2$/C (Pd 20%) was added to a stirred solution of *O*-benzyl precursor of **16** (23 mg, 0.07 mmol) in abs. EtOH (1 ml). The slurry was vigorously stirred for 1 h at RT under $H_2$. $Pd(OH)_2$ was removed by filtration on a Celite pad, and the solvent was removed *in vacuo* to afford 17 mg of pure compound **16** (yield > 98%).

2-Benzo[1,3]dioxol-5-yl-2-phenyl-ethylamine (**12**). Yields: step 1, 63%; step 2 (method B), 60%. $^1$H-NMR ($CD_3OD$, 305 K): 3.20 (d, $J$ = 7.9 Hz, 2 H); 3.94 (t, $J$ = 7.9 Hz, 1 H); 5.86 (s, 2 H); 6.74 (s, 3 H); 7.25 (m, 5 $H_{ar}$).

2-Phenyl-2-(4-trifluoromethyl-phenyl)-ethylamine (**13**). Yields: step 1, 53%; step 2 (method B), 60%. $^1$H-NMR ($CD_3OD$, 305 K): 3.30 (m, 2 H); 4.13 (t, $J$ = 7.5 Hz, 1 H); 7.22 (m, 1 $H_{ar}$); 7.30 (m, 4 $H_{ar}$); 7.47 (d, $J$ = 8.1 Hz, 2 $H_{ar}$); 7.59 (d, $J$ = 8.1 Hz, 2 $H_{ar}$); $^{19}$F-NMR ($CD_3OD$, 305 K): 86.4 (s, 3 F).

2-(2,6-dichloro-phenyl)-2-naphthalen-1-yl-ethylamine (**14**). Yields: step 1, 73%; step 2 (method A), 52%. $^1$H-NMR ($CD_3OD$, 305 K): 3.54 (dd, $J$ = 13.3 and 7.5 Hz, 1 H); 3.78 (dd, $J$ = 13.3 and 7.5 Hz, 1 H); 5.59 (d, $J$ = 7.5 Hz, 1 H); 7.18 (t, $J$ = 8.1 Hz, 1 $H_{ar}$); 7.37 (m, 5 $H_{ar}$); 7.47 (dd, $J$ = 8.1 and 7.5 Hz, 1 $H_{ar}$); 7.78 (d, $J$ = 8.1 Hz, 1 $H_{ar}$); 7.84 (d, $J$ = 7.5 Hz, 1 $H_{ar}$); 7.88 (d, $J$ = 8.1 Hz, 1 $H_{ar}$).

2-Phenyl-2-thiophen-2-yl-ethylamine (**15**). Yields: step 1, 63%; step 2 (method A), 55%. $^1$H- NMR ($CD_3OD$, 305 K): 3.20 (dd, $J$ = 12.7 and 7.5 Hz, 1 H); 3.26 (dd, $J$ = 12.7 and 7.5 Hz, 1 H); 4.25 (t, $J$ = 7.5 Hz); 6.93 (m; 1 $H_{ar}$); 6.95 (dd, $J$ = 5.2 and 3.5 Hz, 1 $H_{ar}$); 7.24 (m, 2 $H_{ar}$); 7.31 (m, 4 $H_{ar}$).

4-(2-Amino-1-phenyl-ethyl)-2-methoxy-phenol (**16**). Yields: step 1, 48%; step 2 (method B), 48%. $^1$H-NMR ($CD_3OD$, 305 K): 3.23 (d, $J$ = 7.5 Hz, 2 H); 3.79 (s, 3 H); 3.96 (t, $J$ = 7.5 Hz, 1 H); 6.74 (m, 2 $H_{ar}$); 6.81 (m, 1 $H_{ar}$); 7.18 (m, 1 $H_{ar}$); 7.27 (m, 4 $H_{ar}$).

2-Naphthalen-1-yl-2-phenyl-ethylamine (**17**). Yields: step 1, 78%; step 2 (method B), 63%. $^1$H- NMR ($CDCl_3$, 305 K): 1.60 (br s, 2 H); 3.40 (dd, $J$ = 12.7 and 7.5 Hz, 1 H); 3.47 (dd, $J$ = 12.7 and 7.5 Hz, 1 H); 4.79 (t, $J$ = 7.5 Hz, 1 H); 7.16 (m, 1 $H_{ar}$); 7.26 (m, 4 $H_{ar}$); 7.44 (m, 4 $H_{ar}$); 7.74 (d, $J$ = 7.5 Hz, 1 $H_{ar}$); 7.82 (m, 1 $H_{ar}$); 8.10 (d, $J$ = 8.7 Hz, 1 $H_{ar}$).

2-(3-Methoxy-phenyl)-2-naphthalen-1-yl-ethylamine (**18**). Yields: step 1, 60%; step 2 (method B), 57%. $^1$H-NMR ($CD_3OD$, 305 K): 3.67 (dd, $J$ = 12.8 and 7.8 Hz, 1 H); 3.74 (s, 3H); 3.77 (m, 1 H); 5.12 (t, $J$ = 7.8 Hz, 1 H); 6.89 (d, $J$ = 8.7 Hz, 2 $H_{ar}$); 7.30 (d, $J$ = 8.7 Hz, 2 $H_{ar}$); 7.55 (m, 4 $H_{ar}$); 7.84 (d, $J$ = 7.8 Hz, 1 $H_{ar}$); 7.88 (d, $J$ = 7.3 Hz, 1 $H_{ar}$); 8.13 (d, $J$ =7.8 Hz, 1 $H_{ar}$).

### 3.1.4 Results

#### 3.1.4.1 Library design

We designed a library of 113 organic compounds, each containing an aromatic ring and at least one positively charged group, considered to be water-soluble at neutral pH (Figure 3.1.2). Furthermore, the compounds should not contain negatively charged moieties, since the EDB domain is highly acidic (net charge = -9 at neutral pH). The molecular weight of the compounds ranged between 95 and 333 Da. The aromatic moieties chosen included phenyl-, naphthyl- and heteroaromatic derivatives. As positively charged groups, at least one primary amino group was present in each molecule. It has been proposed that the hydrophobicity of aromatic rings should ensure high binding affinity towards protein targets with solvent-exposed hydrophobic patches, while charged groups would contribute to the solubility of the low-molecular weight ligands [Park et al., 2000; Berezov et al., 2001] .

#### 3.1.4.2 NMR analysis of EDB binding

Of the 113 compounds composing the library, 85 were soluble in 50mM phosphate buffer, pH = 7.0 at concentrations compatible with NMR analysis, and could readily be mixed with $^{15}$N-labeled EDB to yield a 0.65mM EDB solution. HSQC-screening of 17 mixtures, each containing five 2.5mM concentrated compounds, was performed and the resulting spectra were compared to a reference spectrum of 0.65mM $^{15}$N-labeled EDB. From a separated series of experiments we could conclude that pH-variations of ±0.2 pH-units as well as small variations in ionic strength did not give rise to significant amide resonance shifts (data not shown).

From these 17 experiments, only a single mixture gave rise to a large resonance shift of a single backbone amide group. Deconvolution of this mixture by individually screening the 5 candidate compounds led to the identification of the shift-causing compound, 2,2-diphenylethylamine hydrochloride **(1)** [library number 84 (see Fig. 3.1.2); shifting EDB residue: Y73; $\Delta\partial_1$ = -0.34 ppm, $\Delta\partial_2$ = -0.14 ppm; see Fig. 3.1.3].

**Figure 3.1.2**

Chemical structures of the 113 compounds composing the original library which was subjected to NMR screening (cf. text)

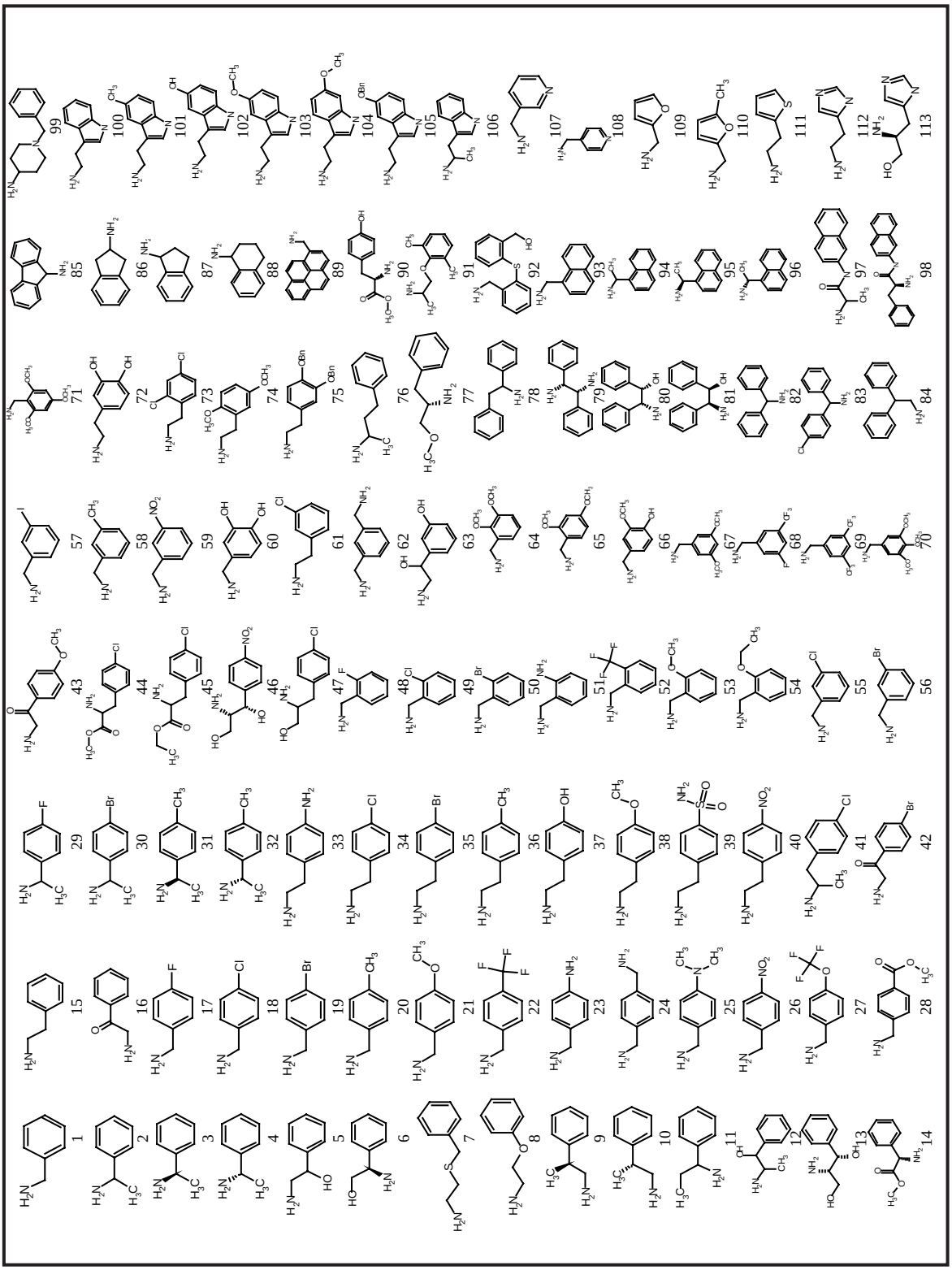

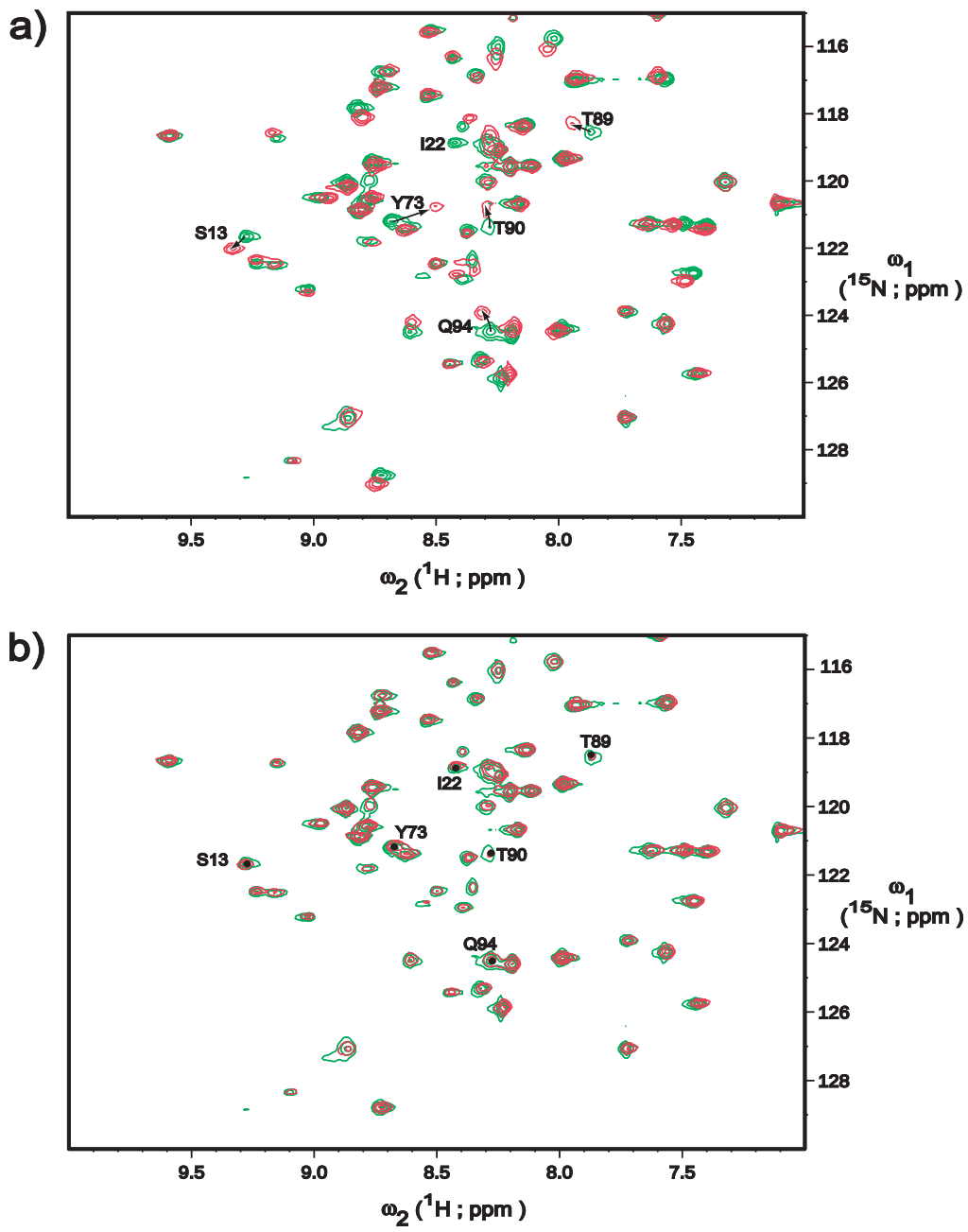


**Figure 3.1.3**

A superposition of [$^{15}$N,$^{1}$H]-HSQC spectra of 0.65mM EDB in the absence (green contours) and a) in the presence (red contours) of the strongly shifting compound 2,2-diphenylethylamine (**1**) (2.5mM); b) in the presence (red contours) of the non-shifting compound 2,3-dimethoxybenzylamine (2.5mM). Assignments are indicated for selected peaks which, in the case of a), exhibit large resonance shift changes.

A 1D-$^{1}$H-NMR line-broadening assay [Fejzo et al., 1999; Moore, 1999] was performed to exclude artefactual resonance shifting [Figure 3.1.4, panel a)].

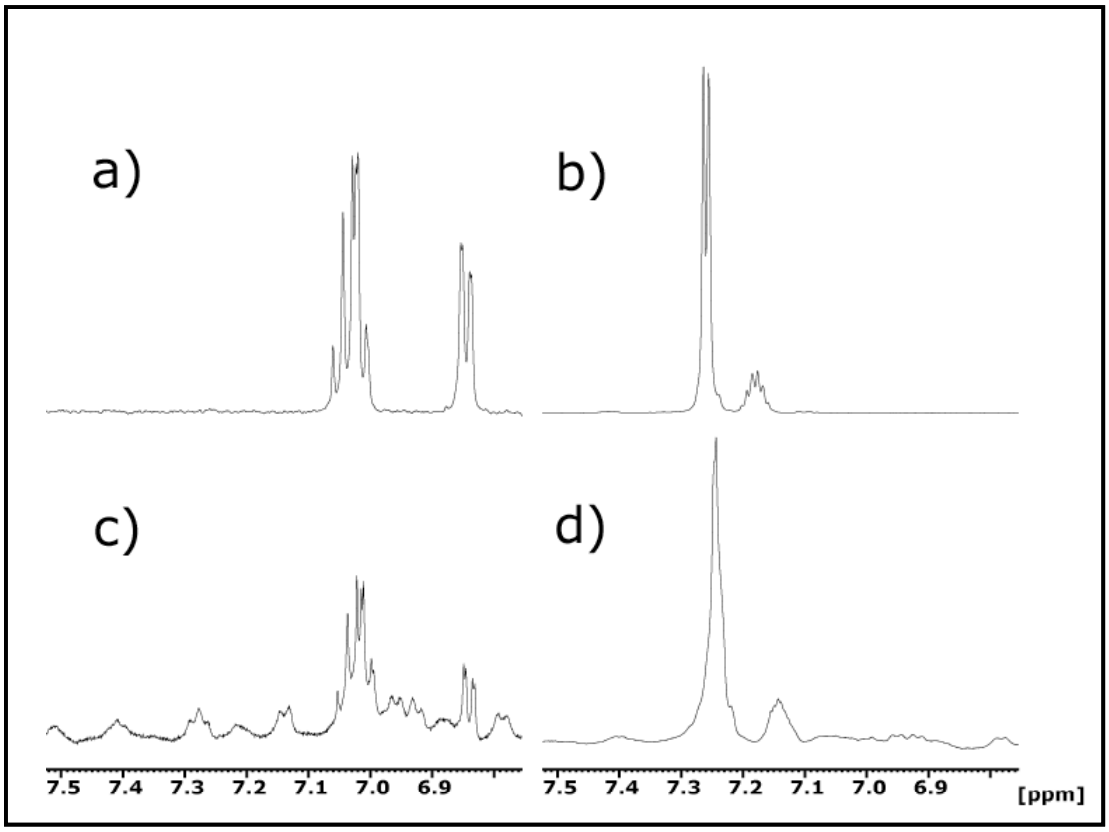


**Figure 3.1.4**

1D-$^{1}$H-NMR spectra of a) 2,3-dimethoxybenzylamine, in the absence of EDB; b) 2,2-diphenylethylamine (**1**), in the absence of EDB; c) 2,3-dimethoxybenzylamine, in the presence of EDB; d) 2,2-diphenylethylamine (**1**), in the presence of EDB.

Binding of 2,2-diphenylethylamine (**1**) to EDB is indicated by the line-broadening and suppression of fine structure as observed in d), but not in b). No line-broadening is observed for 2,3-dimethoxybenzylamine (c) and a)).

The compounds were measured as 2.5mM solutions in 50mM phosphate buffer, pH=7.0 in the absence (a) and b)) resp. presence (c) and d)) of 0.65mM EDB.

The overall correlation time $\tau_c$ of EDB at 1mM solution, 298K, in the used buffer was estimated as 6.8 ns. The value was derived from the ratio of $^{15}$N transverse to longitudinal relaxation rates R2/R1 [Kay et al., 1989] from residues in stably, β-strand folded residues. In the case of weak ligand binding the exchange rate is fast on NMR

time scale [Harris, 1983] and significant line-broadening could be detected for **1** in the presence of EDB. This behavior is manifested by the disappearance of signal-splitting due to more efficient transverse proton relaxation [Figure 3.1.4, panel b) and d)]. In addition, upon binding to EDB the T2 values of protons of the aromatic rings decrease from 2.2 sec to 0.52 sec. Moreover, the translational diffusion coefficient decreases from $8.04*10^{-10}$ $m^2/s$ to $6.63*10^{-10}$ $m^2/s$. Such binding could not be detected for another compound of the same 5 compound-mixture (2,3-dimethoxybenzylamine hydrochloride) that had not shown an amide resonance shift in the $^{15}N$-HSQC experiment, therefore serving as a negative control [Figure 3.1.4, panel a) and c)]. For the negative control, the decrease in T2 from 2.5 sec to 1.3 sec upon addition of EDB was much less pronounced than for **1**. Unfortunately, it was impractical to measure T2 and the translational diffusion constant for all compounds and hence we have focused our estimates of binding on cross-peak shifts in [$^{15}N$,$^{1}H$]-HSQC spectra.

In order to be able to optimize the binding properties of ligands to EDB, we have attempted to measure the dissociation constant $K_D$ in a titration series. In these experiments, aliquots of ligand **1** were added to a 0.65mM EDB solution and the $^{15}N$ and $^{1}H$ chemical shifts were derived from [$^{15}N$,$^{1}H$]-HSQC spectra. The absolute resonance shift values were plotted versus the logarithm of the concentration of the ligand (Figure 3.1.5).

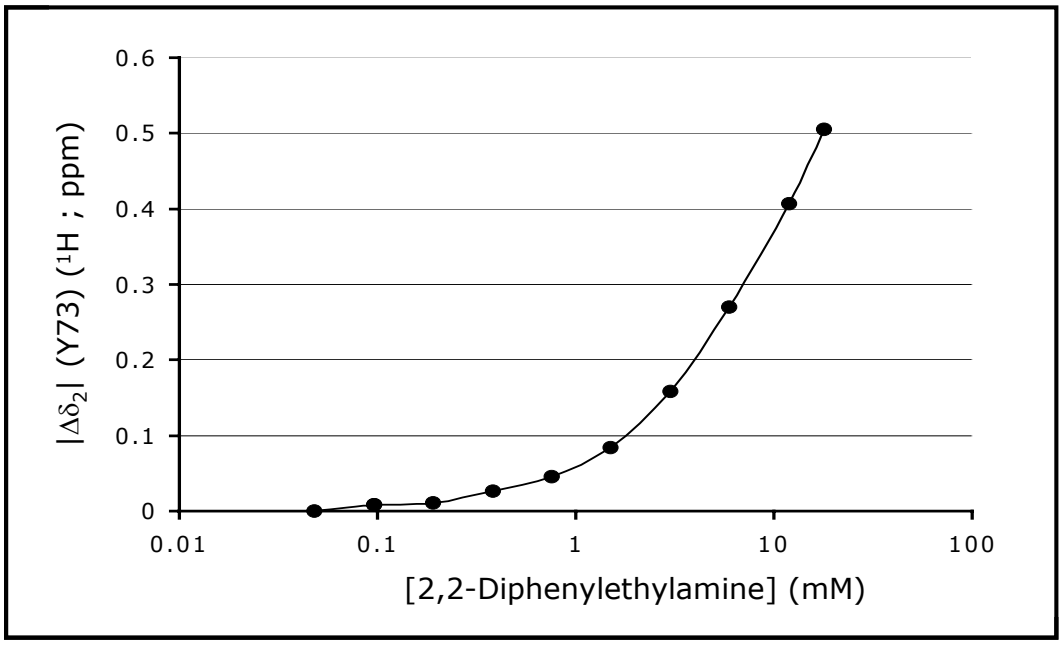


**Figure 3.1.5**

Titration of 0.65mM $^{15}$N-labeled EDB with lead-compound 2,2-diphenylethylamine (**1**), monitored by [$^{15}$N,$^{1}$H]-HSQC: Absolute proton ($\omega_2$) resonance shifts were monitored at increasing concentrations of **1** and plotted against the logarithm of concentration of **1**.

The point of inflection of the resulting curve represents the concentration of ligand at semisaturation of EDB, i.e. $K_D$ = [Ligand]$_{Semisaturation}$. Due to insolubility of the ligand at concentrations larger than 20mM the point of inflection could not be precisely determined, and hence $K_D$ was estimated $\geq$ 5 mM.

Screening of binding by [$^{15}$N,$^{1}$H]-HSQC spectra is unique in its ability to deliver additional information about which residues are involved in forming contacts to the ligand. The spectra surprisingly revealed that the weak binder **1** to EDB does not recognize the hydrophobic patch described in Figure 3.1.1 as intended, but rather recognized a second epitope on the EDB surface (Figure 3.1.6). This stretch contains residue Y73, whose resonances shift to the largest extend, and which is flanked by two Asp residues and is part of the sequence IDYDI. This sequence is characteristic of EDB and not contained in other fibronectin type-III repeats.

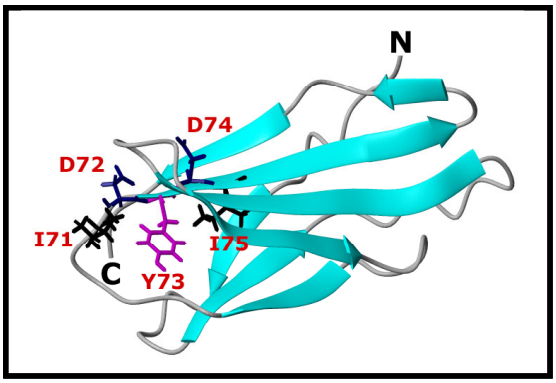


**Figure 3.1.6**

Ribbon drawing of one of the 20 energy-minimized solution structures of the EDB domain of fibronectin. β-strands are depicted in cyan. Residues I71,D72,Y73,D74,I75, forming the binding epitope for 2,2-diphenylethylamine (**1**) and derivatives of **1,** are depicted in black, blue and magenta.

### 3.1.4.3 Derivatives of 2,2-diphenylethylamine

We chemically modified the structure of 2,2-diphenylethylamine **(1)**, with the aim to improve the affinity of this lead EDB binder and to identify sites of this molecule that are amenable to derivatization without loss of binding. Possible changes in this molecule are conceivable either at the aromatic or the alicyclic part of the molecule. We focused our synthetic interest in both extending the molecule at the amino nitrogen and modifying the aromatic moieties, thereby leaving the 2,2-disubstituted ethylamine scaffold intact. As a result, a series of diverse derivatives were chemically synthesized **(5 – 18,** see Table 3.1.1 and Table 3.1.2**)**.

**Table 3.1.1**

| compound | | $\lvert\Delta\delta_1\rvert$ [a] [ppm] | $\lvert\Delta\delta_2\rvert$ [b] [ppm] |
|---|---|---|---|
| 1 | 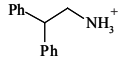 | 0.34 | 0.14 |
| 2 | 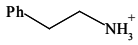 | 0.06 | 0.02 |
| 3 | 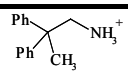 | 0.36 | 0.15 |
| 4 | 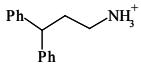 | 0.45 | 0.18 |
| 5 | | 0.19 | 0.09 |
| 6 | 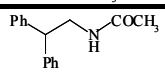 | 0.03 | 0.00 |
| 7 | 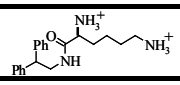 | 0.24 | 0.11 |
| 8 | 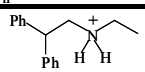 | 0.19 | 0.09 |
| 9 | 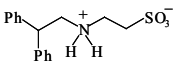 | 0.01 | 0.01 |
| 10 | 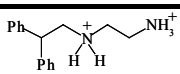 | 0.15 | 0.08 |
| 11 | 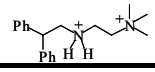 | 0.03 | 0.04 |

**Table 3.1.2**

| | | | $\lvert\Delta\delta_1\rvert$ [a] [ppm] | $\lvert\Delta\delta_2\rvert$ [b] [ppm] |
|---|---|---|---|---|
| | 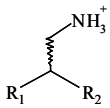 | | | |
| 12 | $R_1$= 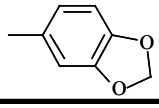 | $R_2$= 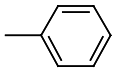 | 0.43 | 0.24 |
| 13 | $R_1$= 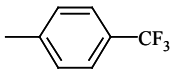 | $R_2$= 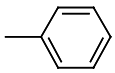 | 0.50 | 0.27 |
| 14 | $R_1$= | $R_2$= 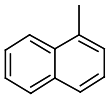 | 0.61 | 0.30 |
| 15 | $R_1$= | $R_2$= 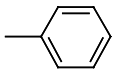 | 0.61 | 0.29 |
| 16 | $R_1$= 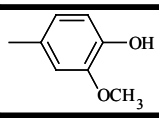 | $R_2$= 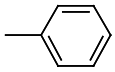 | 0.14 | 0.05 |
| 17 | $R_1$= 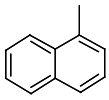 | $R_2$= 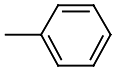 | 0.45 | 0.21 |
| 18 | $R_1$= 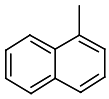 | $R_2$= 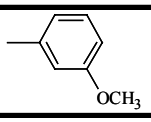 | 0.26 | 0.17 |

[a] absolute resonance-shift change in $\omega_1$ ($^{15}N$)
[b] absolute resonance-shift change in $\omega_2$ ($^{1}H$)

Firstly, we derivatized 2,2-diphenylethylamine **(1)** at the site of the amino nitrogen, and hence tested the role of the primary amino group in EDB binding **(Table I).** Upon acetylation of compound **1** the positive charge was removed resulting in a complete loss of the resonance shift of Y73 in the [$^{15}N$,$^{1}H$]-HSQC experiment for compound **6**. Hence, we conclude that the positive charge is essential for binding. In order to investigate whether the loss of the Y73-peak shift resulting from the loss of the positive charge at the amino group of **1** could be compensated by the introduction of a positive charge at a different position, the amino group was coupled to a C-terminally activated lysine. The resulting molecule **7** again interacted with Y73, however the reduced amount of the peak-shift indicated a reduced affinity to EDB compared to **1**.

Furthermore, a negative charge was introduced into **1** by alkylating the amine nitrogen with a sulfonatoethyl group (**9**). Similar to the uncharged amide **6**, the resulting zwitterionic molecule **9** displayed no binding to EDB. In another synthetic approach, an additional positive charge was introduced by aminoethylating **1**, to yield molecules **10** and **11**, respectively. These compounds showed a decreased resonance shift of the Y73 backbone amide compared to **1**. Without adding an additional charge, *N*-ethylation of the amino nitrogen (to yield **8)** resulted in a larger resonance shift compared to **9** or **10**, yet smaller than the one observed for **1**.

Elongation of the alkyl chain of the 2,2-diphenylethyl scaffold by a methylene group to derive compound **4** gave rise to a somewhat greater resonance shift change as compared to **1**, an additional methyl group at the 2-position of 2,2-diphenylethylamine led to a shift of the resulting molecule **3** comparable to **1**.

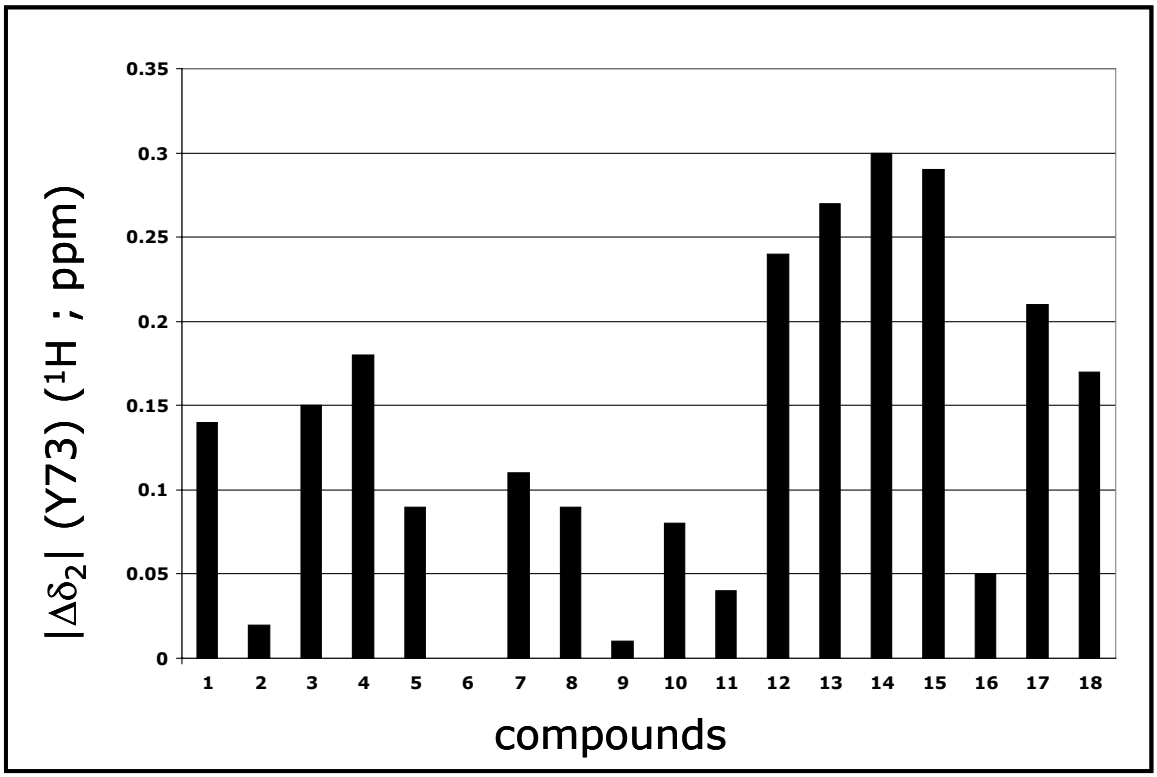


**Figure 3.1.7**

Absolute proton ($\omega_2$) resonance shifts of compounds **1-11** (cf. Table I) and racemates **12-18** (see Table II): [$^{15}$N,$^{1}$H]-HSQC spectra of the compounds resp. racemates were measured at 2.5mM each, together with 0.65mM $^{15}$N-labeled EDB.

Next, we investigated whether a chemical modification of the aromatic moieties of **1** would improve binding affinity **(Table II)**. Compound **1** has many (freely) rotatable bonds and binding of **1** to EDB is expected to lead to a larger loss in entropy. Hence, we rigidified the two phenyl moieties of **1** by introducing a 2',2''-linkage thereby forcing the two π-systems into co-planarity and yielding the fluorenyl derivative **5**. However, this chemical conversion led to a decreased shift, suggesting that the two aromatic rings in the bound conformation are not coplanar.

We then asked ourselves whether the addition of electron-donating or -withdrawing groups, which do not alter the molecular shape significantly, would result in increased EDB binding affinity. In a systematic approach, we synthesized the 7 racemic compounds **12-18** and recorded the proton chemical shifts of the aromatic protons in order to possibly rank them according to their electron-donating/withdrawing capability. With exception of compound **16**, all racemates displayed increased shifts of the Y73 cross-peak compared to **1,** and the largest differences, sorting according to ascending magnitude, were observed for **13**, **15** and **14** (see Figure 3.1.7). Interestingly, both steric and electronic effects seem to contribute to the binding process as observed by NMR. **13** and **14** contain electron-poor aromatic systems. Moreover, the replacement of a phenyl moiety with the larger naphthyl group in compound **17** led to an increased resonance shift of Y73. By contrast, *m*-methoxy substitution in the phenyl ring resulted in loss of the resonance shift, as demonstrated by compounds **16** and **18**. It has to be noted that the resonance shifts of the racemic compounds **12 –18** could be caused by just one of by both of the two stereoisomers. Due to the minute amounts of compound synthesized, chiral resolution of the racemates was impossible.

A summary of the results obtained by altering the molecular scaffold of 2,2-diphenylethylamine (**1**) is given in (Figure 3.1.8): increased resonance shifts could be observed upon addion of a methyl substituent at the 2-position of **1** (compound **3**), as well as upon addition of electron-withdrawing substituents in *o*- or *p*-positions of the aromatic moiety (compounds **13-15**). A reduced resonance shift however was observed when altering the amino nitrogen (compounds **6-11**) or with electron-withdrawing *m*-substituents (**16,18**) at the aromatic ring.

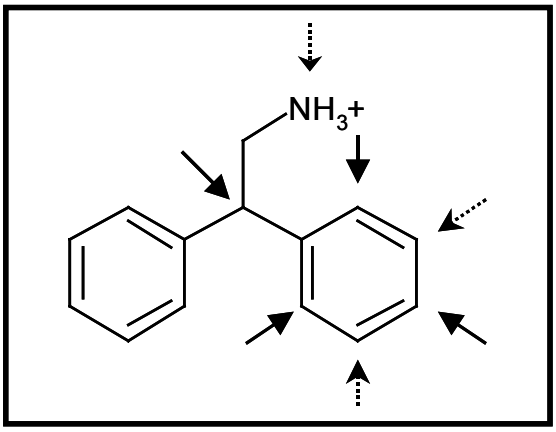


**Figure 3.1.8**

Positions at the scaffold of initial lead-compound **1** that upon chemical modification by attachment of substituents led to a) increased resonance shift (solid arrows); b) decreased resonance shift (dotted arrows).

### 3.1.5 Discussion

There is emerging interest in pharmaceutical sciences to find small molecules that bind to flat protein surfaces [Cochran, 2001]. Promising fields for application would be their use as inhibitors of protein-protein interactions [Cochran, 2000], or as ligands for proteins that lack cavities suitable for binding. Although results exist from combinatorial peptide libraries screened by phage display techniques [Sidhu, 2000], it is not immediately clear how these peptides can be converted into a small-molecule drug. Furthermore, the fact that no recognizable binding cavity exists in the target protein complicates a rational approach to the design of such molecules.

However, even if such detailed information does not exist a combinatorial library may be designed which is based on empirical knowledge about building blocks that have a high tendency to form interactions with proteins. S. Fesik and coworkers have performed a statistical investigation on data from NMR-based screening of 11 protein targets [Hajduk et al., 2000a] to discover functional groups or compounds that are privileged for binding to proteins. In his survey, two classes of compounds were statistically significantly enriched: biphenyl and carboxylic acid containing substructures. The rationale of the presented work was to start from a substructure that has such an increased likelihood to form suitable interactions with EDB and to find improved binders by a combination of directed synthesis and NMR-based screening.

Ligands that bind to cavities of proteins usually form several hydrogen bonds or ionic interactions. In contrast, for binding to flat surfaces, the number of contacts is reduced, simply due to the fact that possible interactions are limited to one side of the molecule and hence the specificity stemming from a three-dimensional fit of interactions is lost. Usually, this lack of interactions has to be compensated by increasing the size of the ligand, which clearly contradicts the pharmaceutical necessity of a small molecule. Hence, if a low-molecular weight compound is desired, interactions are required which are highly specific and contribute most favourably to the free energy of the bound state. Since multiple hydrophobic interactions are only suitable for large binding interfaces the most promising gain in affinity might result from charge complementarity and specific hydrophobic contacts, like aromatic ring stacking.

Nature has overcome the problem of obtaining high-affinity binders to protein surfaces lacking a cavity by using complementary electrostatics. This is nicely demonstrated by the interaction between the RNase barnase and its inhibitor barstar, leading to $K_D=10^{-14}$ M [Schreiber and Fersht, 1993]. Attempts in this respect have been made to optimize the association and affinity between TEM1 β-lactamase and its protein inhibitor BLIP [Selzer et al., 2000]. These examples suggest that electrostatic matching of a binder to the surface of a protein will probably play the most prominent role in future drug design.

In the present work, we have used a focused library of 113 compounds that should incorporate elements for both hydrophobic and electrostatic interactions. For this reason, the compounds contained at least one aromatic ring and a primary amino group. From this library, one lead-compound was identified (2,2-diphenylethylamine) which binds to EDB with a dissociation constant in the millimolar range. Chemical shift mapping which is unique in its ability to detect such weak interactions by [$^{15}$N,$^{1}$H]-HSQC NMR further revealed that the binding site of this compound is on the surface of EDB. Furthermore, chemical modifications of the 2,2-diphenylethylamine scaffold yielded a number of derivatives capable of specific binding to the same epitope on EDB and which exhibited larger changes in cross peak positions upon binding. Systematic variations of the initial hit revealed positions that are accessible to further modifications. Elongation of the molecular framework by using parallel synthesis, which in particular is focused at improving electrostatic interaction with the binding epitope may further improve the affinity of the initial lead-compound.

In the past, low-molecular weight compounds, binding to adjacent but non-overlapping epitopes on target proteins with affinities in the millimolar range, have been chemically linked to provide bidentate binders with much superior affinities [Shuker et al., 1996]. The chelate effect has long been recognized as a very effective means of achieving high binding affinities. This is not only the case for inorganic metal complexes, where it was first discovered [Cotton and Wilkinson, 1988; Huheey et al., 1993], but also for organic ligands [Jencks, 1975; Fersht, 2000] and for macromolecular binders [Neri et al., 1995]. If adjacent sites for binders could be discovered by the technique described above, substantial improvement in binding affinities are expected.

The affinities of the ligands described in this article are in the millimolar range and the complex with EDB is in fast exchange on the NMR time scale. Their binding is drastically poorer than the one of specific human monoclonal antibodies that have recently been reported by our group [Pini et al., 1998]. The failure to derive comparably good binders with the method described in this work might be due to the relatively small size of the library. Assuming that the change that occurs in ligand resonance frequencies upon complexation is less than 2 ppm, corresponding to 1000 Hz at 500 MHz, the decay rate of the complex should be less than 1000 $s^{-1}$ for slow exchange to occur. Since the complex is obviously in fast exchange the data are suggestive of kinetic dissociation constants/complex half-life in the (sub)-millisecond range. The best anti-EDB antibody described so far has a $k_{off} = 6 \times 10^{-6}$ $s^{-1}$, giving rise to a complex with EDB which has a half-life of more than a day. The results obtained, while providing a promising starting point for the design of multidentate EDB binders, underline the difficulty of isolating low-molecular weight binders towards hydrophilic globular proteins that are devoid of crevices. Several components of the extracellular matrix fall into this category. As mentioned above, this difficulty is recognized as a major problem for the pharmaceutical industry today. In the future, it will have to be shown if low-molecular weight binders of antibody-like affinity can be reached in an easy way. This would be of invaluable use for pharmaceutical purposes.

# PART II: High-molecular weight binders to EDB

## 3.2 Unexpected observation of concentration-dependent dissociation rates for antibody-antigen complexes in competition experiments

### 3.2.1 Abstract

The dissociation rate constant of bimolecular complexes between macromolecules ($k_{off}$) is often measured in solution by competition experiments and is generally expected to follow first-order kinetics.

When measuring $k_{off}$ constants by competition for three complexes of high-affinity recombinant antibody fragments with the cognate antigen and for one calmodulin/peptide complex, a surprising dependence between apparent dissociation rate and concentration of competitor (antigen or calmodulin-binding peptide) was observed.

Our results may be characteristic for macromolecules consisting of two domains (such as single-chain Fv fragments) and may reflect a transient opening of the two domains which are involved in the binding reaction, and which are connected by a polypeptide linker.

### 3.2.2 Introduction

A proper characterization of biologically-relevant antibodies often involves measurement of the dissociation constant for the antigen ($K_D$) and of the kinetic association and dissociation rate constants ($k_{on}$ and $k_{off}$) [Neri et al., 1996a]. To name just one application, the tumor-targeting ability of affinity-matured mutants of a monovalent antibody fragment has recently been correlated with the $k_{off}$ values of these antibodies towards the tumor antigen [Adams et al., 2001].
In first-order conditions, the kinetic dissociation constant $k_{off}$ is directly related to the half-life of the bimolecular complex $T_{1/2,off}$ in irreversible dissociation conditions, through the equation:

$$T_{1/2,off} = \ln(2)/ k_{off} = 0.693\ldots/ k_{off} \qquad \text{[Eq. 1]}$$

establishing an intuitive and direct relation between $k_{off}$ and life-time of the complex [Neri et al., 1996a], see Figure 3.2.1

Typically, irreversible dissociation conditions are achieved experimentally either by:

a) infinite dilution of the complex (which may pose sensitivity problems for the quantitation of the free ligand at different time points)

or

b) formation of a complex in which one of the binding partners is labeled, followed by addition of a large excess of unlabeled ligand (in order to prevent rebinding).

For example, $k_{off}$ values for several dozens of complexes between mutants of barnase and its inhibitor barstar have been measured by competition experiments. In most cases, the complex of barnase with tritiated barstar was competed with a molar excess (10-fold) of unlabeled ligand, followed by chromatographic separation of the kinetically stable complex [Schreiber and Fersht, 1993].

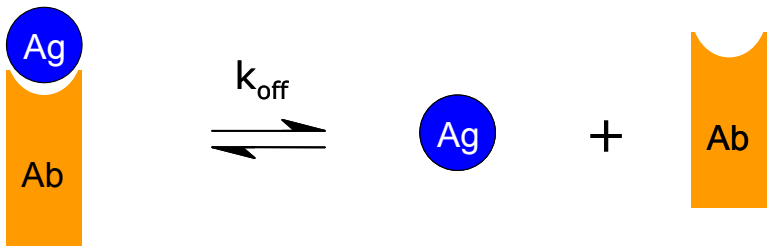


**Figure 3.2.1**

Schematic representation of the equilibrium between a binary antibody-antigen complex and its free components

(Ag = Antigen, Ab = Antibody)

We have recently established a robotic set-up for the high-throughput screening of affinity-matured antibody fragments derived from combinatorial libraries [Elia et al., 2002]. In some experiments, featuring competition ELISAs with well-characterized, monomeric antigens, we have observed a surprising dependence between apparent dissociation rate constants and concentration of competitive ligand used in the assay. Therefore, in order to better characterize to which extent competition experiments can be used for the measurement of $k_{off}$ constants for recombinant antibody fragments, we have investigated the binding properties of three well-characterized antibodies for their antigen, and of calmodulin for a high-affinity peptide.

As model system we chose two anti-lysozyme antibody fragments (D1.3 and HyHEL-10) in scFv format [Huston et al., 1988]. Both antibodies have been used in a variety of immunometric and biophysical assays. Furthermore, the crystal structure of these antibodies in the complex with hen egg lysozyme is known. Furthermore, we analyzed the binding properties of scFv(L19), a high-affinity antibody fragment specific for the EDB domain of fibronectin, a marker of angiogenesis [Pini et al., 1998]. This antibody fragment has been used in a variety of tumor targeting experiments, including a Phase I clinical trial for the immunoscintigraphic detection of solid tumors in patients with cancer [Santimaria et al., 2003].

Furthermore, we chose calmodulin and a high-affinity cognate peptide [Montigiani et al., 1996] (see Figure 3.2.2) as a further model bimolecular complex system, involving macromolecules other than antibodies.

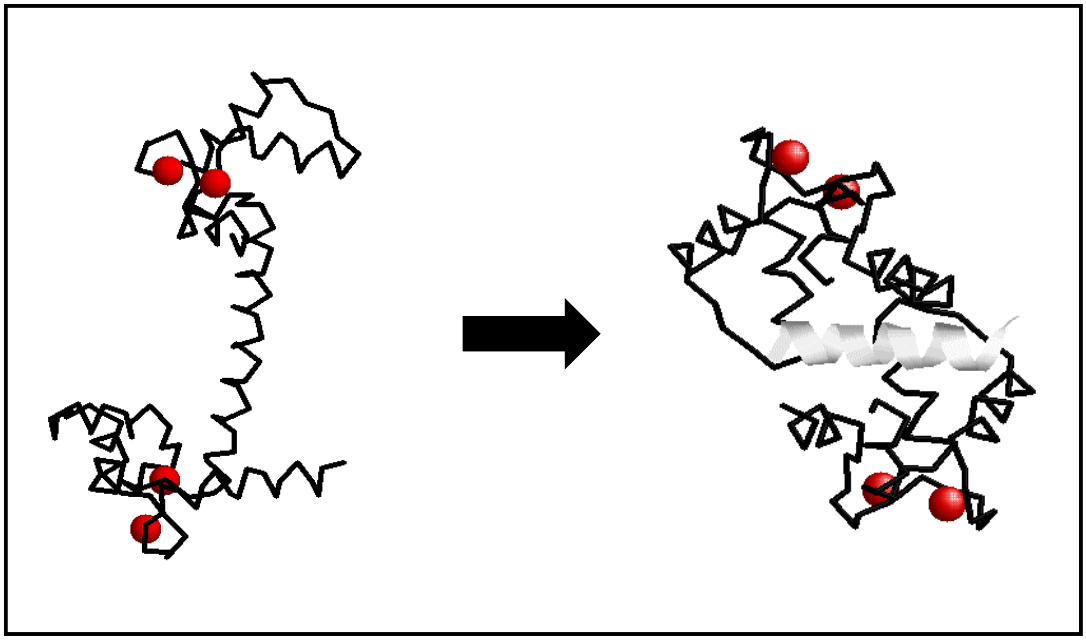

**Figure 3.2.2**

Structures of free Calmodulin (left) and of Calmodulin when bound to a Calmodulin-binding peptide (right)[Chattopadhyaya et al., 1992; Meador et al., 1993].Red balls indicate $Ca^{2+}$.

For all four model systems tested, a surprising dependence was observed between apparent dissociation rates and concentration of competitive ligands. In order to explain the observed deviation from the expected first-order kinetics, we propose a mechanism which features the transient opening of the two domains connected by a polypeptide linker, which are involved in the binding reaction in scFv fragments and in calmodulin.

### 3.2.3 Experiments and Methods

#### 3.2.3.1 Antibodies, antigens and calmodulin

scFv(D1.3), scFv(HyHEL-10) and scFv(L19) were expressed and purified on antigen columns as described [Neri et al., 1996b; Pini et al., 1998]. The three antibody fragments carried a FLAG tag at the C-terminal extremity, provided by the expression vector used.

Calmodulin and hen egg lysozyme were purchased from a commercial supplier (Cat. Nr. P2277 and L6876 respectively; Sigma, Buchs, Switzerland), while the fluorescently Cy5 labeled calmodulin-binding peptide H-CGGGAAARWKKAFIAVSAANRFKKIS-$NH_2$ was synthesized as described [Montigiani et al., 1996]. The iodoacetamido-Cy5 reactive fluorescent dye used for the coupling was purchased from Biological Detection Systems Inc., Pittsburgh, USA. Recombinant EDB and biotin-EDB were prepared as described [Pini et al., 1998]. EDB is biotinylated site specifically at the N-terminus, since this domain lacks lysine residues.

#### 3.2.3.2 Competition experiments

Competition experiments for the measurement of the rate constant for the calmodulin/peptide complex were performed essentially as described [Montigiani et al., 1996]: 250µl of a 1µM solution of calmodulin in TBSC was mixed with 25µl of 10µM Cy5-labeled calmodulin-binding peptide CGGGAAARWKKAFIAVSAANRFKKIS and the complex was allowed to form for 1 minute. 20µl of this solution was aliquoted into 8 tubes. To control tube 1 (no competition), 4µl of TBSC was added. To test tubes 2-8 4µl of a serial dilution of unlabeled calmodulin-binding peptide dissolved in TBSC was added: 2909µM (640x molar excess over Cy5-labeled peptide), 1454.5µM (320x excess), 727µM (160x excess), 363.5µM (80x excess), 181.8µM (40x excess), 90.9µM (20x excess) and 45.5µM (10x excess). In control samples, equilibrium conditions were established by

premixing 1.8µl of 10µM Cy5-labeled peptide with 4µl 45.5µM unlabeled peptide (10x molar excess) and 4µl 90.9µM unlabeled peptide (20x molar excess), respectively, followed by addition of 18.2µl of a 1µM solution of calmodulin in TBSC. All tubes were kept at 4°C for 72h. The samples (20µl of a solution of 24µl of the competition reaction, 24µl of TBSC and 12µl of 5x native loading buffer (TBSC, containing 40% (v/v) glycerol and bromophenol blue)) were analysed by native polyacrylamide gel electrophoresis as described [Montigiani et al., 1996] and the resulting gels were imaged with the DIANA-II CCD-camera system (Raytest, Straubenhardt, Germany) using Cy5 excitation and emission filters.

Competition experiments for the antibody/antigen complexes were performed as follows. Microtiter plates (NUNC, Roskilde, Danmark) were coated overnight (100µl/well) with 20 µg/ml of the FLAG-specific M2 antibody (F3165; Sigma, Buchs, Switzerland) in PBS (50 mM sodium phosphate + 100 mM NaCl, pH 7.4) containing 0.1% sodium azide. The plates were blocked for 3h at RT with 200µl/well PBS containing 4% dried skimmed milk and washed 3 times each with PBS containing 0.1% Tween-20 and PBS. The scFv antibody fragment (HyHEL-10, D1.3 and L19, each 7.5µg/ml, 100µl/well) in PBS containing 1% dried skimmed milk was allowed to bind at RT for 45 min. The plates were then washed 3 times with PBS containing 0.1% Tween-20 and 3 times with PBS. The biotinylated antigen was then applied (100µl/well of 4µg/ml biotinylated lysozyme and biotinylated EDB, respectively) and allowed to bind at RT for 30 min.
At different time points, 20µl of a solution of unlabeled antigen in PBS (240µg/ml, 600µg/ml, 1200µg/ml, 2400µg/ml, 4800µg/ml and 9600µg/ml, giving rise to a 12-, 30-, 60-, 120-, 240- and 480-fold excess of unlabeled antigen over biotinylated antigen) were added and the competition was stopped by washing the plates 5 times each with PBS containing 0.1% Tween-20 and PBS. 100µl/well of a 1:500 dilution of streptavidin-HRP conjugate (Amersham Pharmacia Biotech, Buckinghamshire, UK) in PBS was added and allowed to bind to the biotinylated antigen at RT for 15 min. The plates were washed 5 times with PBS containing 0.1% Tween-20 and 5 times with PBS and developed by addition of 100µl/well POD blue substrate (Roche

Diagnostics, Mannheim, Germany). The color reaction was quenched by addition of 60µl/well of 1M sulphuric acid and absorbance values determined at 450nm using a VERSAmax plate reader (Molecular Devices, Sunnyvale, CA, USA).

### 3.2.4 Results and Discussion

Figure 3.2.3 a) shows a representation of the experimental scheme used for the measurement of $k_{off}$ constants for scFv(D1.3), scFv(HyHEL-10) and scFv(L19). The FLAG-tagged scFv fragments were captured on a microtiter plate, coated with the anti-FLAG M2 monoclonal antibody, in a fashion that does not interfere with antigen binding. After saturation of the plate with biotinylated antigen, a molar excess of unlabeled antigen (acting as competitor) was added and the competition reaction allowed to proceed for different time values.

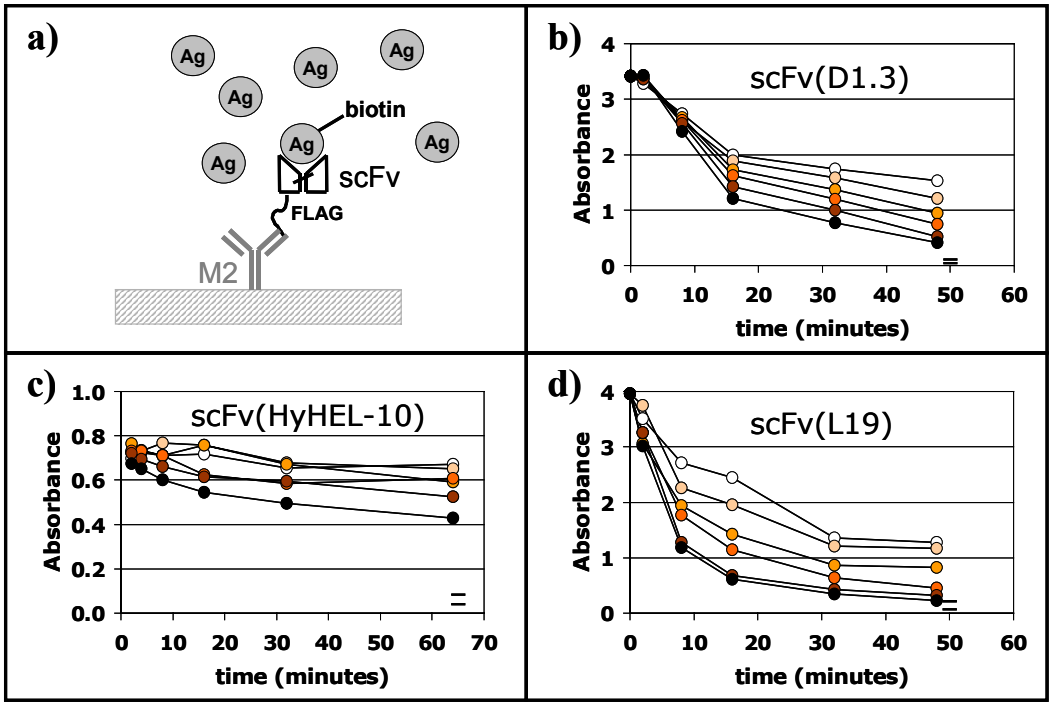


**Figure 3.2.3**

a) Schematic representation of the competition ELISA used. The complex between scFv antibody and biotinylated antigen is competed with unlabeled antigen at different molar excess over biotinylated antigen (Ag = Antigen; scFv = scFv antibody fragment; FLAG = DYKDDDK peptidic tag)

b)–d) Results of the kinetic competition ELISA with the following antibody complexes: b) scFv(D1.3) / lysozyme; c) scFv(HyHEL-10) / lysozyme and d) scFv(L19) / EDB. Concentration series of molar excess of antigen over biotinylated antigen (12-, 30-, 60-, 120-, 240- and 480-fold excess) with a color coding, ranging from white (○: 12-fold) to black (●: 480-fold)). The minimum and maximum ELISA signal of the equilibrium reaction, obtained by premixing biotinylated antigen with a 12 -, 30-, 60-, 120-, 240- and 480-fold excess of unlabeled antigen, respectively, are represented by two lines at the the end of the time-frame of b) – d)

At the end of the competition time, plates were washed and the residual biotinylated antigen was detected using a streptavidin-based colorimetric assay.
Figure 3.2.3 b)-d) shows the time course of the competition experiment for scFv(D1.3), scFv(HyHEL-10) and scFv(L19), respectively. In all cases, a concentration dependence was observed, in the sense that competition was faster, with increasing concentrations of competitor (ranging between 12-fold and 480-fold excess of unlabeled competitor antigen, relative to the concentration of labeled antigen). The extent of competition reaction was lower for scFv(HyHEL-10), consistent with the extremely high kinetic stability of this complex [Neri et al., 1996b]. For all competition reactions (and for each concentration of competitor), the equilibrium level was experimentally measured by simultaneous incubation of the antibody with both biotinylated and unlabeled antigen. As expected, the ELISA levels of these equilibrium reactions, performed with the various molar excesses of competitor, were very low and close to the background of the assay Figure 3.2.3 b)-d). The competition experiments depicted in Figure 3.2.3 a) were also performed using radioiodinated antigen, obtaining results similar to the ones depicted in Figure 3.2.3 b)-d) [data not shown].

In order to further validate the generality of the findings, we investigated a competition reaction in solution of a well-characterized, non-antibody-based bimolecular complex. Calmodulin is a 148-aminoacid protein, capable of $Ca^{2+}$ -dependent binding to specific peptides with dissociation constants in the picomolar range [Montigiani et al., 1996]. Calmodulin consists of two structurally-homologous domains, connected by a short peptidic linker, which are able to wrap around amphipathic target peptides. The specific calmodulin-binding peptide CGGGAAARWKKAFIAVSAANRFKKIS [Montigiani et al., 1996] was labeled with the fluorescent dye Cy5 at the N-terminus in order to monitor the competition reaction, without interfering with calmodulin binding. The competition reaction was performed in solution, and monitored by native polyacrylamide gel electrophoresis as described [Montigiani et al., 1996]. Interestingly, also in this case the rate of competition (reflecting an apparent dissociation rate) was clearly dependent on the concentration of unlabeled competitor peptide [Figure 3.2.4 a)].

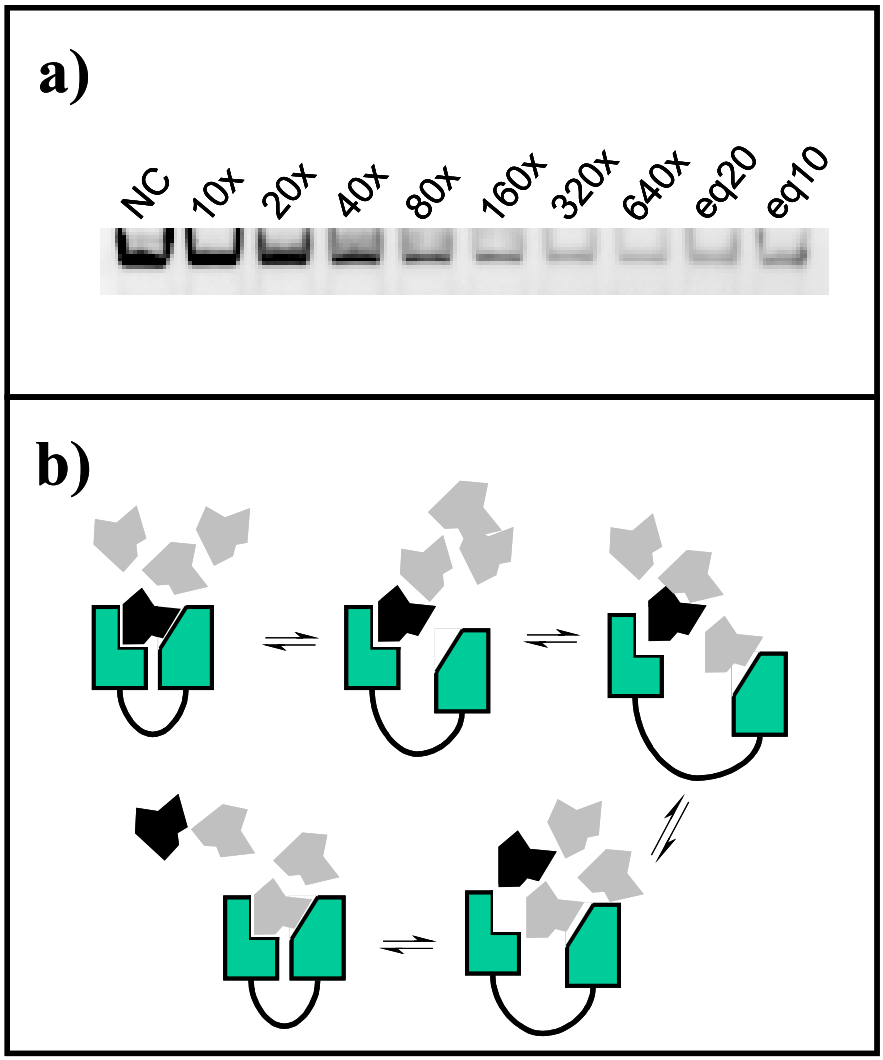


**Figure 3.2.4**

a) Results of the competition of the complex between calmodulin and Cy5-labeled calmodulin binding peptide with unlabeled calmodulin binding peptide. The complex containing Cy5-labeled peptide is monitored by native polyacrylamide gel electrophoresis by means of the Cy5-fluorescence of its corresponding band (NC = no competitor; 10-fold – 640-fold excess of unlabeled peptide over Cy5-labeled peptide; eq20 (eq10) = complex formation between calmodulin and a 20:1 (10:1) molar excess of unlabeled peptide and Cy5-labeled peptide, representing the equilibrium state).

b) schematic representation of the suggested two-step mechanism for the displacement of bound antigen (black) from a bidentate binder (green) by an excess of antigen (gray), consistent with the observed concentration dependence in the rate of the competition reactions.

The results obtained in this article, which are in contrast with first-order competition kinetics often used to describe the irreversible dissociation of bimolecular complexes, can be rationalized with the following model. Both scFv fragments and calmodulin consist of two interconnected domains, which are essential for the high-affinity binding to the target polypeptide. If at a certain time point one of the two domains transiently detaches from the target antigen (or peptide), rebinding could be inhibited by increasingly high concentration of competitor, therefore effectively speeding up competitions [Figure 3.2.4 b)].

## 3.3 Robotic Isolation of EDB-specific derivatives of the L19 antibody

### 3.3.1 Abstract

The human antibody fragment scFv(L19), specific for the EDB domain of fibronectin, has been used as a selective targeting agent for neo-vasculature in animal models of angiogenesis-related diseases and patients with cancer. It would be desirable to select L19 variants with higher affinity towards the antigen, particularly for applications in which the antibody fragment is used in monomeric form.

Here we describe the construction of a library obtained by partial randomization of the CDR3 loop of the VL domain of the L19 antibody. After biopanning using biotinylated EDB as capture reagent, a variety of L19 derivatives were obtained, which were characterized by DNA sequencing and by robotic ELISA assays. A number of L19 derivatives with binding properties comparable to the one of L19 were identified. The new robotic station for antibody screening allows the rapid analysis of > 1000 antibody clones. The observation that the L19 sequence can accommodate mutations without loss of functional affinity suggests that a more radical mutagenesis approach, combined with extensive screening of EDB binders, may yield affinity matured derivatives of the L19 antibody.

### 3.3.2 Introduction

Angiogenesis, i.e., the proliferation of new blood vessels from pre-existing ones, is an underlying process in many human diseases, including cancer, blinding ocular disorders and rheumatoid arthritis. The ability to selectively target and occlude neovasculature will be potentially useful in diagnosis and treatment of angiogenesis-related diseases [Folkman, 1995; Carmeliet, 2000; Carmeliet and Jain, 2000].

A good-quality marker for both tumoral and non-tumoral neovasculature is the extra-domain B (EDB) of fibronectin, a sequence of 91 aminoacids that can be inserted into the fibronectin molecule by a mechanism of alternative splicing [Zardi et al., 1987].

To date, the production of monoclonal antibodies directly recognising the EDB domain has not been possible using hybridoma technology, because of tolerance. In collaboration with Prof. Dr. Luciano Zardi (Istituto Nazionale per la Ricerca sul Cancro, Genova, Italy), we have overcome this problem using large synthetic antibody phage libraries, generating several high-affinity antibody fragments specific for fibronectin containing the EDB domain, and mapping their epitope onto the three-dimensional structure of the antigen (see Chapter 2.3.2). These antibodies stain vascular structures in tumor sections and selectively target tumor neovasculature, as shown in tumor-bearing mice using infrared fluorescence and radioactive techniques. Increased binding affinity leads to improved targeting of tumoral angiogenesis, as demonstrated by biodistributions studies performed using the L19 antibody fragment with affinity for the EDB domain in the picomolar range and L19 mutants with reduced affinity [Viti et al., 1999].

Recently, the ability of the antibody fragment scFv(L19) to target the tumor neo-vasculature in patients with cancer has been demonstrated [Santimaria et al., 2003].

The binding properties of the L19 antibody appear to be sufficient to provide an efficient tumor targeting in a variety of antibody formats [Borsi et al., 2002] and for a variety of antibody derivatives [Birchler et al., 1999a ; Nilsson et al., 2001; Carnemolla et al., 2002]. However, in some *in vivo* applications, particularly when scFv(L19) derivatives were used in monomeric format, the tumor targeting performance was not spectacular [Viti et al., 1999; Halin et al., 2002b], suggesting

that affinity-matured versions of the L19 antibody may perform better in *in vivo* targeting experiments when used as monomers.

For chemical equilibria describing a bimolecular complex formation, the affinity of one binding partner for the other is expressed by the the affinity constant $K_A$, or by its reciprocal $K_D$ (i.e. $K_A = 1/ K_D$).

The dissociation constant $K_D$ is also linked to the kinetic association and dissociation constants, $k_{on}$ and $k_{off}$, through the relation:

$$K_D = k_{off} / k_{on} \qquad \text{[eq. 1]}$$

In conditions of irreversible dissociation of the antibody-antigen complex (e.g., when one of the binding partners is anchored on a solid support and the other one is washed away, as soon as the complex dissociates), the half life of the complex ($T_{1/2}^{off}$) is independent of concentration and is expressed by the equation (Neri et al., 1996b):

$$T_{1/2}^{off} = \ln(2) / k_{off} \approx 0.69 / k_{off} \qquad \text{[eq. 2]}$$

For example, a kinetic dissociation constant of $10^{-3}$ $s^{-1}$ would correspond to a complex half-life of 690 s = 11.5 min; a kinetic dissociation constant of $10^{-5}$ $s^{-1}$ would result in a half-life of 20 hours. One would be tempted to conclude that parameters such as residence time of a targeting agent at the tumor site could be directly predicted on the basis of Eq. 2. Even though knowledge of the $k_{off}$ constant is a precious information when planning tumor targeting experiments, in practice rebinding effects and multivalent binding can significantly increase residence time on tumor.

Velocity of complex formation, in the initial rate approximation, is a function of ligand concentration and of the kinetic association constant, $k_{on}$. It could therefore be expected, that tumor targeting agents with high $k_{on}$ values would target tumors more rapidly than agents with low $k_{on}$. However, tumor targeting is a multi-compartment pharmacokinetic problem (blood and perivascular spaces representing at least two of the compartments), and the influence of $k_{on}$ values on tumor targeting remains to be experimentally addressed. Fast association kinetics are likely to be important for one-compartment systems such as targeting of tumoral new-forming blood vessels

(angiogenesis) [Otte et al., 1998]. High affinity constants (and possibly high kinetic association constants) are probably important determinants of the good tumor targeting performance of small tumor targeting agents such as radiobiotin ([Paganelli et al., 1991b] ; Avicidin™, NeoRX Corporation, Seattle, U.S.A.) and octreotide derivatives [Otte et al., 1998].

A number of techniques can be used for the measurement of antibody affinity and kinetic constants [Neri et al., 1996a; Huber et al., 1999]. The approach generally used to determine affinity constants consists in determining at equilibrium the ratio of the concentrations of the antibody (or antigen) free and engaged in complex, at several total antibody (or antigen) concentrations. This ratio is measured either directly (for example by physically separating bound and unbound species by equilibrium dialysis or gel electrophoresis) or indirectly (by monitoring a reporter, such as fluorescence variation, which is diagnostic for antibody binding to its antigen).

The kinetic association constants for the binding reaction between scFv(L19) and recombinant EDB has been measured by BIAcore surface plasmon technology [Huber et al., 1999], as being $k_{on} = 1.1 \times 10^5\ s^{-1}M^{-1}$. The kinetic dissociation constant was measured with different experimental techniques and gave different values. Competition experiments (e.g., with ELISA detection or electrochemiluminescence) showed a very long half-life for the L19-EDB complex ([Pini et al., 1998]; see chapter 2.3.2). However, while homodimeric preparations of scFv(L19) gave long half-lives of the L19-EDB complex on the BIAcore in irreversible dissociation conditions ([Pini et al., 1998], monomeric preparations of scFv(L19) yielded BIAcore values of $k_{off}$ in the order of $10^{-2} – 10^{-3}\ s^{-1}$ (see Figure 3.3.1) It is not clear, at present, whether these values are the real $k_{off}$ values for the bimolecular complex between monomeric scFv(L19) and EDB, or whether these values are higher due to electrostatic repulsion on the negatively charged BIAcore microsensor chip, or to suboptimal folding of the antibody in bacterial preparations [Nowakowski et al., 2002].

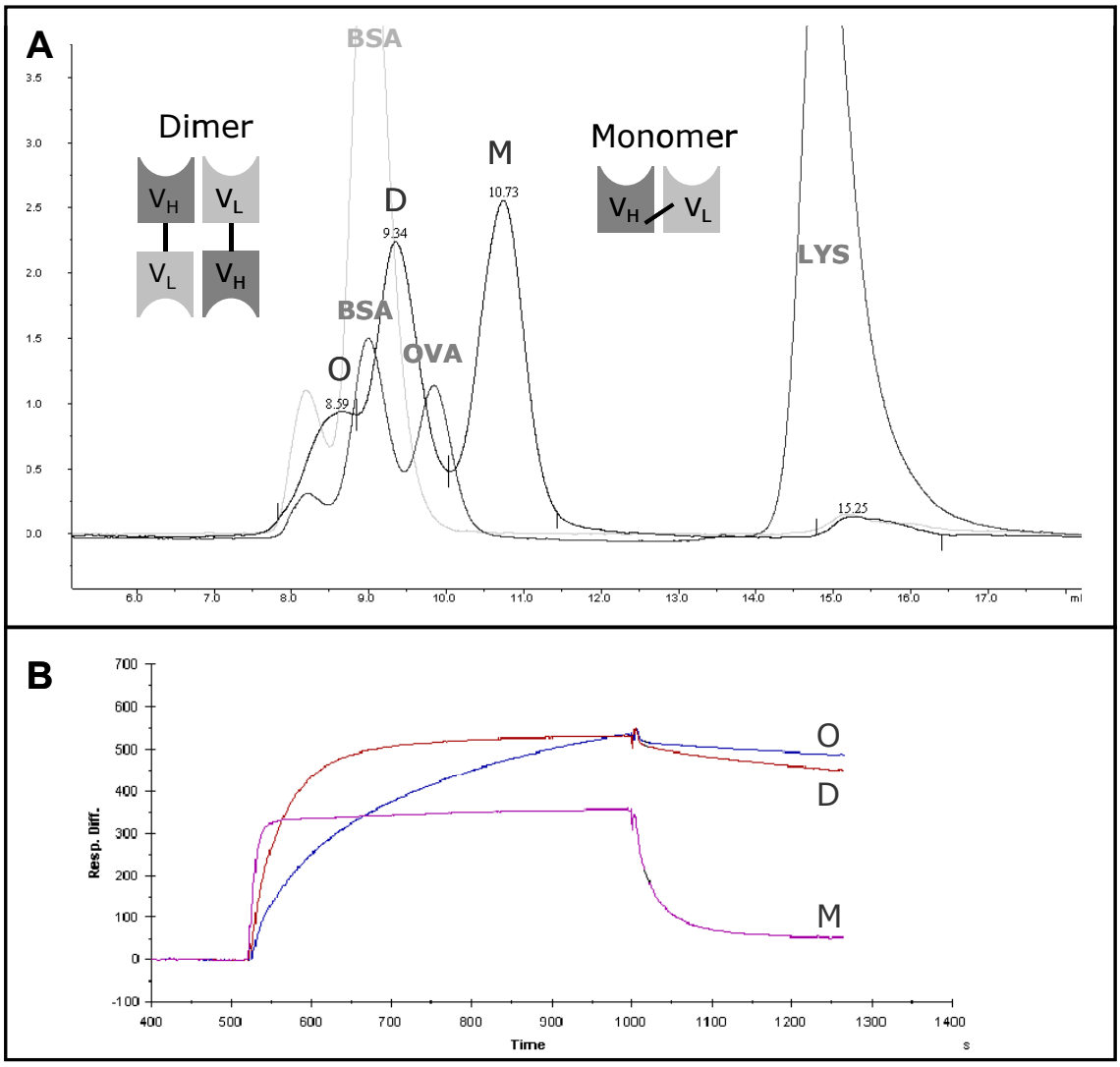


**Figure 3.3.1**

**A)** Size-exclusion chromatogram of affinity-purified L19 derivative supernatant using a Superdex 75 HR 10/30 column (Amersham Pharmacia, Uppsala, Sweden) and PBS as buffer. Absorbance at 280nm is plotted over elution volume in ml. For calibration bovin serum albumin (BSA, 67 kDa), Ovalbumin (OVA, 45 kDa) and hen egg white lysozyme (LYS, 14 kDa) were used. Monomeric (M, MW approx. 27 kDa), dimeric (D, MW approx. 54 kDa) and oligomeric (O) scFv eluted at 10.73, 9.34 and 8.59 ml, respectively.

**B)** BIAcore surface plasmon resonance sensorgram of above mentioned heteromeric scFv on a EDB-coated CM5 chip: Resonance Units (RU) are plotted over time. In the dissociation phase, monomeric scFv give rise to a fast decay of the signal while dimeric and oligomeric preparations exhibit signal stability, thus having much better apparent $k_{off}$ values, due to avidity.

Due to the fact that bacterial supernatants of clones expessing scFv antibody fragment always contain monomeric, homodimeric and homooligomeric scFv species in varying amounts, screening of these supernatants by surface plasmon resonance in oder to rank these scFv producing clones according to their affinity to the cognate antigen is impossible. The same, of course, is true when using an ELISA assay which does not prevent avidity artifacts (as e.g. the SA-ELISA, see below).

In order to solve this problem, we have set-up an ELISA assay (M2-ELISA, see below) which gives results independent of the oligomeric state of the scFv antibody.

By performing this ELISA as a competition ELISA, $k_{off}$ values of the different antibodies can be obtained and ranked, according to the scheme depicted in Figure 3.3.2.

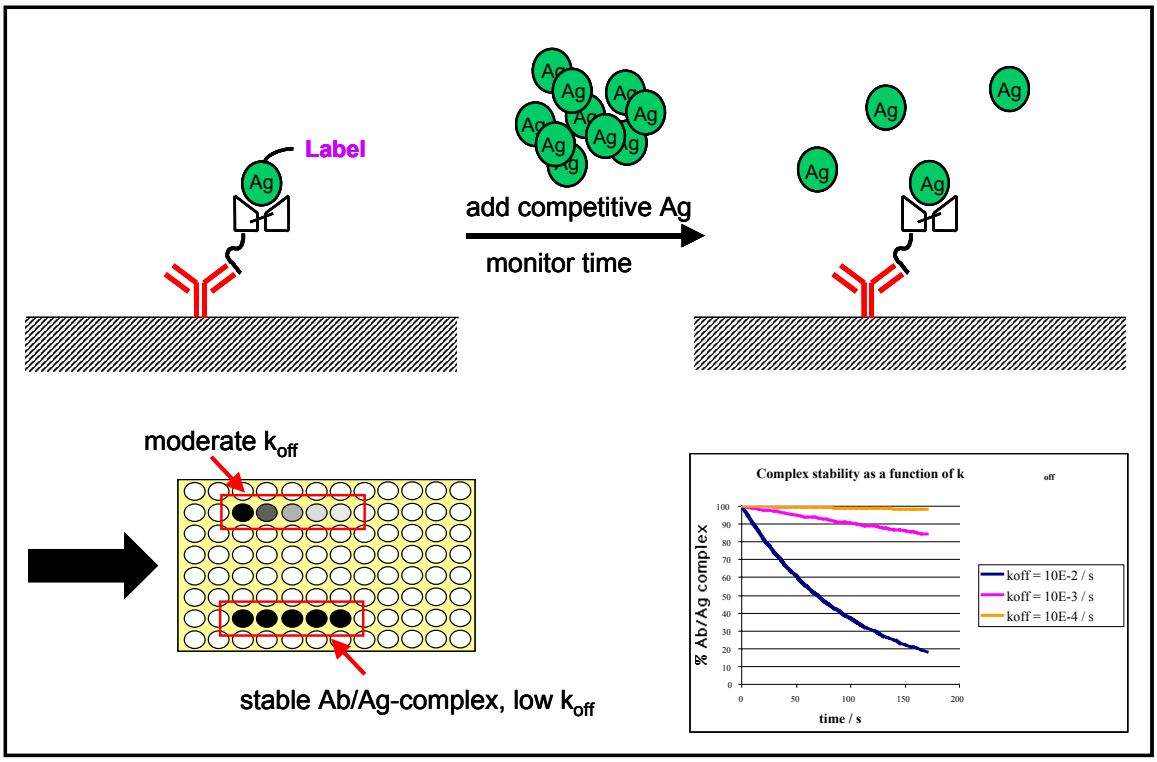


**Figure 3.3.2** Screening strategy for better $k_{off}$ by competition ELISA independent of the oligomeric state of the scFv antibody fragments. Clones exhibiting signal stability have low $k_{off}$ values.

As a first step towards affinity-maturing the scFv(L19), we have cloned a phage-display library of scFv(L19) mutants, partially randomized at the level of the CDR3 loop of the VL domain. Several EDB binders were isolated by biopanning and characterized by means of a robotic ELISA assay.

### 3.3.3 Materials and Methods

#### 3.3.3.1 Library construction

Library cloning and construction was performed essentially as described by Viti el al. [Viti et al., 2000]:

Preparation of phagemid vector

purified phagemid vector pDNEK [Pini et al., 1998] was prepared using the QIAfilter Plasmid Maxi Kit (Qiagen, Basel, Switzerland).

The vector was double digested with NcoI/NotI (NcoI: 1U/µg DNA; NotI: 2U/µg DNA; DNA concentration in the digestion mixture was lower than 0.1µg /µl) for 4h, at 37°C.

Double digested vector was purified by cutting the corresponding band from a 1.4% agarose gel and reeluting it from the gel according to the QIAEX II Gel Extraction Kit (Qiagen, Basel, Switzerland). (The double digested vector could easily be separated from single digested vector and the 1600bp stuffer fragment between the NcoI and NotI restriction site. The resulting vector was stored until use at –80°C.

PCR products: VH-, VL-randomized genes, PCR3-product

Heavy and light chain V gene PCR-products and PCR3-product were prepared in parallel PCR reactions:

20 pmoles of non-degenerate primer, 40 pmoles of degenerate primer, < 30 ng scFv template, 5mM dNTPs, appropriate Taq polymearse buffer were used in a total reaction volume of 50 µl. Reaction vessels were transferred to a thermal cycler and subjected to the following cycling program: 94°C(3') - [94°C(1')-60°C(1')-72°C(1')]$_{25\ cycles}$- 65°C(2'). When the samples had reached the temperature of 94°C, 3U of Taq polymerase (Appligen Oncor, Basel, Switzerland) were added. Two pairs of oligonucleotide primers were used (see Table 3.3.1): LMB3long and fo1_VH for the generation of the degenerate VH fragment, CDR3balong and fo2_VL for the generation of the degenerate VL fragment and VLCDR3toNotBa and LMB5 for the generation of PCR3-product. PCR products of the correct size were purified by

agarose gel extraction using a commercially available kit (QIAquick Gel Extraction, Qiagen, Basel, Switzerland).

PCR Assembly of VH fragment, VL fragment and the PCR3-product

PCR assembly was performed in 42 parallel reactions of 50µl reaction volume, using as templates 100ng of each of the previously described PCR-products. 5mM dNTPs, appropriate Taq polymearse buffer, 20 pmoles of primers LMB3long and FdSeq1long and 100U of Taq polymerase (Appligen Oncor, Basel, Switzerland) were used and the reaction vessels ransferred to a thermal cycler and subjected to the following cycling program: 94°C(3') - [94°C(45'')-65°C(45'')-72°C(2')]$_{25\ cycles}$- 72°C(5'). The resulting PCR-product of correct size was purified using the QIAquick PCR Purification kit (Qiagen) and sequentially digested for 4h at RT with restriction enzymes NcoI and NotI, respectively (NcoI: 2U/µg DNA; NotI: 4U/µg DNA; DNA concentration in the digestion sol.: lower than 0.1 µg/µl).

The digested PCR-fragment of correct size was purified by agarose gel extraction using the QIAquick Gel Extraction kit (Qiagen, Basel, Switzerland) and stored until use at –80°C.

Ligation

3µg of NcoI/NotI digested vector and 2µg of NcoI/NotI digested VH-VL PCR-product were ligated for 14-18 hours at 15°C using 50 Weiss-Units of T4 DNA Ligase (Böhringer Mannheim, Mannheim, Germany). The quality of the ligation was controlled on a 0.8% agarose gel and the DNA was purified by Phenol extraction, followed by Ethanol / sodium acetate precipitation and two 70% Ethanol washes, according to standard protocols. Finally, the precipitated DNA was dissolved in 100 µl of sterile water.

Electrocompetent *E.Coli* TG1 cells

Electrocompetent *E. coli* TG1 cells were prepared as follows:

1 liter of 2xYT growth medium was inoculated with 1/100 volume of an overnight culture of TG1 bacteria and grown to $OD_{600}$ = 0.5-0.7. In a prechilled rotor and prechilled bottles the cells were centrifuged at 4000 g for 15 min, resuspended in the

original volume of ice cold 1mM Hepes pH 7.0 in water, containing 5% glycerol and centrifuged as before.

The cells were then resuspended in half of the original volume of ice cold 1mM Hepes pH 7.0 in water, containing 5% glycerol and centrifuged as before, followed by 2 times resuspension in 40ml of ice cold 10% glycerol and centrifugation as before. Finally, the cells were resuspended in 2ml of ice cold 10% glycerol and immediately used for electroporation.

Electroporation of *E.coli* TG1 cells with the DNA construct

100µl of ligated DNA was mixed with 2 ml of fresh electrocompetent *E.coli* TG1 cells. Aliquots of 100µl were electroporated (Gene Pulser II Electroporation System, BioRad, California 94547, U.S.A., Set parameters: Capacitance: 25 µF; Voltage: 2.5 kV; Resistance: 200 Ω). Immediately after every electroporation 100 µl of sterile 2xYT, containing 100µg/ml ampicillin and 1% (w/v) glucose, were added and the electroporation plated on a plate of 20 cm diameter (2xYT, containing 100µg/ml ampicillin and 1% (w/v) glucose) by gently spreading with a sterile glass loop on half of the plate's surface. Appropriate dilution series of transformed bacteria were prepared after the $5^{th}$ and $10^{th}$ electroporation round and plated on standard petri dishes with 2xYT, containing 100µg/ml ampicillin and 1% (w/v) glucose, in order to calculate the size of the library. The big electroporation plates were incubated overnight at 30°C. The size of the resulting library [Size = (number of colonies on a plate) x (dilution factor) x (number of electroporations)] was determined to be $2 \times 10^7$ bacterial clones.

Rescue and aliquoting of the library

5 ml of 2xYT, containing 100µg/ml ampicillin, 1% (w/v) glucose and 25% (v/v) glycerol, was applied to each plate and bacteria gently loosened with a sterile glass spreader until a homogeneous suspension resulted. The suspensions obatined from all the plates were mixed and aliquoted (500µl/sterile tube), frozen in liquid nitrogen and stored at –80°C.

Library quality control

PCR screening of individual colonies of the library (for detection of the presence of the scFv coding sequence) and Dot Blot analysis (for detection of clones expressing soluble scFv fragments) were used to assess the quality of the library.

PCR screening: In a total reaction volume of 20µl 20 pmoles of each primer [LMB1bis (5' - GCG GCC CAG CCG GCC ATG GCC GAG -3') and JforNot (5'- TCA TTC TCG ACT TGC GGC CGC TTT GAT TTC CAC CTT GGT CCC TTG GCC GAA CG -3')] , 5mM dNTPs, appropriate Taq polymerase buffer, 0.3 U Taq polymerase (Appligen Oncor, Basel, Switzerland) were used. As template, individual bacterial colonies were picked and added to the reaction, then the PCR reaction was started on the above mentioned thermal cycler, using the program: 94°C(10') - [94°C(1')-60°C(1')-72°C(2')]$_{30\ cycles}$-65°C(2'). 20 out of 20 clones showed to be positive for the scFv gene insert.

Dot Blot analysis of soluble scFv fragments: Individual bacterial clones were picked with a toothpick and inoculated into 96-well plates with 130µl/well of 2xYT, containing 100µg/ml ampicillin and 1% (w/v) glucose. Colonies were allowed to grow for 3 h at 37°C (shaking at 220 rpm) and then induced by addition of 50 µl/well of 2xYT, containing 100µg/ml ampicillin and 10 mM Isopropyl-β-D-1-thiogalactopyranoside (IPTG). The plates were then incubated for 16 h at 30°C (shaking at 220 rpm), centrifuged at 1800 x g for 10 min and 2 x 3µl/well were applied to a nitrocellulose membrane which was then blocked for 30 min with 4% MPBS, washed 3 times with PBS/0.1 % Tween-20 and 3 times with PBS (5 min each).

The FLAG tag of the scFv fragments could then eventually be detected with M2 anti-FLAG antibody (1:1000 dilution, Cat.Nr. F-3165, Sigma, Buchs, Switzerland; 40 min incubation, followed by washing 3 times with PBS/0.1 % Tween-20 and 3 times with PBS) and anti-mouse-HRP antibody (1:1000 dilution, Cat.Nr. A-2554 Sigma, Buchs, Switzerland; 40 min incubation, followed by washing 3 times with PBS/0.1 % Tween-20 and 3 times with PBS) which gave rise to an enzymatic reaction generating luminescence (ECL-Plus Kit according to manufacturer instructions, Amersham Pharmacia Biotech, Uppsala, Sweden). The majority of the clones showed expression of soluble scFv fragments (see Figure 3.3.7)

### 3.3.3.2 Biopanning

Phage preparation

Phage preparation of the L19-MAT1 library was performed as described by Viti et al. [Viti et al., 2000]. In short, a bacterial culture harboring clones of the library was grown and infected with non-lytic helper phage VCS-M13 ($10^{12}$ t.u.) and infected clones were allowed to grow at 30°C over night. The bacterial culture was centrifuged and the produced phages were PEG-precipitated from the bacterial supernatant. After a further PEG-precipitation, the phages were redissolved in 5ml PBS and aliquoted. After addition of glycerol, the phages were frozen with liquid nitrogen and stored at –20°C. The titer of produced phages was determined to be 1.8 x $10^{12}$ t.u./ml.

Selection SEL_1, SEL_2 and control selection

SEL_1 was performed essentially as described by Pini et al [Pini et al., 1998]:
Phages ($10^{11}$ t.u., dissolved in 250µl PBS) were mixed with 250µl of 4% MPBS, 5µl of Tween-20 and 0.4µl of biotinylated EDB [Biot.-S-S-EDB, see [Viti et al., 2000]] (final concentration: 50 nM) in a 1.5ml tube. After 25 minutes, this mixure was applied to 150µl magnetic Dynabeads M-280 Streptavidin (Dynal, Oslo, Norway), preblocked at RT for 1 h with 4% MPBS. The beads were resuspended in the phage mix and incubated for 25 min at RT (gently rotating). The beads were separated by means of a magnet and the phage containing supernatant was removed. 5 cycles of washing, i.e. addition of ca. 1 ml of PBS/0.1% Tween-20, magnetic bead separation and removal of the supernatant were performed, followed by 5 further washing cycles performed with PBS alone. Phages still bound to the beads were then eluted with 300µl of a 50 mM solution of dithiothreitol (Cleland's reagent) in PBS and directly used for infection of exponentially growing *E. coli* TG1 ($OD_{600}$ = 0.5).
SEL_2 was performed essentially the same way as SEL_1, but an additional competition step was carried out: 10 minutes after mixing the phages ($10^{11}$ t.u.) with MPBS, Tween-20 and biotinylated EDB, a 1000-fold molar excess of unbiotinylated antigen (final concentration: 50 µM) was added and allowed to compete out kinetically weakly binding phages for 15 minutes.

A control selection was performed likewise SEL_1, but omitting the addition of biotinylated EDB.
Titers of the phages after selection were determined to be 1.1 x $10^6$ t.u./ml (SEL_1), 4.2 x $10^4$ t.u./ml (SEL_2) and 3 x $10^3$ t.u./ml (control selection), respectively.

Growth of library after selection

Exponentially growing *E. coli* TG1 were infected at $OD_{600}$ = 0.5 with the collected phages for 40 minutes at 37°C. For titration dilution series of phage-infected bacteria were plated and kept at 30°C over night. The remaining infected TG1 were centrifuged at 3000 x g for 10 min resuspended in 500µl 2xYT and plated on a 20 cm diameter plate with 2xYT, containing 100µg/ml ampicillin and 1% (w/v) glucose. After overnight growth at 30°C, the bacteria were rescued by loosening them from the agar, using 5 ml of 2xYT, containing 100µg/ml ampicillin, 1% (w/v) glucose and 25% (v/v) glycerol. The homogeneous suspensions obtained were frozen in liquid nitrogen and stored at –80°C.

#### 3.3.3.3 ELISA

M2-ELISA and M2-competition ELISA (96-well format)

Microtiter plates (Maxisorp, NUNC, Roskilde, Danmark) were coated overnight at 4°C with 20 µg/ml of the FLAG-specific M2 antibody (F3165; Sigma, Buchs, Switzerland) in PBS containing 0.1% sodium azide (100µl/well). The plates were blocked for >3h at RT with 200µl/well 4% MPBS, then washed 3 times with PBS/0.1% Tween-20 and PBS alone. scFv supernatants in PBS containing 1% dried skimmed milk were allowed to bind at RT for 45 min. The plates were then washed 3 times with PBS containing 0.1% Tween-20 and 3 times with PBS. The biotinylated antigen was then applied (100µl/well of biotinylated EDB, typically at 2 µg/ml) and allowed to bind at RT for 30 min. When performed as a competition experiment, 20µl of a solution of unlabeled EDB in PBS (typically at 50 µg/ml) was added at different time points, and the competition was stopped by washing the plates 5 times each with

PBS containing 0.1% Tween-20 and PBS alone. 100µl/well of a 1:500 dilution of streptavidin-HRP conjugate (Amersham Pharmacia Biotech, Buckinghamshire, UK) in PBS was then added and allowed to bind to the biotinylated antigen at RT for 15 min. The plates were washed 5 times with PBS containing 0.1% Tween-20 and 5 times with PBS and developed by addition of 100µl/well POD blue substrate (Roche Diagnostics, Mannheim, Germany). The color reaction was quenched by addition of 60µl/well of 1M sulphuric acid and absorbance values determined at 450nm using a VERSAmax plate reader (Molecular Devices, Sunnyvale, CA, USA

SA-ELISA and SA-competition ELISA (96well format)

SA-coated microtiter plates (Roche Diagnostics, Mannheim, Germany) were incubated for 1h at RT with typically 2 µg/ml biotinylated EDB in PBS containing 3% dried skimmed milk. The plates were then washed 3 times with PBS/0.1% Tween-20 and PBS alone. scFv containing supernatants (in PBS containing 1% dried skimmed milk) were allowed to bind for 45 min at RT. The plates were washed again 3 times with PBS/0.1% Tween-20 and with PBS alone. When performed as a competition experiment, 100µl of a solution of unbiotinylated EDB (typically at 50 µg/ml) in PBS containing 1% dried skimmed milk was added at different time points, and the competition was stopped by washing the plates 5 times each with PBS containing 0.1% Tween-20 and PBS alone. FLAG-tagged scFv still binding to EDB were then detected by addition (100µl/well) of a 1:1000 dilution of the FLAG-specific M2 antibody (F3165; Sigma, Buchs, Switzerland) in PBS containing 1% dried skimmed milk (20 minutes incubation at RT), followed by 3 washing steps with PBS containing 0.1% Tween-20 and PBS alone, addition (100µl/well) of a 1:1000 dilution of anti-mouse IgG peroxidase conjugate (Cat. Nr. A2554, Sigma, Buchs, Switzerland), 5 washing steps with PBS containing 0.1% Tween-20 and PBS alone and final addition of 100µl/well POD blue substrate (Roche Diagnostics, Mannheim, Germany). The color reaction was quenched by addition of 60µl/well of 1M sulphuric acid and absorbance values determined at 450nm using a VERSAmax plate reader (Molecular Devices, Sunnyvale, CA, USA

#### 3.3.3.4 Robotization

For colony picking, bacterial clones of the above mentioned library were plated at different dilutions overnight at 30°C on 2xYT plates, containing 100µg/ml ampicillin and 1% (w/v) glucose. Plates with bacterial clones of optimal density and size were used for picking which was performed by the QpixII colony picker (Genetix Ltd., New Milton, Hampshire, UK) following the manufacturer's instruction. In short, several hundreds of clones of appropriate diameter and roundness were selected by imaging the plate with the built-in camera and processing the resulting image with the manufacturer's software. The selected clones were picked by a 96 tip picking head, the tips of each picking round were then inoculated sequentially in two prepared 96well plates, containing 180 µl of 2xYT medium (with 100µg/ml ampicillin and 1% (w/v) glucose. The bacteria were grown overnight at 30°C (shaking at 200 rpm) and one of the two replica plates was stored at –80°C after addition of glycerol to a final concentration of 20% (v/v) whereas 10 µl the other replica plate was used to freshly inoculate another 96well plate, containing 180 µl of 2xYT medium (with 100µg/ml ampicillin and 0.1% (w/v) glucose). Typically after 3 hours growth at 37°C (shaking at 200 rpm) these bacterial plates were induced by addition of Isopropyl-β-D-1-thiogalactopyranoside (IPTG) (final concentration: 1mM) and allowed to produce scFv at 30°C overnight. The plates were then centrifuged at 3000 x g for 10 min using the Heraeus MULTIFUGE 3L (Kendro, Zürich, Switzerland) and the supernatants were either directly used for the robotic M2-ELISA or stored at –20°C.

Robotic M2-ELISA was performed on a TECAN Gemini RWS 200 Workstation (TECAN AG, Männedorf , Switzerland) which was recently implemented at the the Functional Genomics Center Zurich, Winterthurerstr. 190, Y 32 H52, 8057 Zurich.

For this purpose, the robotic workstation features 8-channel simultaneous micropipetting up to the 384-well microtiter plate scale, transfer of microtiter plates to different positions at the worktable by means of a robotic manipulator arm, washing of 384-well microtiter plates with a 384 washing head (PW 384) and absorbance (or fluorescence) reading of plates up to the 384-well microtiter plate scale.

Programming of the workstation was performed using the manufacturer's Gemini V3.5 software which allows to program events in sequential fashion. In brief, the M2-competition ELISA was carried out essentially in the same manner as described above: 384 well microtiter plates (Maxisorp, NUNC, Roskilde, Danmark) were coated overnight at 4°C with 20 µg/ml of the FLAG-specific M2 antibody (F3165; Sigma, Buchs, Switzerland) in PBS containing 0.1% sodium azide (50µl/well). Afterwards, the coating solution was aspirated with the PW384 and the plates were blocked for >3h at RT with 90µl/well 4% MPBS. The plates were then washed with PBS/0.1% Tween-20 and PBS alone using the PW384. scFv supernatants (50µl/well) in PBS containing 1% dried skimmed milk were then applied and allowed to bind at RT for 40 min. The plates were then washed again with the PW384, using first PBS containing 0.1% Tween-20 and then 3 PBS. The biotinylated EDB was then applied (50µl/well, at 2 µg/ml) and allowed to bind at RT for 40 min. To the left 2 quadrants of each 384-well microtiter plate 20µl of 1% MPBS were added to each well, whereas 20 µl of EDB in 1% MPBS (typically at 50 µg/ml) were added to the two right quadrants. Competition time was typically 40 minutes. The plates were then washed as before with the PW 384 and a 1:500 dilution of streptavidin-HRP conjugate (Amersham Pharmacia Biotech, Buckinghamshire, UK) in PBS was then added and allowed to bind to the biotinylated antigen at RT for 15 min. The plates were washed again as before and developed by addition of 50µl/well POD blue substrate (Roche Diagnostics, Mannheim, Germany). The color reaction was quenched by addition of 20µl/well of 1M sulphuric acid and absorbance values determined at 450nm using the GENIOS reader (TECAN AG, Männedorf , Switzerland).

The resulting raw-data could be displayed by the manufacturer's MAGELLAN software using a color scale (but unfortunately not in a grayscale) ranging from blue (lowest value) to red (highest value). Data displayed in a black color code account for signal overflow.

### 3.3.4 Results and Discussion

#### 3.3.4.1 Robotization of antibody screening

Antibody phage technology represents a robust avenue towards the isolation of specific binding specificities for a large variety of different antigens [Winter et al., 1994]. However, during the affinity maturation of antibodies (e.g., by construction of affinity-maturation secondary libraries, derived from good-quality antibodies) the number of antigen binders isolated at the end of a biopanning experiment can be very high [Pini et al., 1998]. A robotic screening of several hundred different antibodies is therefore often necessary, in order to isolate novel antibodies with superior antigen binding properties.

In our laboratory, in the frame of an initiative of the Functional Genomics Center Zurich (FGCZ), we have set up a robotic system, which facilitates the screening of large libraries of antibodies (Figure 3.3.3).

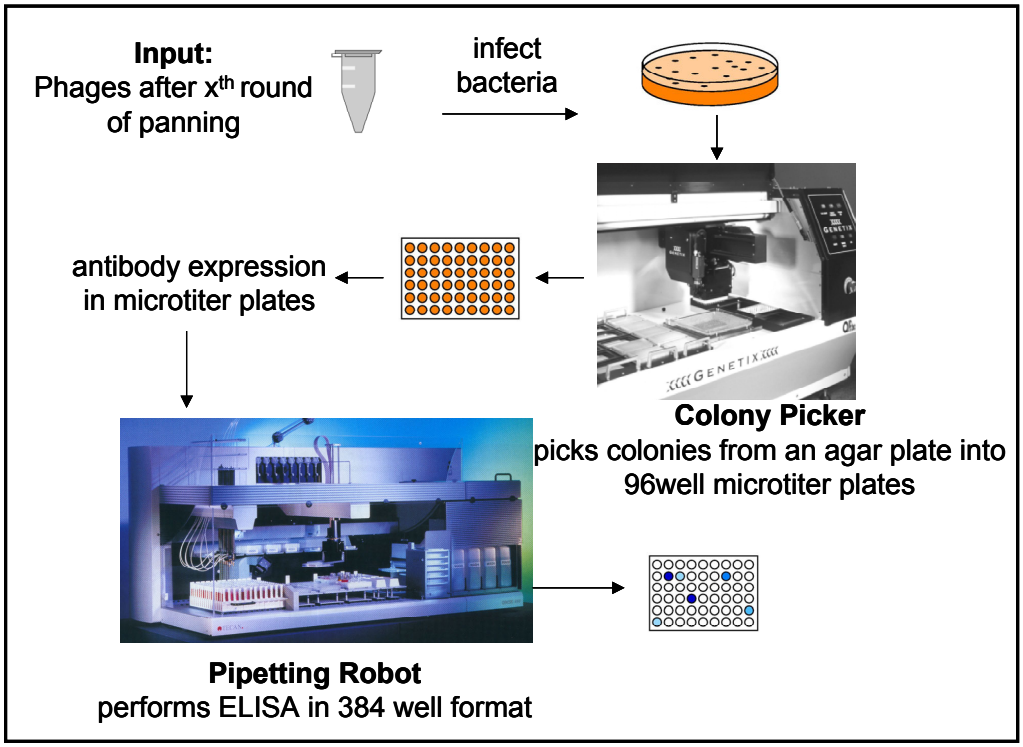


**Figure 3.3.3** Automating antibody fragment selection from antibody phage display libraries. Implementation of robotic stations for automatic picking and gridding of bacterial colonies from agar plates and for the automatic immunometric analysis of antibody-containing supernatants

A colony picker (QpixII; Genetix Ltd., New Milton, Hampshire, UK) can identify bacterial colonies from agar plates (standard Petri dish format or large 20 x 20 cm square plates) and pick them with a 96-pin head in a sequential fashion. The 96 picked colonies can then be inoculated into microtitre plates with suitable growth medium, and duplicated into replica plates (e.g., for the preparation of glycerol cultures). The instrument can pick up to 4'000 colonies/hour, depending on plate shape and colony density.

Microtitre plates allow the growth of individual colonies in distinct wells, by incubation in a thermostated shaker (typically overnight). Microtitre plates are then centrifuged in a dedicated plate centrifuge (Sorvall Heraeus MULTIFUGE 3L, Kendro Zürich, Switzerland) and the resulting supernatants from distinct wells, containing the different monoclonal antibodies, are amenable to robotic ELISA screening using a TECAN Gemini RWS 200 Workstation (TECAN AG, Männedorf , Switzerland)

The TECAN Gemini RWS 200 Workstation features a liquid handling system with 8-tip micropipetting options, a robotic manipulator arm for transport of plates, a magnetic bead separation unit (TeMag), a 384-well microplate washer (POWER WASHER 384) and a plate reader (GENIOS), which can operate in absorption or fluorescence.

In a typical experiment, microtitre plates with antibody supernatants are loaded onto the TECAN robot after centrifugation. The robot dispenses either antigen solutions or antibody capture reagents (e.g., monoclonal antibodies against the peptidic tag of recombinant antibodies) to 384-well microtitre plates and blocks them with milk. After washing, antibody-containing supernatants are dispensed onto the capture plates. ELISA experiments are then performed robotically as described in the next section.

#### 3.3.4.2 ELISA screening of antibody fragments with improved dissociation rate for the antigen

ELISA experiments for testing the antigen binding ability of monoclonal antibodies are typically performed by coating antigen solutions onto plastic microtitre plates.
In the case of the L19 antibody and its derivatives, biotinylated recombinant EDB was applied to streptavidin-coated microtitre plates, in order to facilitate coating of this small protein antigen and to preserve it in the native conformation.

For the measurement of kinetic dissociation constants $k_{off}$, two different ELISA experiments were used (Figure 3.3.4).
In a first experimental set-up (termed "SA-ELISA"), antibody-containing supernatants were applied to microtitre plates, carrying biotin-EDB immobilized onto streptavidin.
At a later time point, recombinant EDB was added (typically at micromolar concentrations), in order to compete-out kinetically labile scFv-EDB complexes immobilized onto plastic. The residual amount of scFv on the microtitre plate at the end of the competition reaction could then be detected by means of secondary antibodies and of a colorimetric enzymatic reaction.
In a second implementation (termed "M2-ELISA"), microtitre plates were coated with the M2 monoclonal antibody, specific for the FLAG peptidic tag at the C-terminal end of the recombinant antibody [Pini et al., 1998]. Antibody-containing supernatants are then applied to the M2-coated plates, allowing a site-specific antibody immobilization which does not interfere with antigen binding. At a later time point, biotinylated EDB was added, followed by the addition of unlabeled EDB (typically at micromolar concentrations), in order to compete-out kinetically labile scFv-(EDB-biotin) complexes immobilized onto plastic. The residual amount of biotinylated EDB on the plate was eventually detected by means of horseradish peroxidase-conjugated streptavidin and chromogenic substrates.

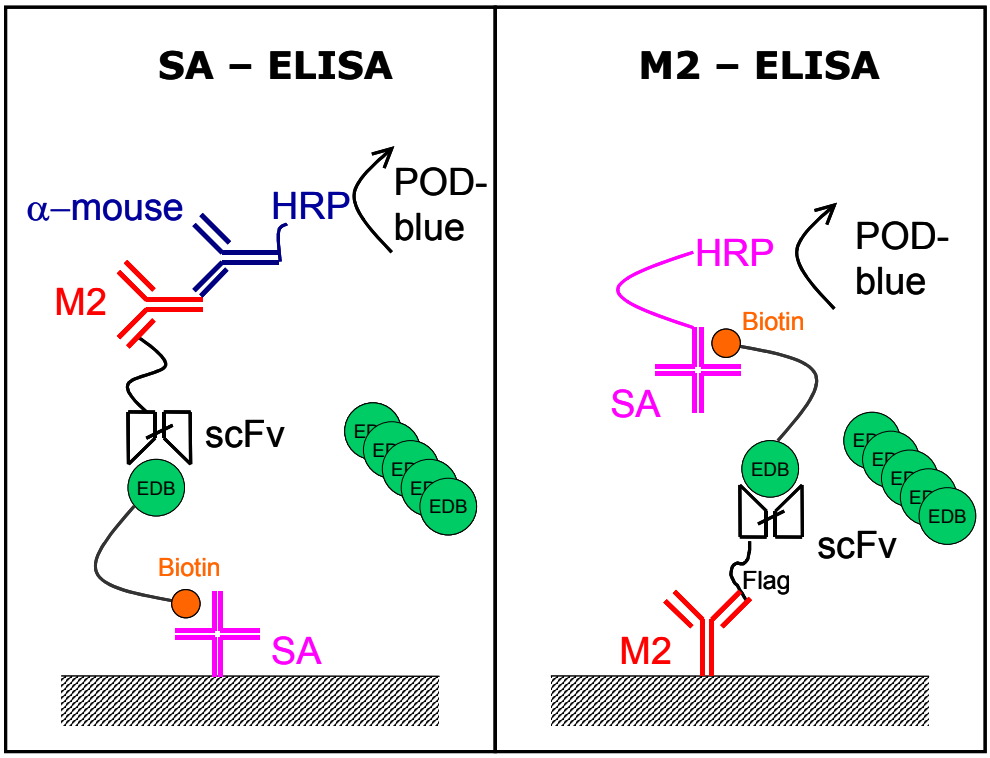


**Figure 3.3.4** **Graphic representation of the "SA-ELISA" and the "M2-ELISA".**

In the **SA-ELISA**, biotinylated antigen (here: EDB) is applied to a streptavidin (SA) coated microtiter plate followed by bacterial supernatants eventually containing FLAG-tagged antigen-binding scFv fragments. When perfomed as a competition assy, a large molar excess of unbiotinylated antigen is applied at different timepoints. Binding FLAG-tagged scFvs are then detected via murine M2 anti-FLAG antibody, horse radish peroxidase (HRP) conjugated anti-mouse antibody by means of a chromogenic reaction catalysed by HRP.

In the **M2-ELISA**, microtiter plates are coated with M2 anti-FLAG antibody before applying the eventually antigen-binding FLAG-tagged scFv fragments. Biotinylated antigen (here: EDB) is applied and in a competition-ELISA format afterwards eventually competed-out by a large molar excess of unbiotinylated antigen at different timepoints. Binding FLAG-tagged scFvs are then detected via horse radish peroxidase (HRP) conjugated streptavidin by means of a chromogenic reaction catalysed by HRP.

Figure 3.3.5 shows the results of SA-ELISA and M2-ELISA assays performed with scFv(L19). The apparent fitted $k_{off}$ values for the two experiments were $4x10^{-4}$ $s^{-1}$ and $1x10^{-3}$ $s^{-1}$, respectively. Please note that the apparent $k_{off}$ values obtained by M2-ELISA appear to depend on the concentration of competing antigen used (see chapter 3.2)!

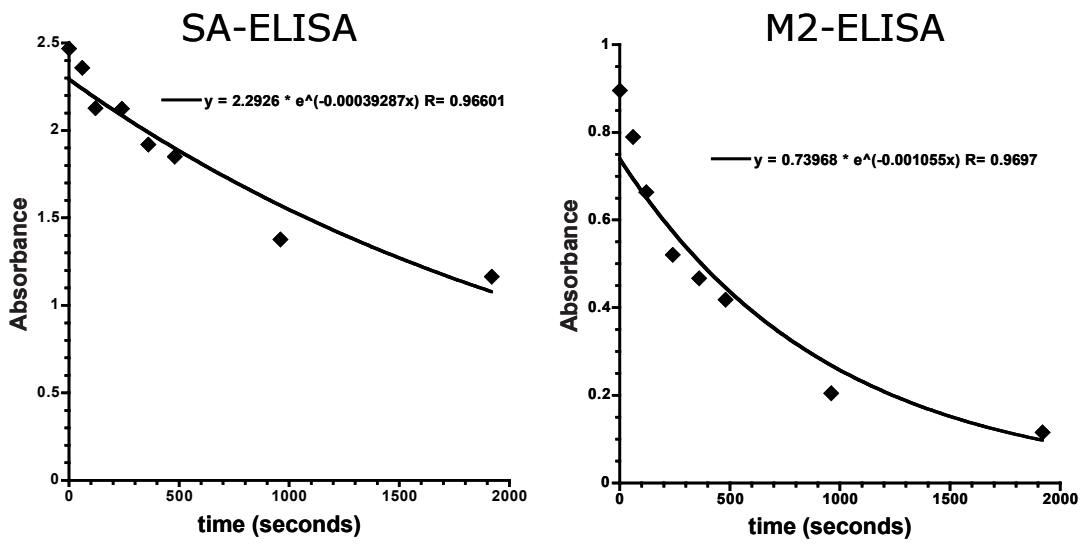


**Figure 3.3.5**

Fit of a competition "SA-ELISA" and competition "M2-ELISA" using L19 supernatant

Since, in principle the SA-ELISA experimental set-up may give rise to avidity artifacts (e.g., if homobivalent antibodies are simultaneously engaged to two EDB molecules immobilized onto the solid surface), the M2-ELISA screening was used for the analysis of L19-derived clones (see next paragraphs).

### 3.3.4.3 Construction of a library of L19 mutants

As a first step towards the isolation of affinity-matured L19 mutants, we asked whether the CDR3 loops of the L19 antibody correspond to the only sequence capable of yielding high-affinity antigen binding, or whether other aminoacid sequences would be compatible with antigen binding.

Using the experimental strategy of Nakayama et al. [Nakayama et al., 2001], we randomized the CDR3 loops of VH and VL by means of "doped" oligonucleotides, which allow a 15% mutagenesis probability for each base in the sequence coding for the CDR3 loops (Table 3.3.1).

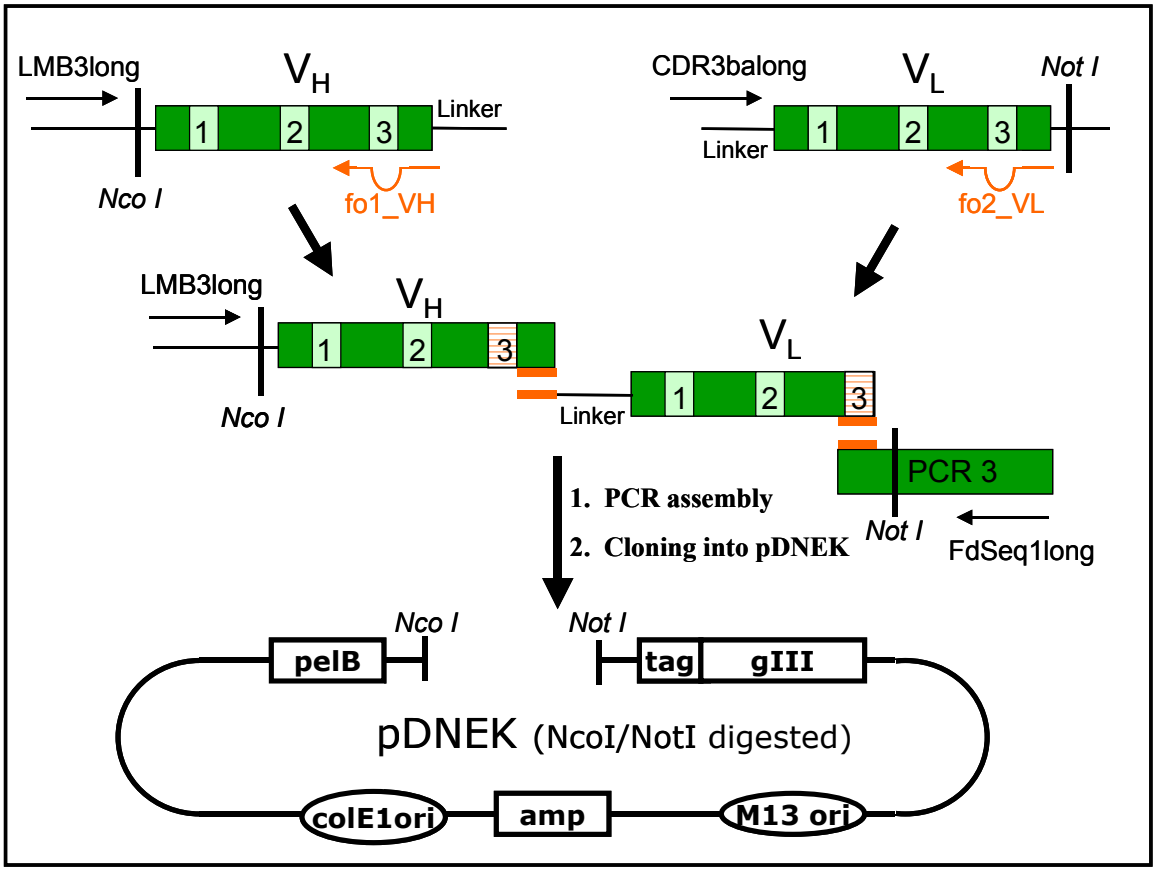


**Figure 3.3.6** Cloning strategy used for the construction of the L19-MAT1 library

| | |
|---|---|
| LMB3long | 5′- CAG GAA ACA GCT ATG ACC ATG ATT AC -3′ |
| CD47CDR2ba | 5′- ACA TAC TAC GCA GAC TCC GTG AAG -3′ |
| CDR3balong | 5′- TTT GAC TAC TGG GGC CAG GGA ACC CTG GTC -3′ |
| VLCDR3toNotBa | 5'-TTC GGC CAA GGG ACC AAG GTG GAA ATC -3′ |
| fo1_VH | 5′- GAC CAG GGT TCC CTG GCC CCA GTA GTC AAA A**21 644 511 644** TTT CGC ACA GTA ATA TAC GGC C- 3′ |
| fo2_VL | 5′- GAT TTC CAC CTT GGT CCC TTG GCC GAA **642 644 644 512 534 533 642 627 627** ACA GTA ATA CAC TGC -3′ |
| JforNotLong | 5′- TCA TTC TCG ACT TCA TTC TCG ACT TGC GGC CGC TTT GAT TTC CAC CTT GGT CCC TTG GCC G -3′ |
| FdSeq1long | 5′- GAC GTT AGT AAA TGA ATT TTC TGT ATG AGG -3′ |
| LMB5 | 5′- TGG CCT TGA TAT TCA CAA ACG AAT -3′ |

**Table 3.3.1** Sequences of primers used for construction and sequencing of the L19-MAT1 library. Digits displayed in bold code for the use of the following phosphoramidite mixtures in the synthesis: **1**: 85%A, 5% each T,C,G; **2**: 85%T, 5% each A,C,G; **3**: 85%C, 5% each A,T,G; **4**: 85%G, 5% each A,T,C; **5**: 85%A, 15%C; **6**: 85%C, 15%A; **6**: 80%G, 10%T, 10%C

The L19 antibody derivatives were cloned into pDNEK [Pini et al., 1998], using an experimental strategy similar to the one described by Viti et al. [Viti et al., 2000] (Figure 3.3.6). The resulting library was termed “L19-MAT1”. It contained 2 x $10^7$ individual clones. A sequence analysis of library clones before biopanning revealed that the CDR3 loops had been randomized as expected for the VL domain, whereas a lower mutagenesis rate was observed for the VH domain, most probably due to a bad synthesis of the commercial oligonucleotide fo1_VH.

A dot blot analysis of bacterial supernatants corresponding to individual colonies revealed that the majority of library clones expressed FLAG-tagged antibody fragments (Figure 3.3.7).

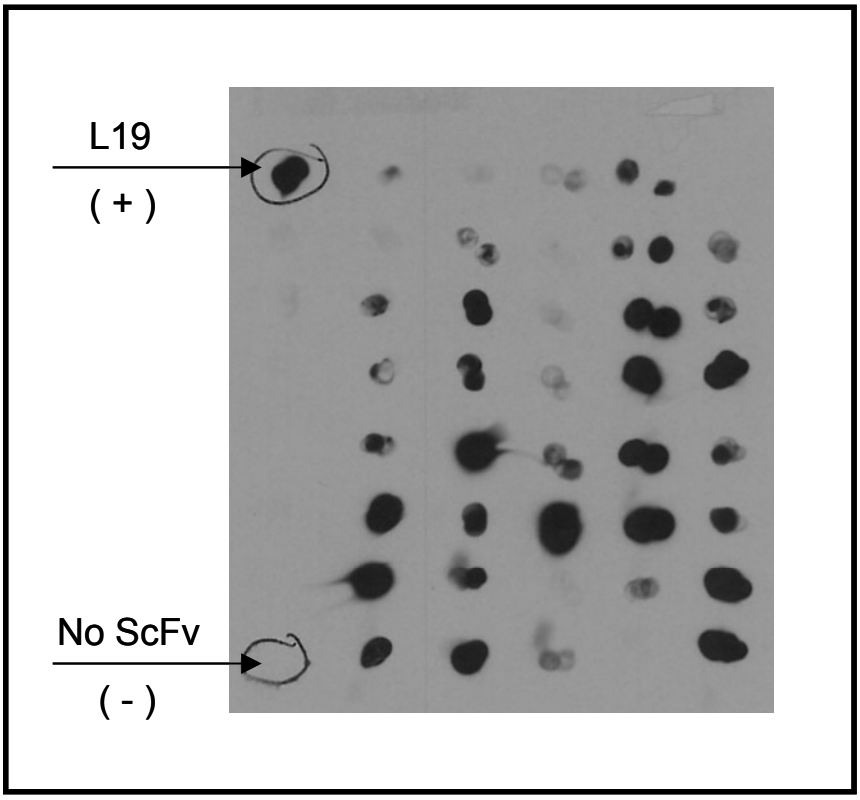


**Figure 3.3.7** Dot blot analysis of clones of the L19-MAT1 library. Clones expressing FLAG-tagged scFv antibody fragments. Each clone's supernatant was dotted twice (eventually giving rise to two small spots). A positive control (L19-Flag) and a negative control (no antibody) were also applied.

#### 3.3.4.4 Biopanning experiment

The antibody phage library L19-MAT1 was biopanned (see Figure 2.3.1) with biotinylated EDB as described by Pini et al. [Pini et al., 1998].
In a first experimental set-up [“SEL_1”], > $10^{11}$ phage particles were incubated with biotinylated EDB and captured on streptavidin-coated magnetic beads. As the biotin moiety was linked to EDB by means of a disulfide-containing cleavable linker, bound phage could be eluted by addition of dithiothreitol after washing.
In a second experimental set-up [“SEL_2”], antibody phage particles bound to biotin-EDB (captured on streptavidin-coated dybabeads) were competed with a molar excess of unlabeled EDB before elution.
As negative control, a selection omitting biotinylated EDB was performed.

Figure 3.3.8 shows representative robotic SA-ELISA results obtained with clones from a single round of biopanning according to the SEL_1 and SEL_2 protocols. SEL-1 yielded a large proportion of EDB binders, indistinguishable in this assay. The proportion of EDB binders from the SEL-2 selection was lower, but the positive clones gave very strong SA-ELISA signals. As expected, clones from the negative control selection did not give antigen binders, indicating that the proportion of EDB binders in the L19-MAT1 library was < 10%.

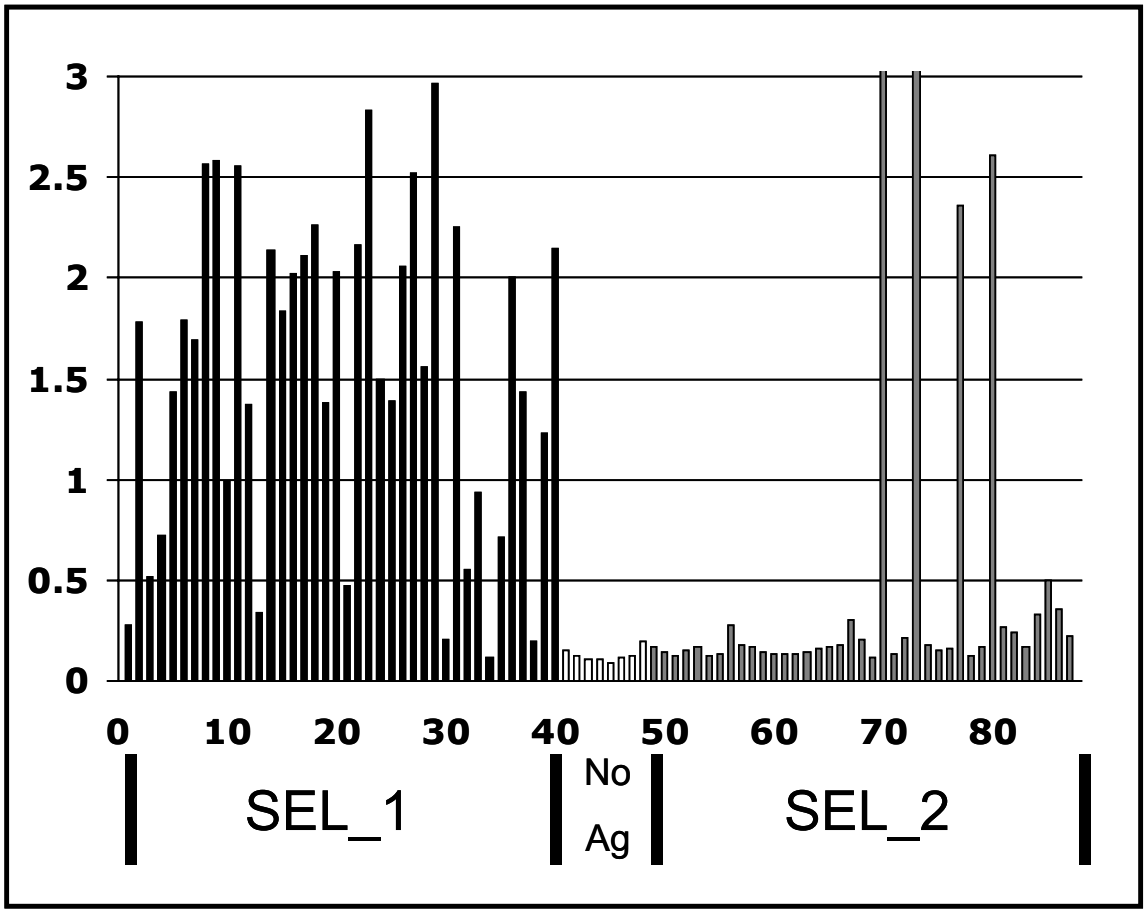


**Figure 3.3.8** SA-ELISA of clones after 1 round of biopanning: Clones 1-40 resulting from SEL_1, clones 41-49 from a control selection performed without biotinylated EDB, clones 50-88 resulting from SEL_2, in which unbiotinylated EDB was added later on in order to compete out EDB-binding phages of lower affinity.

### 3.3.4.5 Characterization of L19 mutants

Figure 3.3.9 shows the result of an M2-ELISA of L19 derivatives resulting from SEL_2 selections. The figure consists of four quadrants. The two left quadrants present ELISA results of 192 individual clones, according to an M2-ELISA experimental scheme in which the competition with soluble EDB had been omitted (Figure 3.3.9). The two right quadrant of the figure present the results of the M2-ELISA experiment with soluble EDB competition (5µM; 30 min.) for the same clones as in the left two panels. Interesting clones which exhibited stable antigen binding (e.g., F5 and F10 in the upper left panel, I8 in the lower left panel) were then subjected to a second M2-ELISA experiment, in which the time course of the competition reaction with soluble EDB was studied.

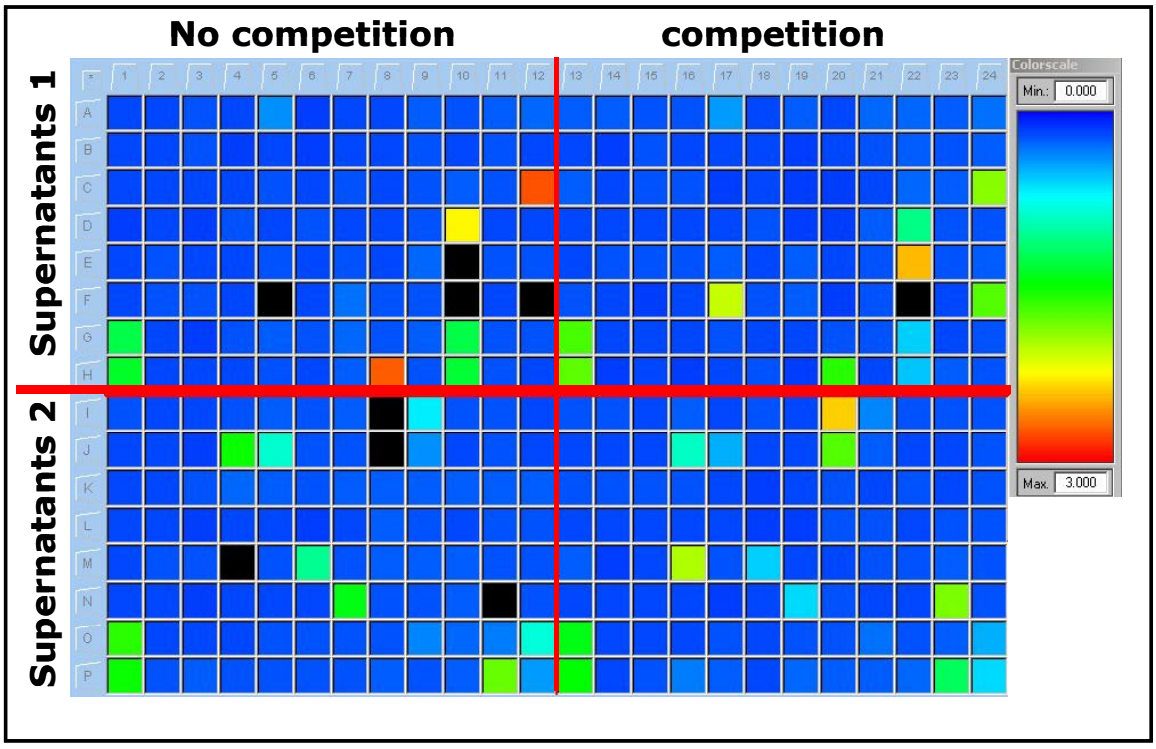


**Figure 3.3.9** M2-ELISA performed with supernatants of 192 clones (left two quadrants). The same supernatants were used for M2-competition ELISA using a 25x molar excess of unlabelled EDB over biotinylated EDB (right two quadrants).ELISA absorbance is color coded, ranging from blue(0) to red (3) (see color scale). Black color coded clones gave rise to an "overflow"signal (absorbance > 3). As positive controls, L19 clones were used in the lower left two wells of each supernatant plate [1G,1H (= 13G,13H), and 1O,1P (=13O,13P), respectively].

Figure 3.3.10 shows representative results of this second M2-ELISA screening. A large proportion of the clones tested exhibited a strong ELISA signal, with a competition half-life of approx. 30-60 minutes.

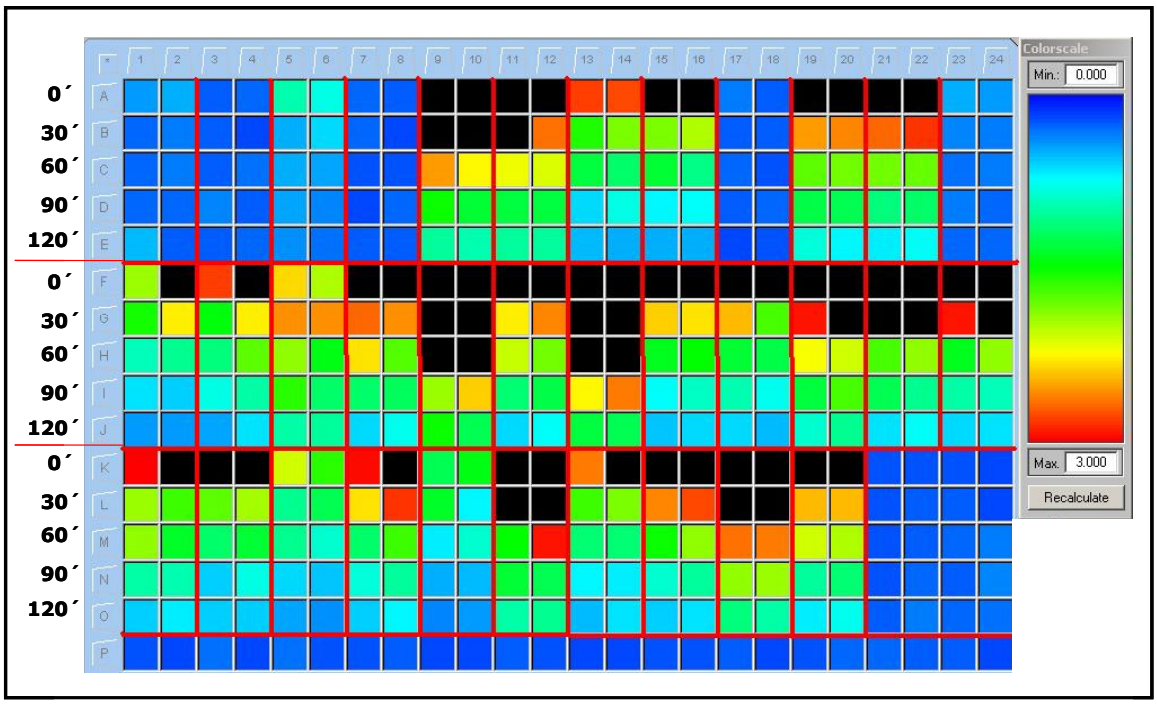


**Figure 3.3.10** M2-competition ELISA of clones exhibiting signal stability upon competition in the experiment depicted in Figure 3.3.9: Each supernatant of an individual clone was applied 10 times (red lined rectangles). Each supernatant was competed with a molar excess of unlabeled EDB in duplicate (left/right) for 4 timepoints (120, 90, 60, 30 minutes competition, 0 minutes: no addition of competitor). ELISA absorbance is color coded, ranging from blue(0) to red (3) (see color scale). Black color coded clones gave rise to an "overflow"signal (absorbance > 3).

Table 3.3.2 shows the sequence of a portion of the CDR3 loop of the VL domain of the isolated antibodies, revealing a number of different aminoacid sequences which were compatible with high-affinity binding. Some sequences turned out to be identical to the original L19 sequence (in terms of aminoacids, but not of nucleotides,

confirming that the mutagenesis reaction used for library construction had worked). In all cases, the aminoacid sequence of the CDR3 loop of the CH domain was identical to the one of the parental L19 antibody.

| Clone | $V_L$ |
|---|---|
| L19 | Q Q T G R I P P T |
| 1 | **E** Q T G R I P P T |
| 2 | Q Q T G R **M** P P **S** |
| 3 | Q Q T G R I P P *T* |
| 4 | Q Q *T* G R I P *P* *T* |
| 5 | Q Q T G R I P P *T* |
| 6 | Q Q **M** **A** *R* **V** *P* P T |
| 7 | **E** Q T G R I P *P* T |
| 8 | Q Q T G R I P P T |
| 9 | Q Q T G R I P *P* *T* |
| 10 | **E** Q *T* G R I P P *T* |
| 11 | **E** Q *T* **S** R **F** P P T |
| 12 | Q Q T *G* *R* I P P T |
| 13 | Q Q T G **W** I **A** P *T* |
| 14 | Q Q T G R **V** P P T |
| 15 | Q Q *T* *G* R I P P *T* |
| 16 | Q **H** T *G* R **V** P P *T* |
| 17 | Q **H** T G R I P P **A** |

**T able 3.3.2**

amino acid sequences of the CDR3 segment of VL - mutagenization of the DNA bases of these amino acid residues were introduced by means of "doped" oligonucleotide primer (see above) - of clones which, after 1 round of biopanning, gave rise to stable signals over time in M2-competition ELISA. On top, the original sequence of L19 is given. Mutated amino acid residues are marked in bold, silent mutations in the DNA sequence not giving rise an amino acid mutation are marked in italic.

A similar M2-ELISA analysis of clones from the SEL-1 selection gave similar results (data not shown).

In summary, M2-ELISA appears to be a stringent method for the identification of kinetically stable antibody-EDB complexes, which may be suitable for biomedical applications (e.g., *in vivo* tumor targeting).

# 4 CONCLUSIONS

In the first part of my thesis, a small-sized library of chemical compounds has been screened using two-dimensional heteronuclear NMR technology (SAR by NMR), aiming at the discovery of low-molecular weight binders to the EDB domain of fibronectin.

Out of this library, one binder could be detected (2,2-diphenylethylamine), which binds to EDB with millimolar affinity.

This initial binder was further investigated by chemical modifications, in order to characterize the structural determinants required for binding and to assess molecular sites amenable to modification without loss of binding affinity.

We are currently using ESACHEL technology (Encoded Self-Assembling Chemical Libraries; Neri, D., Melkko, S. (2002) International patent application E1105-WO), in order to convert 2,2-diphenylethylamine into a high-affinity bidentate ligand for EDB (see Figure 4.1).

Like SAR by NMR, ESACHEL technology exploits the chelate effect. Sublibraries are created by covalently linking chemical compounds (typically hundreds or thousands) to oligonucleotides carrying a distinctive code for each compound and an oligomerizing domain (e.g. an oligonucleotide which can dimerize with its counterpart to form duplex-DNA). After mixing of the sublibraries, the individual library members of the sublibraries form stable heteroduplexes, leading to an effective library size which is the product of the size of the two sublibraries. This assembled library is then selected for binding and "decoded" by DNA sequencing methodology.

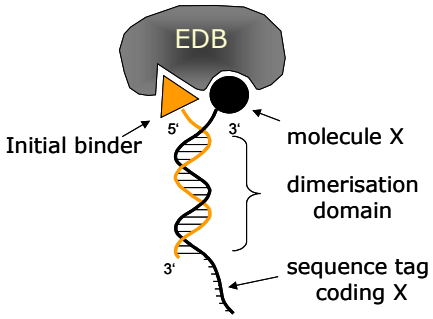


**Figure 4.1**

ESACHEL affinity maturation strategy for binders to EDB: The initial EDB binder is combined with a sublibrary of chemical compounds and the resulting library is selected for high-affinity EDB binders.

In the second part of this thesis, a novel antibody kinetic screening methodology is described, which was developed in order to allow the fast, high-throughput ELISA-screening of antibodies according to the kinetic dissociation rates of the binary antibody-antigen complex.
A library of scFv antibody fragments was created by partial randomization of the CDR3 loop of the VL domain of the L19 antibody. After enrichment of binders to EDB by performing one round of biopanning, robotic M2-competition-ELISA screening led to the discovery of a number of L19 derivatives with binding properties comparable to the one of L19. The observation that the L19 sequence can accommodate mutations without loss of functional affinity suggests that a more radical mutagenesis approach, combined with extensive screening of EDB binders, may yield affinity matured derivatives of the L19 antibody.

When measuring kinetic dissociation rate constants by competition for three complexes of high-affinity recombinant antibody fragments with their cognate antigens and for one calmodulin/peptide complex, a surprising dependence between apparent dissociation rate and concentration of competitor (antigen or calmodulin-binding peptide) was observed which contrasts with the generally expected first-order kinetic for the decay of a bimolecular complex.
Our findings may be characteristic for macromolecules consisting of two domains (such as single-chain Fv fragments) and may reflect a transient opening of the two domains which are involved in the binding reaction.

# 5 REFERENCES

Adams GP, McCartney JE, Tai MS, Oppermann H, Huston JS, Stafford WF, 3rd, Bookman MA, Fand I, Houston LL and Weiner LM. (1993). Highly specific in vivo tumor targeting by monovalent and divalent forms of 741F8 anti-c-erbB-2 single-chain Fv. *Cancer Res* 53: 4026-4034.

Adams GP, Schier R, Marshall K, Wolf EJ, McCall AM, Marks JD and Weiner LM. (1998). Increased affinity leads to improved selective tumor delivery of single-chain Fv antibodies. *Cancer Res* 58: 485-490.

Adams GP, Schier R, McCall AM, Simmons HH, Horak EM, Alpaugh RK, Marks JD and Weiner LM. (2001). High affinity restricts the localization and tumor penetration of single-chain fv antibody molecules. *Cancer Res* 61: 4750-4755.

Alitalo K and Vaheri A. (1982). Pericellular matrix in malignant transformation. *Adv Cancer Res* 37: 111-158.

Amit AG, Mariuzza RA, Phillips SE and Poljak RJ. (1986). Three-dimensional structure of an antigen-antibody complex at 2.8 A resolution. *Science* 233: 747-753.

Aronov AM, Munagala NR, Ortiz De Montellano PR, Kuntz ID and Wang CC. (2000). Rational design of selective submicromolar inhibitors of Tritrichomonas foetus hypoxanthine-guanine-xanthine phosphoribosyltransferase. *Biochemistry* 39: 4684-4691.

Barbas CF, 3rd, Kang AS, Lerner RA and Benkovic SJ. (1991). Assembly of combinatorial antibody libraries on phage surfaces: the gene III site. *Proc Natl Acad Sci U S A* 88: 7978-7982.

Barre S, Greenberg AS, Flajnik MF and Chothia C. (1994). Structural conservation of hypervariable regions in immunoglobulins evolution. *Nat Struct Biol* 1: 915-920.

Bartels C, Xia T-h, Billeter M, Güntert P and Wüthrich K. (1995). The program XEASY for computer-supported spectral analysis of biological macromolecules. *J Biomol NMR* 6: 1-10.

Bass S, Greene R and Wells JA. (1990). Hormone phage: an enrichment method for variant proteins with altered binding properties. *Proteins* 8: 309-314.

Baxter CA, Murray CW, Waszkowycz B, Li J, Sykes RA, Bone RG, Perkins TD and Wylie W. (2000). New approach to molecular docking and its application to virtual screening of chemical databases. *J Chem Inf Comput Sci* 40: 254-262.

Behr TM, Becker WS, Klein MW, Bair HJ, Scheele JR and Wolf FG. (1995). Diagnostic accuracy and tumor-targeting kinetics of complete versus fragmented 99mTc-labeled anti-carcinoembryonic antigen antibodies: an intraindividual comparison. *Cancer Res* 55: 5786s-5793s.

Berezov A, Zhang HT, Greene MI and Murali R. (2001). Disabling erbB receptors with rationally designed exocyclic mimetics of antibodies: structure-function analysis. *J Med Chem* 44: 2565-2574.

Berkower I. (1996). The promise and pitfalls of monoclonal antibody therapeutics. *Curr Opin Biotechnol* 7: 622-628.

Better M, Chang CP, Robinson RR and Horwitz AH. (1988). Escherichia coli secretion of an active chimeric antibody fragment. *Science* 240: 1041-1043.

Bhattacharyya S. (2000). Polymer-supported reagents and catalysts: recent advances in synthetic applications. *Comb Chem High Throughput Screen* 3: 65-92.

Birchler M, Viti F, Zardi L, Spiess B and Neri D. (1999a). Selective targeting and photocoagulation of ocular angiogenesis mediated by a phage-derived human antibody fragment. *Nat Biotechnol* 17: 984-988.

Birchler M, Neri G, Tarli L, Halin C, Viti F and Neri D. (1999b). Infrared photodetection for the in vivo localisation of phage-derived antibodies directed against angiogenic markers. *J Immunol Methods* 231: 239-248.

Bodenhausen G and Ruben DJ. (1980). Natural Abundance Nitrogen-15 NMR by Enhanced Heteronuclear Spectroscopy. *Chem Phys Lett* 69: 185-189.

Boehm HJ, Boehringer M, Bur D, Gmuender H, Huber W, Klaus W, Kostrewa D, Kuehne H, Luebbers T, Meunier-Keller N and Mueller F. (2000). Novel inhibitors of DNA gyrase: 3D structure based biased needle screening, hit validation by biophysical methods, and 3D guided optimization. A promising alternative to random screening. *J Med Chem* 43: 2664-2674.

Borsi L, Allemanni G, Castellani P, Rosellini C, Di Vinci A and Zardi L. (1985). Structural differences in the cell binding region of human fibronectin

molecules isolated from cultured normal and tumor-derived human cells. *FEBS Lett* 192: 71-74.

Borsi L, Carnemolla B, Castellani P, Rosellini C, Vecchio D, Allemanni G, Chang SE, Taylor-Papadimitriou J, Pande H and Zardi L. (1987). Monoclonal antibodies in the analysis of fibronectin isoforms generated by alternative splicing of mRNA precursors in normal and transformed human cells. *J Cell Biol* 104: 595-600.

Borsi L, Balza E, Allemanni G and Zardi L. (1992). Differential expression of the fibronectin isoform containing the ED-B oncofetal domain in normal human fibroblast cell lines originating from different tissues. *Exp Cell Res* 199: 98-105.

Borsi L, Balza E, Bestagno M, Castellani P, Carnemolla B, Biro A, Leprini A, Sepulveda J, Burrone O, Neri D and Zardi L. (2002). Selective targeting of tumoral vasculature: Comparison of different formats of an antibody (L19) to the ED-B domain of fibronectin. *Int J Cancer* 102: 75-85.

Bothmann H and Plückthun A. (1998). Selection for a periplasmic factor improving phage display and functional periplasmic expression. *Nat Biotechnol* 16: 376-380.

Broach JR and Thorner J. (1996). High-throughput screening for drug discovery. *Nature* 384: 14-16.

Bronson JJ and Barrett JF. (2001). Quinolone, everninomycin, glycylcycline, carbapenem, lipopeptide and cephem antibacterials in clinical development. *Curr Med Chem* 8: 1775-1793.

Bunin BA and Ellman JA. (1992). A general and expedient method for the solid-phase synthesis of 1,4-benzodiazepine derivatives. *J Am Chem Soc* 114: 10997-10998.

Burkhard P, Hommel U, Sanner M and Walkinshaw MD. (1999). The discovery of steroids and other novel FKBP inhibitors using a molecular docking program. *J Mol Biol* 287: 853-858.

Camps F, Castells J, Ferrando MJ and Font J. (1971). Organic syntheses with functionalized polymers. I. Preparation of polymeric substrates and alkylation of esters. *Tetrahedron Lett* 20: 1713-1714.

Camps F, Cartells J and Pi J. (1974). Organic systheses with functionalized polymers. IV. Synthesis of 1,3-dihydro-5-phenyl-2H-1,4-benzodiazepin-2-ones. *An Quim* 70: 848-849.

Carmeliet P and Jain RK. (2000). Angiogenesis in cancer and other diseases. *Nature* 407: 249-257.

Carmeliet P. (2000). Mechanisms of angiogenesis and arteriogenesis. *Nat Med* 6: 389-395.

Carnemolla B, Balza E, Siri A, Zardi L, Nicotra MR, Bigotti A and Natali PG. (1989). A tumor-associated fibronectin isoform generated by alternative splicing of messenger RNA precursors. *J Cell Biol* 108: 1139-1148.

Carnemolla B, Leprini A, Allemanni G, Saginati M and Zardi L. (1992). The inclusion of the type III repeat ED-B in the fibronectin molecule generates conformational modifications that unmask a cryptic sequence. *J Biol Chem* 267: 24689-24692.

Carnemolla B, Neri D, Castellani P, Leprini A, Neri G, Pini A, Winter G and Zardi L. (1996). Phage antibodies with pan-species recognition of the oncofoetal angiogenesis marker fibronectin ED-B domain. *Int J Cancer* 68: 397-405.

Carnemolla B, Borsi L, Balza E, Castellani P, Meazza R, Berndt A, Ferrini S, Kosmehl H, Neri D and Zardi L. (2002). Enhancement of the antitumor properties of interleukin-2 by its targeted delivery to the tumor blood vessel extracellular matrix. *Blood* 99: 1659-1665.

Carr R and Jhoti H. (2002). Structure-based screening of low-affinity compounds. *Drug Discov Today* 7: 522-527.

Carter P, Kelley RF, Rodrigues ML, Snedecor B, Covarrubias M, Velligan MD, Wong WL, Rowland AM, Kotts CE, Carver ME and et al. (1992). High level Escherichia coli expression and production of a bivalent humanized antibody fragment. *Biotechnology (N Y)* 10: 163-167.

Castellani P, Siri A, Rosellini C, Infusini E, Borsi L and Zardi L. (1986). Transformed human cells release different fibronectin variants than do normal cells. *J Cell Biol* 103: 1671-1677.

Castellani P, Viale G, Dorcaratto A, Nicolo G, Kaczmarek J, Querze G and Zardi L. (1994). The fibronectin isoform containing the ED-B oncofetal domain: a marker of angiogenesis. *Int J Cancer* 59: 612-618.

Castellani P, Borsi L, Carnemolla B, Biro A, Dorcaratto A, Viale GL, Neri D and Zardi L. (2002). Differentiation between High- and Low-Grade Astrocytoma Using a Human Recombinant Antibody to the Extra Domain-B of Fibronectin. *Am J Pathol* 161: 1695-1700.

Charifson PS, Corkery JJ, Murcko MA and Walters WP. (1999). Consensus scoring: A method for obtaining improved hit rates from docking databases of three-dimensional structures into proteins. *J Med Chem* 42: 5100-5109.

Chattopadhyaya R, Meador WE, Means AR and Quiocho FA. (1992). Calmodulin structure refined at 1.7 A resolution. *J Mol Biol* 228: 1177-1192.

Chen H and McLennan AG. (1993). The bis(adenosin-N6-yl) alkanes, a family of potential dinucleoside polyphosphate analogue precursors. Mechanism of growth inhibition and suppression of adenosine toxicity in lymphoid cells. *Eur J Biochem* 215: 465-471.

Cho CY, Moran EJ, Cherry SR, Stephans JC, Fodor SP, Adams CL, Sundaram A, Jacobs JW and Schultz PG. (1993). An unnatural biopolymer. *Science* 261: 1303-1305.

Cochran AG. (2000). Antagonists of protein-protein interactions. *Chem Biol* 7: R85-94.

Cochran AG. (2001). Protein-protein interfaces: mimics and inhibitors. *Curr Op ChemBiol* 5: 654-659.

Cotton FA and Wilkinson G. (1988). Advanced inorganic chemistry. New York: John Wiley, pages

Crothers DM and Metzger H. (1972). The influence of polyvalency on the binding properties of antibodies. *Immunochemistry* 9: 341-357.

Curfs JH, Meis JF and Hoogkamp-Korstanje JA. (1997). A primer on cytokines: sources, receptors, effects, and inducers. *Clin Microbiol Rev* 10: 742-780.

Demartis S, Huber A, Viti F, Lozzi L, Giovannoni L, Neri P, Winter G and Neri D. (1999). A strategy for the isolation of catalytic activities from repertoires of enzymes displayed on phage. *J Mol Biol* 286: 617-633.

Demartis S, Tarli L, Borsi L, Zardi L and Neri D. (2001). Selective targeting of tumour neovasculature by a radiohalogenated human antibody fragment specific for the ED-B domain of fibronectin. *Eur J Nucl Med* 28: 534-539.

DeWitt SH, Kiely JS, Stankovic CJ, Schroeder MC, Cody DM and Pavia MR. (1993). "Diversomers": an approach to nonpeptide, nonoligomeric chemical diversity. *Proc Natl Acad Sci U S A* 90: 6909-6913.

Diercks T, Coles M and Kessler H. (2001). Applications of NMR in drug discovery. *Curr Opin Chem Biol* 5: 285-291.

Dina R and Jafari M. (2000). Angiotensin II-receptor antagonists: an overview. *Am J Health Syst Pharm* 57: 1231-1241.

Dolle RE. (1998). Comprehensive survey of chemical libraries yielding enzyme inhibitors, receptor agonists and antagonists, and other biologically active agents: 1992 through 1997. *Mol Divers* 3: 199-233.

D'Ovidio MC, Mastracchio A, Marzullo A, Ciabatta M, Pini B, Uccini S, Zardi L and Ruco LP. (1998). Intratumoral microvessel density and expression of ED-A/ED-B sequences of fibronectin in breast carcinoma. *Eur J Cancer* 34: 1081-1085.

Drews J. (2000). Drug discovery: a historical perspective. *Science* 287: 1960-1964.

Elia G, Silacci M, Bumke MA, Scheurer S and Neri D. (2002). Visualizing the proteome in structurally intact samples. *BioWorld* 3: 16-17.

Fattorusso R, Pellecchia M, Viti F, Neri P, Nerio D and Wüthrich K. (1999). NMR structure of the human oncofoetal fibronectin ED-B domain, a specific marker for angiogenesis. *Structure* 7: 381-390.

Fejzo J, Lepre CA, Peng JW, Bemis GW, Ajay MA, Murcko MA and Moore JM. (1999). The shapes strategy: an NMR-based approach for lead generation in drug discovery. *Chem Biol* 6: 755-769.

Fersht A. (2000). Structure and mechanism in protein science: a guide to enzyme catalysis and protein folding. New York: Freeman, pages

Ffrench-Constant C and Hynes RO. (1989). Alternative splicing of fibronectin is temporally and spatially regulated in the chicken embryo. *Development* 106: 375-388.

Ffrench-Constant C, Van de Water L, Dvorak HF and Hynes RO. (1989). Reappearance of an embryonic pattern of fibronectin splicing during wound healing in the adult rat. *J Cell Biol* 109: 903-914.

Ffrench-Constant C. (1995). Alternative splicing of fibronectin--many different proteins but few different functions. *Exp Cell Res* 221: 261-271.

Fielding L. (2000). Determination of Association Constants (Ka) from Solution NMR Data. *Tetrahedron* 56: 6151-6170.

Filikov AV, Mohan V, Vickers TA, Griffey RH, Cook PD, Abagyan RA and James TL. (2000). Identification of ligands for RNA targets via structure-based virtual screening: HIV-1 TAR. *J Comput Aided Mol Des* 14: 593-610.

Floyd CD, Leblanc C and Whittaker M. (1999). Combinatorial chemistry as a tool for drug discovery. *Prog Med Chem* 36: 91-168.

Fodor SP, Read JL, Pirrung MC, Stryer L, Lu AT and Solas D. (1991). Light-directed, spatially addressable parallel chemical synthesis. *Science* 251: 767-773.

Folkman J. (1995). Angiogenesis in cancer, vascular, rheumatoid and other disease. *Nat Med* 1: 27-31.

Frank R, Heikens W, Heisterberg-Moutsis G and Blocker H. (1983). A new general approach for the simultaneous chemical synthesis of large numbers of oligonucleotides: segmental solid supports. *Nucleic Acids Res* 11: 4365-4377.

Frechet JM. (1981). Synthesis and applications of organic polymers as supports and protecting groups. *Tetrahedron* 37: 663-683.

Frodin JE, Lefvert AK and Mellstedt H. (1992). The clinical significance of HAMA in patients treated with mouse monoclonal antibodies. *Cell Biophys* 21: 153-165.

Furka A, Sebestyen F, Asgedom M and Dibo G. (1991). General method for rapid synthesis of multicomponent peptide mixtures. *Int J Pept Protein Res* 37: 487-493.

Gane PJ and Dean PM. (2000). Recent advances in structure-based rational drug design. *Curr Opin Struct Biol* 10: 401-404.

Garrard LJ, Yang M, O'Connell MP, Kelley RF and Henner DJ. (1991). Fab assembly and enrichment in a monovalent phage display system. *Biotechnology (N Y)* 9: 1373-1377.

George EL, Georges-Labouesse EN, Patel-King RS, Rayburn H and Hynes RO. (1993). Defects in mesoderm, neural tube and vascular development in mouse embryos lacking fibronectin. *Development* 119: 1079-1091.

Geysen HM, Meloen RH and Barteling SJ. (1984). Use of peptide synthesis to probe viral antigens for epitopes to a resolution of a single amino acid. *Proc Natl Acad Sci U S A* 81: 3998-4002.

Good A. (2001). Structure-based virtual screening protocols. *Curr Opin Drug Discov Devel* 4: 301-307.

Goodnow RA, Jr. (2001). Current practices in generation of small molecule new leads. *J Cell Biochem Suppl* Suppl 37: 13-21.

Grana C, Chinol M, Robertson C, Mazzetta C, Bartolomei M, De Cicco C, Fiorenza M, Gatti M, Caliceti P and Paganelli G. (2002). Pretargeted adjuvant radioimmunotherapy with yttrium-90-biotin in malignant glioma patients: a pilot study. *Br J Cancer* 86: 207-212.

Gravert DJ and Janda KD. (1997). Organic Synthesis on Soluble Polymer Supports: Liquid-Phase Methodologies. *Chem Rev* 97: 489-510.

Greenwood J, Willis AE and Perham RN. (1991). Multiple display of foreign peptides on a filamentous bacteriophage. Peptides from Plasmodium falciparum circumsporozoite protein as antigens. *J Mol Biol* 220: 821-827.

Gruneberg S, Stubbs MT and Klebe G. (2002). Successful virtual screening for novel inhibitors of human carbonic anhydrase: strategy and experimental confirmation. *J Med Chem* 45: 3588-3602.

Grzesiek S and Bax A. (1993). The importance of not saturating H2O in protein NMR. Application to sensitivity enhancement and NOE measurement. *J Am Chem Soc* 115: 12593-12594.

Hajduk PJ, Meadows RP and Fesik SW. (1997a). Discovering high-affinity ligands for proteins. *Science* 278: 497,499.

Hajduk PJ, Dinges J, Miknis GF, Merlock M, Middleton T, Kempf DJ, Egan DA, Walter KA, Robins TS, Shuker SB, Holzman TF and Fesik SW. (1997b). NMR-based discovery of lead inhibitors that block DNA binding of the human papillomavirus E2 protein. *J Med Chem* 40: 3144-3150.

Hajduk PJ, Sheppard G, Nettesheim DG, Olejniczak ET, Shuker SB, Meadows RP, Steinman DH, Carrera GM, Marcotte PA, Severin J, Walter K, Smith H, Gubbins E, Simmer R, Holzman TF, Morgan DW, Davidsen SK, Summers JB and Fesik SW. (1997c). Discovery Of Potent Nonpeptide Inhibitors Of Stromelysin Using Sar By Nmr. *Journal of the American Chemical Society* 119: 5818-5827.

Hajduk PJ, Meadows RP and Fesik SW. (1999). NMR-based screening in drug discovery. *Quart Rev Biophys* 32: 211-240.

Hajduk PJ, Gerfin T, Boehlen JM, Haberli M, Marek D and Fesik SW. (1999a). High-throughput nuclear magnetic resonance-based screening. *J Med Chem* 42: 2315-2317.

Hajduk PJ, Zhou MM and Fesik SW. (1999b). NMR-based discovery of phosphotyrosine mimetics that bind to the Lck SH2 domain. *Bioorg Med Chem Lett* 9: 2403-2406.

Hajduk PJ, Dinges J, Schkeryantz JM, Janowick D, Kaminski M, Tufano M, Augeri DJ, Petros A, Nienaber V, Zhong P, Hammond R, Coen M, Beutel B, Katz L and Fesik SW. (1999c). Novel inhibitors of Erm methyltransferases from NMR and parallel synthesis. *J Med Chem* 42: 3852-3859.

Hajduk PJ, Bures M, Praestgaard J and Fesik SW. (2000a). Privileged molecules for protein binding identified from NMR-based screening. *J Med Chem* 43: 3443-3447.

Hajduk PJ, Boyd S, Nettesheim D, Nienaber V, Severin J, Smith R, Davidson D, Rockway T and Fesik SW. (2000b). Identification of novel inhibitors of urokinase via NMR-based screening. *J Med Chem* 43: 3862-3866.

Hajduk PJ, Augeri DJ, Mack J, Mendoza R, Yang J, Betz SF and Fesik SW. (2000c). NMR-Based Screening of Proteins Containing 13C-Labeled Methyl Groups. *Journal of the American Chemical Society* 122: 7898-7904.

Hakimi J, Chizzonite R, Luke DR, Familletti PC, Bailon P, Kondas JA, Pilson RS, Lin P, Weber DV, Spence C and et al. (1991). Reduced immunogenicity and improved pharmacokinetics of humanized anti-Tac in cynomolgus monkeys. *J Immunol* 147: 1352-1359.

Halin C, Zardi L and Neri D. (2001). Antibody-based targeting of angiogenesis. *News Physiol Sci* 16: 191-194.

Halin C, Rondini S, Nilsson F, Berndt A, Kosmehl H, Zardi L and Neri D. (2002a). Enhancement of the antitumor activity of interleukin-12 by targeted delivery to neovasculature. *Nat Biotechnol* 20: 264-269.

Halin C, Rondini S, Nilsson F, Berndt A, Kosmehl H, Zardi L and Neri D. (2002b). Enhancement of the anti-tumor activity of interleukin-12 by targeted delivery to neovasculature. *Nat Biotechnol* 20: 264-269.

Hanauske AR. (1996). The development of new chemotherapeutic agents. *Anticancer Drugs* 7 Suppl 2: 29-32.

Harris RK. (1983). Nuclear Magnetic Resonance Spectroscopy, A Physiochemical View. New York: Longman Scientific & Technical, pages

Hermkens PHH, Ottenheijm HCJ and Rees D. (1997). Solid-phase organic reactions. II: a review of the literature Nov 95-Nov 96. *Tetrahedron* 53: 5643-5678.

Hertzberg RP and Pope AJ. (2000). High-throughput screening: new technology for the 21st century. *Curr Opin Chem Biol* 4: 445-451.

Hoogenboom HR, Griffiths AD, Johnson KS, Chiswell DJ, Hudson P and Winter G. (1991). Multi-subunit proteins on the surface of filamentous phage: methodologies for displaying antibody (Fab) heavy and light chains. *Nucleic Acids Res* 19: 4133-4137.

Hopkins SC, Vale RD and Kuntz ID. (2000). Inhibitors of kinesin activity from structure-based computer screening. *Biochemistry* 39: 2805-2814.

Houghten RA. (1985). General method for the rapid solid-phase synthesis of large numbers of peptides: specificity of antigen-antibody interaction at the level of individual amino acids. *Proc Natl Acad Sci U S A* 82: 5131-5135.

Houghten RA, Pinilla C, Blondelle SE, Appel JR, Dooley CT and Cuervo JH. (1991). Generation and use of synthetic peptide combinatorial libraries for basic research and drug discovery. *Nature* 354: 84-86.

Huber A, Demartis S and Neri D. (1999). The use of biosensor technology for the engineering of antibodies and enzymes. *J Mol Recognit* 12: 198-216.

Huheey JE, Keiter EA and Keiter RL. (1993). Inorganic chemistry: principles of structure and reactivity. New York: Harper Collins, pages

Huston JS, Levinson D, Mudgett-Hunter M, Tai MS, Novotny J, Margolies MN, Ridge RJ, Bruccoleri RE, Haber E, Crea R and et al. (1988). Protein engineering of antibody binding sites: recovery of specific activity in an anti-digoxin single-chain Fv analogue produced in Escherichia coli. *Proc Natl Acad Sci U S A* 85: 5879-5883.

Hwang TL and Shaka AJ. (1995). Water suppression that works. Excitation sculpting using arbitrary waveforms and pulsed field gradients. *J Magn Reson A* 112: 275-279.

Hynes R. (1985). Molecular biology of fibronectin. *Annu Rev Cell Biol* 1: 67-90.

Hynes RO. (1990). Fibronectins. New York: Springer-Verlag, pages

Iannolo G, Minenkova O, Petruzzelli R and Cesareni G. (1995). Modifying filamentous phage capsid: limits in the size of the major capsid protein. *J Mol Biol* 248: 835-844.

Isaacs JD, Watts RA, Hazleman BL, Hale G, Keogan MT, Cobbold SP and Waldmann H. (1992). Humanised monoclonal antibody therapy for rheumatoid arthritis. *Lancet* 340: 748-752.

Jacobsohn DA. (2002). Novel therapeutics for the treatment of graft-versus-host disease. *Expert Opin Investig Drugs* 11: 1271-1280.

Jahnke W. (2002) The Use of Spin Labels in NMR-Supported Lead Finding and Optimization. In: O Zerbe (Ed) BioNMR in Drug Research, Vol. 16, Methods and Principles in Medicinal Chemistry. Wiley-VCH, Weinheim, Germany, 341-354.

Jain RK and Baxter LT. (1988). Mechanisms of heterogeneous distribution of monoclonal antibodies and other macromolecules in tumors: significance of elevated interstitial pressure. *Cancer Res* 48: 7022-7032.

Jakobovits A. (1998). Production and selection of antigen-specific fully human monoclonal antibodies from mice engineered with human Ig loci. *Adv Drug Deliv Rev* 31: 33-42.

James IW. (1999). Linkers for solid phase organic synthesis. *Tetrahedron* 55: 4855-4946.

Jencks WP. (1975). Binding energy, specificity, and enzymic catalysis: the circe effect. *Adv Enzymol Relat Areas Mol Biol* 43: 219-410.

Jespers LS, Messens JH, De Keyser A, Eeckhout D, Van den Brande I, Gansemans YG, Lauwereys MJ, Vlasuk GP and Stanssens PE. (1995). Surface expression and ligand-based selection of cDNAs fused to filamentous phage gene VI. *Biotechnology (N Y)* 13: 378-382.

Johnson CS. (1999). Diffusion-ordered nuclear magnetic resoance spectroscopy:principles and applications. *Prog NMR Spectrosc* 34: 203-256.

Jones PT, Dear PH, Foote J, Neuberger MS and Winter G. (1986). Replacing the complementarity-determining regions in a human antibody with those from a mouse. *Nature* 321: 522-525.

Kaczmarek J, Castellani P, Nicolo G, Spina B, Allemanni G and Zardi L. (1994). Distribution of oncofetal fibronectin isoforms in normal, hyperplastic and neoplastic human breast tissues. *Int J Cancer* 59: 11-16.

Karelina TV and Eisen AZ. (1998). Interstitial collagenase and the ED-B oncofetal domain of fibronectin are markers of angiogenesis in human skin tumors. *Cancer Detect Prev* 22: 438-444.

Kay LE, Torchia DA and Bax A. (1989). Backbone dynamics of proteins as studied by 15N inverse detected heteronuclear NMR spectroscopy: application to staphylococcal nuclease. *Biochemistry* 28: 8972-8979.

Keeler J, Clowes RT, Davis AL and Laue ED. (1994). Pulsed-field gradients: theory and practice. *Methods Enzymol* 239: 145-207.

Kerbel RS. (1997). A cancer therapy resistant to resistance. *Nature* 390: 335-336.

King DJ, Turner A, Farnsworth AP, Adair JR, Owens RJ, Pedley RB, Baldock D, Proudfoot KA, Lawson AD, Beeley NR and et al. (1994). Improved tumor targeting with chemically cross-linked recombinant antibody fragments. *Cancer Res* 54: 6176-6185.

Klebe G. (2000). Recent developments in structure-based drug design. *J Mol Med* 78: 269-281.

Klungel OH, Heckbert SR, de Boer A, Leufkens HG, Sullivan SD, Fishman PA, Veenstra DL and Psaty BM. (2002). Lipid-lowering drug use and cardiovascular events after myocardial infarction. *Ann Pharmacother* 36: 751-757.

Kohler G and Milstein C. (1975). Continuous cultures of fused cells secreting antibody of predefined specificity. *Nature* 256: 495-497.

Kosmehl H, Berndt A and Katenkamp D. (1996). Molecular variants of fibronectin and laminin: structure, physiological occurrence and histopathological aspects. *Virchows Arch* 429: 311-322.

Krebber A, Bornhauser S, Burmester J, Honegger A, Willuda J, Bosshard HR and Pluckthun A. (1997). Reliable cloning of functional antibody variable domains from hybridomas and spleen cell repertoires employing a reengineered phage display system. *J Immunol Methods* 201: 35-55.

Kristensen P and Winter G. (1998). Proteolytic selection for protein folding using filamentous bacteriophages. *Fold Des* 3: 321-328.

Lahana R. (1999). How many leads from HTS? *Drug Discov Today* 4: 447-448.

Laitinen L, Vartio T and Virtanen I. (1991). Cellular fibronectins are differentially expressed in human fetal and adult kidney. *Lab Invest* 64: 492-498.

Lam KS, Salmon SE, Hersh EM, Hruby VJ, Kazmierski WM and Knapp RJ. (1991). A new type of synthetic peptide library for identifying ligand-binding activity. *Nature* 354: 82-84.

Lam KS. (1997). Application of combinatorial library methods in cancer research and drug discovery. *Anticancer Drug Des* 12: 145-167.

Leahy DJ, Aukhil I and Erickson HP. (1996). 2.0 A crystal structure of a four-domain segment of human fibronectin encompassing the RGD loop and synergy region. *Cell* 84: 155-164.

Lepre CA. (2001). Library design for NMR-based screening. *DDT* 6: 133-140.

Leznoff CC and Wong JY. (1972). Use of polymer supports in organic synthesis. Synthesis of monotrityl ethers of symmetrical diols. *Can J Chem* 50: 2892-2893.

Li E, Pedraza A, Bestagno M, Mancardi S, Sanchez R and Burrone O. (1997). Mammalian cell expression of dimeric small immune proteins (SIP). *Protein Eng* 10: 731-736.

Lipinski CA, Lombardo F and Dominy B. (1997). Experimental and computational approaches to estimate solubility and permeability in drug discovery and development settings. *Adv Drug Deliv Rev* 23: 3-25.

Lipinski CA. (2000). Drug-like properties and the causes of poor solubility and poor permeability. *J Pharmacol Toxicol Methods* 44: 235-249.

Lonberg N, Taylor LD, Harding FA, Trounstine M, Higgins KM, Schramm SR, Kuo CC, Mashayekh R, Wymore K, McCabe JG and et al. (1994). Antigen-specific human antibodies from mice comprising four distinct genetic modifications. *Nature* 368: 856-859.

Lowman HB, Bass SH, Simpson N and Wells JA. (1991). Selecting high-affinity binding proteins by monovalent phage display. *Biochemistry* 30: 10832-10838.

Magnusson MK and Mosher DF. (1998). Fibronectin: structure, assembly, and cardiovascular implications. *Arterioscler Thromb Vasc Biol* 18: 1363-1370.

Maher VE, Drukman SJ, Kinders RJ, Hunter RE, Jennings J, Brigham C, Stevens S and Griffin TW. (1992). Human antibody response to the intravenous and intraperitoneal administration of the F(ab')2 fragment of the OC125 murine monoclonal antibody. *J Immunother* 11: 56-66.

Marchioro C, Davalli S, Provera S, Heller M, Ross A and Senn H. (2002) Experiments in NMR-based Screening. In: O Zerbe (Ed) BioNMR in Drug Research, Vol. 16, Methods and Principles in Medicinal Chemistry. Wiley-VCH, Weinheim, Germany, 321-340.

Mariani G, Lasku A, Balza E, Gaggero B, Motta C, Di Luca L, Dorcaratto A, Viale GA, Neri D and Zardi L. (1997a). Tumor targeting potential of the monoclonal antibody BC-1 against oncofetal fibronectin in nude mice bearing human tumor implants. *Cancer* 80: 2378-2384.

Mariani G, Lasku A, Pau A, Villa G, Motta C, Calcagno G, Taddei GZ, Castellani P, Syrigos K, Dorcaratto A, Epenetos AA, Zardi L and Viale GA. (1997b). A pilot pharmacokinetic and immunoscintigraphic study with the technetium-99m-labeled monoclonal antibody BC-1 directed against oncofetal fibronectin in patients with brain tumors. *Cancer* 80: 2484-2489.

McCafferty J, Griffiths AD, Winter G and Chiswell DJ. (1990). Phage antibodies: filamentous phage displaying antibody variable domains. *Nature* 348: 552-554.

McCafferty J. (1996) Phage display: factors affecting panning efficiency. In: B Kay, L Winter and J McCafferty (Eds), Phage display of peptides and proteins. Academic Press, San Diego, 261-276.

McDevitt MR, Barendswaard E, Ma D, Lai L, Curcio MJ, Sgouros G, Ballangrud AM, Yang WH, Finn RD, Pellegrini V, Geerlings MW, Jr., Lee M, Brechbiel MW, Bander NH, Cordon-Cardo C and Scheinberg DA. (2000). An alpha-particle emitting antibody ([213Bi]J591) for radioimmunotherapy of prostate cancer. *Cancer Res* 60: 6095-6100.

Meador WE, Means AR and Quiocho FA. (1993). Modulation of calmodulin plasticity in molecular recognition on the basis of x-ray structures. *Science* 262: 1718-1721.

Meiboom S and Gill D. (1958). Modified spin-echo method for measuring spin-relaxation rates. *Rev Sci Instrum* 29: 688-691.

Merrifield RB. (1963). Solid phase peptide synthesis. I. The synthesis of a tetrapeptide. *J Am Chem Soc* 85: 2149-2154.

Merritt AT. (1998). Uptake of new technology in lead optimization for drug discovery. *Drug Discovery Today* 3: 505-510.

Midulla M, Verma R, Pignatelli M, Ritter MA, Courtenay-Luck NS and George AJ. (2000). Source of oncofetal ED-B-containing fibronectin: implications of production by both tumor and endothelial cells. *Cancer Res* 60: 164-169.

Montigiani S, Neri G, Neri P and Neri D. (1996). Alanine substitutions in calmodulin-binding peptides result in unexpected affinity enhancement. *J Mol Biol* 258: 6-13.

Moore JM. (1999). NMR Techniques for Characterization of Ligand Binding: Utility for Lead Genereation and Optimization in Drug Discovery. *Biopolymers* 51: 221-243.

Nakayama M, Neri D and Ohara O. (2001). A new simplified method for preparation of a synthetic phage antibody with practically acceptable detection sensitivity on immunoblots. *Hum Antibodies* 10: 55-65.

Neri D, Momo M, Prospero T and Winter G. (1995). High-affinity antigen binding by chelating recombinant antibodies (CRAbs). *J Mol Biol* 246: 367-373.

Neri D, Montigiani S and Kirkham PM. (1996a). Biophysical methods for the determination of antibody-antigen affinities. *Trends Biotechnol* 14: 465-470.

Neri D, Petrul H, Winter G, Light Y, Marais R, Britton KE and Creighton AM. (1996b). Radioactive labeling of recombinant antibody fragments by phosphorylation using human casein kinase II and [gamma-32P]-ATP. *Nat Biotechnol* 14: 485-490.

Neri D, Carnemolla B, Nissim A, Leprini A, Querze G, Balza E, Pini A, Tarli L, Halin C, Neri P, Zardi L and Winter G. (1997). Targeting by affinity-matured recombinant antibody fragments of an angiogenesis associated fibronectin isoform. *Nat Biotechnol* 15: 1271-1275.

Nicolo G, Salvi S, Oliveri G, Borsi L, Castellani P and Zardi L. (1990). Expression of tenascin and of the ED-B containing oncofetal fibronectin isoform in human cancer. *Cell Differ Dev* 32: 401-408.

Nilsson F, Kosmehl H, Zardi L and Neri D. (2001). Targeted delivery of tissue factor to the ED-B domain of fibronectin, a marker of angiogenesis, mediates the infarction of solid tumors in mice. *Cancer Res* 61: 711-716.

Nissim A, Hoogenboom HR, Tomlinson IM, Flynn G, Midgley C, Lane D and Winter G. (1994). Antibody fragments from a 'single pot' phage display library as immunochemical reagents. *Embo J* 13: 692-698.

Nowakowski A, Wang C, Powers DB, Amersdorfer P, Smith TJ, Montgomery VA, Sheridan R, Blake R, Smith LA and Marks JD. (2002). Potent neutralization of botulinum neurotoxin by recombinant oligoclonal antibody. *Proc Natl Acad Sci U S A* 99: 11346-11350.

Otte A, Mueller-Brand J, Dellas S, Nitzsche EU, Herrmann R and Maecke HR. (1998). Yttrium-90-labelled somatostatin-analogue for cancer treatment. *Lancet* 351: 417-418.

Oyama F, Hirohashi S, Shimosato Y, Titani K and Sekiguchi K. (1989). Deregulation of alternative splicing of fibronectin pre-mRNA in malignant human liver tumors. *J Biol Chem* 264: 10331-10334.

Oyama F, Hirohashi S, Shimosato Y, Titani K and Sekiguchi K. (1990). Oncodevelopmental regulation of the alternative splicing of fibronectin pre-messenger RNA in human lung tissues. *Cancer Res* 50: 1075-1078.

Pack P, Kujau M, Schroeckh V, Knupfer U, Wenderoth R, Riesenberg D and Pluckthun A. (1993). Improved bivalent miniantibodies, with identical avidity as whole antibodies, produced by high cell density fermentation of Escherichia coli. *Biotechnology (N Y)* 11: 1271-1277.

Paganelli G, Magnani P, Zito F, Villa E, Sudati F, Lopalco L, Rossetti C, Malcovati M, Chiolerio F, Seccamani E and et al. (1991a). Three-step monoclonal antibody tumor targeting in carcinoembryonic antigen-positive patients. *Cancer Res* 51: 5960-5966.

Paganelli G, Malcovati M and Fazio F. (1991b). Monoclonal antibody pretargetting techniques for tumour localization: the avidin-biotin system. International Workshop on Techniques for Amplification of Tumour Targetting. *Nucl Med Commun* 12: 211-234.

Paganelli G, Grana C, Chinol M, Cremonesi M, De Cicco C, De Braud F, Robertson C, Zurrida S, Casadio C, Zoboli S, Siccardi AG and Veronesi U. (1999). Antibody-guided three-step therapy for high grade glioma with yttrium-90 biotin. *Eur J Nucl Med* 26: 348-357.

Pankov R and Yamada KM. (2002). Fibronectin at a glance. *J Cell Sci* 115: 3861-3863.

Park BW, Zhang HT, Wu C, Berezov A, Zhang X, Dua R, Wang Q, Kao G, O'Rourke DM, Greene MI and Murali R. (2000). Rationally designed anti-HER2/neu peptide mimetic disables P185HER2/neu tyrosine kinases in vitro and in vivo. *Nat Biotechnol* 18: 194-198.

Parmley SF and Smith GP. (1988). Antibody-selectable filamentous fd phage vectors: affinity purification of target genes. *Gene* 73: 305-318.

Patchornik A and Kraus MA. (1970). Reactive species mutually isolated on insoluble polymeric carriers. I. Directed monoacylation of esters. *J Amer Chem Soc* 92: 7587-7589.

Pedersen H, Holder S, Sutherlin DP, Schwitter U, King DS and Schultz PG. (1998). A method for directed evolution and functional cloning of enzymes. *Proc Natl Acad Sci U S A* 95: 10523-10528.

Pellecchia M, Sem DS and Wuthrich K. (2002). NMR in drug discovery. *Nat Rev Drug Discov* 1: 211-219.

Peng JW, Lepre CA, Fejzo J, Abdul-Manan N and Moore JM. (2001). Nuclear magnetic resonance-based approaches for lead generation in drug discovery. *Methods Enzymol* 338: 202-230.

Perola E, Xu K, Kollmeyer TM, Kaufmann SH, Prendergast FG and Pang YP. (2000). Successful virtual screening of a chemical database for farnesyltransferase inhibitor leads. *J Med Chem* 43: 401-408.

Petsko GA. (1996). For medicinal purposes. *Nature* 384: 7-9.

Pini A, Viti F, Santucci A, Carnemolla B, Zardi L, Neri P and Neri D. (1998). Design and use of a phage display library. Human antibodies with subnanomolar affinity against a marker of angiogenesis eluted from a two-dimensional gel. *J Biol Chem* 273: 21769-21776.

Pujuguet P, Hammann A, Moutet M, Samuel JL, Martin F and Martin M. (1996). Expression of fibronectin ED-A+ and ED-B+ isoforms by human and experimental colorectal cancer. Contribution of cancer cells and tumor-associated myofibroblasts. *Am J Pathol* 148: 579-592.

Ravi Kumar A and Kurup PA. (2000). Digoxin and membrane sodium potassium ATPase inhibition in cardiovascular disease. *Indian Heart J* 52: 315-318.

Riechmann L, Clark M, Waldmann H and Winter G. (1988). Reshaping human antibodies for therapy. *Nature* 332: 323-327.

Roberts GCK. (2000). Applications of NMR in drug discovery. *DDT* 5: 230-240.

Roques BP and Noble F. (1996). Association of enkephalin catabolism inhibitors and CCK-B antagonists: a potential use in the management of pain and opioid addiction. *Neurochem Res* 21: 1397-1410.

Rosenberg SA, Yang JC, White DE and Steinberg SM. (1998). Durability of complete responses in patients with metastatic cancer treated with high-dose interleukin-2: identification of the antigens mediating response. *Ann Surg* 228: 307-319.

Ross A, Schlotterbeck G, Klaus W and Senn H. (2000). Automation of NMR measurements and data evaluation for systematically screening interactions of small molecules with target proteins. *J Biomol NMR* 16: 139-146.

Ruef C and Coleman DL. (1990). Granulocyte-macrophage colony-stimulating factor: pleiotropic cytokine with potential clinical usefulness. *Rev Infect Dis* 12: 41-62.

Ruoslahti E. (1988). Fibronectin and its receptors. *Annu Rev Biochem* 57: 375-413.

Santimaria M, Moscatelli G, Giovannoni L, Leprini A, Neri G, Neri D, Zardi L and Riva P. (2003). Immunoscintigraphic detection of the ED-B domain of fibronectin, a marker of angiogenesis, in patients with cancer. *Clin Cancer Res*: in the press.

Schapira M, Raaka BM, Samuels HH and Abagyan R. (2000). Rational discovery of novel nuclear hormone receptor antagonists. *Proc Natl Acad Sci U S A* 97: 1008-1013.

Schneider G and Bohm HJ. (2002). Virtual screening and fast automated docking methods. *Drug Discov Today* 7: 64-70.

Schneider WP, Glaser SM, Kondas JA and Hakimi J. (1993). The anti-idiotypic response by cynomolgus monkeys to humanized anti-Tac is primarily directed to complementarity-determining regions H1, H2, and L3. *J Immunol* 150: 3086-3090.

Schreiber G and Fersht AR. (1993). Interaction of barnase with its polypeptide inhibitor barstar studied by protein engineering. *Biochemistry* 32: 5145-5150.

Selzer T, Albeck S and Schreiber G. (2000). Rational design of faster associating and tighter binding protein complexes. *Nat Struct Biol* 7: 537-541.

Shuker SB, Hajduk PJ, Meadows RP and Fesik SW. (1996). Discovering high-affinity ligands for proteins: SAR by NMR. *Science* 274: 1531-1534.

Sidhu SS. (2000). Phage display in pharmaceutical biotechnology. *Curr Opin Biotechnol* 11: 610-616.

Sieber V, Pluckthun A and Schmid FX. (1998). Selecting proteins with improved stability by a phage-based method. *Nat Biotechnol* 16: 955-960.

Skerra A and Plückthun A. (1988). Assembly of a functional immunoglobulin Fv fragment in Escherichia coli. *Science* 240: 1038-1041.

Smith GP. (1985). Filamentous fusion phage: novel expression vectors that display cloned antigens on the virion surface. *Science* 228: 1315-1317.

Smith GP. (1991). Surface presentation of protein epitopes using bacteriophage expression systems. *Curr Opin Biotechnol* 2: 668-673.

Stephens S, Emtage S, Vetterlein O, Chaplin L, Bebbington C, Nesbitt A, Sopwith M, Athwal D, Novak C and Bodmer M. (1995). Comprehensive pharmacokinetics

of a humanized antibody and analysis of residual anti-idiotypic responses. *Immunology* 85: 668-674.

Stockman BJ. (1998). NMR spectroscopy as a tool for structure-based drug design. *Prog NMR Spectrosc* 33: 109-151.

Studer A, Hadida S, Ferritto R, Kim SY, Jeger P, Wipf P and Curran DP. (1997). Fluorous synthesis: a fluorous-phase strategy for improving separation efficiency in organic synthesis. *Science* 275: 823-826.

Tarli L, Balza E, Viti F, Borsi L, Castellani P, Berndorff D, Dinkelborg L, Neri D and Zardi L. (1999). A high-affinity human antibody that targets tumoral blood vessels. *Blood* 94: 192-198.

Taylor LD, Carmack CE, Schramm SR, Mashayekh R, Higgins KM, Kuo CC, Woodhouse C, Kay RM and Lonberg N. (1992). A transgenic mouse that expresses a diversity of human sequence heavy and light chain immunoglobulins. *Nucleic Acids Res* 20: 6287-6295.

Taylor LD, Carmack CE, Huszar D, Higgins KM, Mashayekh R, Sequar G, Schramm SR, Kuo CC, O'Donnell SL, Kay RM and et al. (1994). Human immunoglobulin transgenes undergo rearrangement, somatic mutation and class switching in mice that lack endogenous IgM. *Int Immunol* 6: 579-591.

Tondi D, Slomczynska U, Costi MP, Watterson DM, Ghelli S and Shoichet BK. (1999). Structure-based discovery and in-parallel optimization of novel competitive inhibitors of thymidylate synthase. *Chem Biol* 6: 319-331.

Tsung K, Meko JB, Peplinski GR, Tsung YL and Norton JA. (1997). IL-12 induces T helper 1-directed antitumor response. *J Immunol* 158: 3359-3365.

Tuaillon N, Taylor LD, Lonberg N, Tucker PW and Capra JD. (1993). Human immunoglobulin heavy-chain minilocus recombination in transgenic mice: gene-segment use in mu and gamma transcripts. *Proc Natl Acad Sci U S A* 90: 3720-3724.

Tucker TJ, Lumma WC, Lewis SD, Gardell SJ, Lucas BJ, Sisko JT, Lynch JJ, Lyle EA, Baskin EP, Woltmann RF, Appleby SD, Chen IW, Dancheck KB, Naylor-Olsen AM, Krueger JA, Cooper CM and Vacca JP. (1997). Synthesis of a series of potent and orally bioavailable thrombin inhibitors that utilize 3,3-

disubstituted propionic acid derivatives in the P3 position. *J Med Chem* 40: 3687-3693.

Vartio T, Laitinen L, Narvanen O, Cutolo M, Thornell LE, Zardi L and Virtanen I. (1987). Differential expression of the ED sequence-containing form of cellular fibronectin in embryonic and adult human tissues. *J Cell Sci* 88: 419-430.

Viswanadhan VN, Balan C, Hulme C, Cheetham JC and Sun Y. (2002). Knowledge-based approaches in the design and selection of compound libraries for drug discovery. *Curr Opin Drug Discov Devel* 5: 400-406.

Viti F, Tarli L, Giovannoni L, Zardi L and Neri D. (1999). Increased binding affinity and valence of recombinant antibody fragments lead to improved targeting of tumoral angiogenesis. *Cancer Res* 59: 347-352.

Viti F, Nilsson F, Demartis S, Huber A and Neri D. (2000). Design and use of phage display libraries for the selection of antibodies and enzymes. *Methods Enzymol* 326: 480-505.

Walters WP, Stahl MT and Murcko MA. (1998). Virtual screening - an overview. *Drug Discovery Today* 3: 160-178.

Webster R. (1996) Biology of the filamentous bacteriophage. In: B Kay, L Winter and J McCafferty (Eds), Phage display of peptides and proteins. Academic Press, San Diego, 1-20.

Weller HN, Young MG, Michalczyk SJ, Reitnauer GH, Cooley RS, Rahn PC, Loyd DJ, Fiore D and Fischman SJ. (1997). High throughput analysis and purification in support of automated parallel synthesis. *Mol Divers* 3: 61-70.

Winter G, Griffiths AD, Hawkins RE and Hoogenboom HR. (1994). Making antibodies by phage display technology. *Annu Rev Immunol* 12: 433-455.

Wise R. (1999). A review of the mechanisms of action and resistance of antimicrobial agents. *Can Respir J* 6 Suppl A: 20A-22A.

Wu D, Chen CS and Johnson CS. (1995). An improved diffusion-ordered spectroscopy experiment incorporating bipolar-gradient pulses. *J Magn Reson A* 115: 260-264.

Yamada KM. (1983). Cell surface interactions with extracellular materials. *Annu Rev Biochem* 52: 761-99.

Yokota T, Milenic DE, Whitlow M and Schlom J. (1992). Rapid tumor penetration of a single-chain Fv and comparison with other immunoglobulin forms. *Cancer Res* 52: 3402-3408.

Zardi L, Carnemolla B, Siri A, Petersen TE, Paolella G, Sebastio G and Baralle FE. (1987). Transformed human cells produce a new fibronectin isoform by preferential alternative splicing of a previously unobserved exon. *Embo J* 6: 2337-42.

Zeng L, Burton L, Yung K, Shushan B and Kassel DB. (1998). Automated analytical/preparative high-performance liquid chromatography-mass spectrometry system for the rapid characterization and purification of compound libraries. *Journal of Chromatography, A* 794: 3-13.

Zerbe O (Ed.). (2002). BioNMR in Drug Research. Vol. 16. Weinheim, Germany: Wiley-VCH, 484 pages

Zuckermann RN, Kerr JM, Siani MA and Banville SC. (1992). Design, construction and application of a fully automated equimolar peptide mixture synthesizer. *Int J Pept Protein Res* 40: 497-506.

# 6 ABBREVIATIONS

| | |
|---|---|
| ACD | Available Chemicals Directory database |
| AMP | ampicillin |
| CaM | calmodulin |
| Cy5 | name of a fluorescent dye |
| DEAE | diethylaminoethyl- |
| DMF | *N*,*N*-dimethylformamide |
| DMSO | dimethylsulfoxide |
| DNA | desoxyribonucleic acid |
| EDB | Extra-domain B of fibronectin |
| ELISA | enzyme-linked immunosorbent assay |
| ESACHEL | encoded self-assembling chemical libraries |
| Hepes | (*N*-[2-Hydroxyethyl]piperazine-*N'*-[2-ethanesulfonic acid]) |
| HPLC | high-performance liquid chromatography |
| HRP | horseradish peroxidase |
| HSQC | heteronuclear single quantum coherence |
| HTS | high-throughput screening |
| IgG | immunoglobulin G |
| MPBS | PBS containing dried skimmed milk |
| NMR | nuclear magnetic resonance |
| $k_{on}$ | kinetic association constant |
| $k_{off}$ | kinetic dissociation constant |
| $K_D$ | dissociation constant |
| PBS | phosphate buffered saline: |
| | 50mM sodium phosphate, 100mM NaCl, pH 7.4 |
| PCR | polymerase chain reaction |
| PDB | Protein Data Bank, http://www.rcsb.org/pdb/index.html |
| RNA | ribonucleic acid |
| RT | room temperature |
| mRNA | messenger RNA |
| SAR | structure-activity relationship |
| scFv | single-chain antibody variable fragment |
| SDS | sodium dodecyl sulfate |
| SA | streptavidin |
| TBSC | Tris buffered saline with calcium |
| TFA | trifluoroacetic acid |
| TLC | thin layer chromatography |
| VH | variable domain of the heavy chain (of an antibody) |
| VL | variable domain of the light chain (of an antibody) |
| 2xYT | bacterial growth medium |

# 7 CURRICULUM VITAE

**Personal Data**


| | |
|---|---|
| *Name:* | Scheuermann |
| *First name:* | Jörg |
| *Address:* | Überlandstr. 17, 8953 Dietikon |
| *Working address:* | ETH Zürich, Institut für Pharmazeutische Wissenschaften<br>Y17 M94, Winterthurerstr. 190, 8057 Zürich |
| *e-mail:* | joerg.scheuermann@pharma.anbi.ethz.ch |
| *Phone:* | work: +41-1-635 60 79 ; private: +41-1-742 31 47 |
| *Birthday:* | April 16, 1970 |
| *Birth place:* | Mannheim, Germany |
| *Nationality:* | German |
| *Civil state:* | Married |


**Education**

| | | |
|---|---|---|
| *Primary school:* | 1976 – 1980 | Gebrüder-Grimm-Grundschule<br>Mannheim, Germany |
| *Gymnasium:*<br>*(humanistic)* | 1980-1989 | Karl-Friedrich-Gymnasium<br>Mannheim, Germany |
| *University:* | 1990-1994 | Ruprecht-Karls-Universität<br>Heidelberg, Germany |
| | 1994-1999 | ETH Zürich<br>Zürich, Switzerland |
| | Studies in Chemistry | |
| | Diploma Thesis: Prof. Steven A. Benner:<br>Chemische Synthese eines strukturanalogen Derivats von Xanthosin, einem Baustein des erweiterten genetischen Codes | |
| *PhD:* | Aug. 1999–today | Ph.D. thesis<br>Group of Prof. Dr. Dario Neri<br>ETH Zürich<br>Institute of Pharmaceutical Sciences |

**Languages**

| | |
|---|---|
| *German:* | Mother language |
| *English:* | Good knowledge in speaking and writing |
| *French:* | Good knowledge in speaking and writing |
| *Italian:* | Basic knowledge in speaking |
| *Chinese:* | Basic knowledge in speaking |

**Scientific publications**

Scheuermann, J., Volonterio, A., Zerbe, O., Zanda, M. and Neri, D.
Discovery and investigation of lead-compounds as binders to the extra-domain B of fibronectin, a marker of angiogenesis. *Drug Discovery Research* (2003, in the press)

Scheuermann, J., Viti, F. and Neri, D.
Unexpected observation of concentration-dependent dissociation rates for antibody-antigen complexes and other macromolecular complexes in competition experiments. *Journal of Immunological Methods* (2003, in the press)

Ebbinghaus, C., Scheuermann, J. and Neri, D.
Selection of recombinant antibodies specific for the EDB domain of fibronectin, a marker of angiogenesis. *Current Cancer Drug Targets* (2003, in the press)

Elia, G., Silacci, M., Scheurer, S., Scheuermann, J. and Neri, D. (2002)
Affinity-capture reagents for protein arrays. *Trends in Biotechnology* **20**(12), S19-S22

# 8 ACKNOWLEDGEMENTS

I would like to express my special thanks to my supervisor, Prof. Dr. Dario Neri for giving me the opportunity to work in his laboratory on a challenging project.
I am very grateful for his always giving me motivating support, and for all the instructive and fruitful scientific discussions we had together.

I am very grateful to Prof. Dr. Leonardo Scapozza and Dr. Oliver Zerbe for accepting to be co-examiners of my thesis.

I feel very much obliged to Dr. Oliver Zerbe and his coworkers Dr. Reto Bader and Mirjam Lerch, for sharing their expertise with me in NMR and for their great help during the course of my thesis.

I am especially grateful to Dr. Cornelia Halin which established the first contact to this research group, and to Dr. Salvatore Demartis who was so kind and introduced me into the world of phage display and cloning.

I am grateful to Dr. Matteo Zanda and Dr. Alessandro Volonterio of the Politechnico di Milano for their help in organic synthesis.
I would also like to thank Dr. Oliver Zerbe, Dr. Giuliano Elia and Christina Ebbinghaus for writing papers together with me.

I always was and I still am extremely happy about the incomparably nice and funny atmosphere in our group, the experimental help, and the serious and not so serious discussions:
Dr. Francesca Viti, Dr. Salvatore Demartis, Dr. Lorenzo Tarli, Dr. Adrian Huber, Dr. Fredrik Nilsson, Dr. Cornelia Halin, Dr. Maja Bumke, Samu Melkko — with whom I am very glad to be able to continue working —, Christian Heinis, Julian Bertschinger, Christina Ebbinghaus, Simone Scheurer, Elisabetta Piras, Patrizia Alessi, Simon Brack, Michela Silacci, Verena Gafner, Eveline Trachsel and Jascha Rybak, to mention the former and present PhD students, our Oberassistent Dr. Giuliano Elia and all the former and present diploma and semester students.

I am very grateful to our secretary, Pia Steinbak and to René Bemsel and his team who were always very nice and helpful.

I would also like to thank Prof. Dr. Steven A. Benner for giving me the opportunity to perform my diploma thesis in his laboratory and to Dr. Michael Lutz for his great supervision at that time.

I am extraordinarily greatful to Diana and Oskar Schmid, who always took and still take great care about my wife and me, and to Dr. Thomas Gilbert who supported me a lot.

My deepest thanks go to my wife Xiaoqin and to my parents for their love and supply. I would like to dedicate my thesis to them.